Charles University in Prague, Third Faculty of Medicine

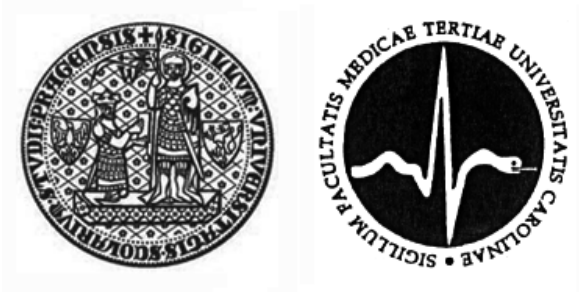

Laboratories of Molecular and Cell Biology,
Department of Pneumology and Thoracic Surgery, Hospital Bulovka

Expression of apoptosome pathway regulators and activation of apoptosome apparatus in non-small cell lung carcinoma

Ph.D. Thesis

Ing. Erika Moravčíková

Thesis Supervisor

MUDr. Evžen Křepela, CSc.

Prague 2013

Statement of authorship

I hereby certify that this thesis represents valid work elaborated under the supervision of MUDr. Evžen Křepela, CSc. and that neither this manuscript nor one with substantially similar content under my authorship has been submitted in support of an application for any other academical degree. I have participated in the conception of this work, performing the experiments described in this thesis, analysis and interpretation of the data.

Prague

. . . . . .
Ing. Erika Moravčíková

Statement of co-authors

I hereby certify that Ing. Erika Moravčíková substantially contributed to the work described in this thesis and to writing of the papers this thesis is based on.

Prague

. . . . . .
MUDr. Evžen Křepela, CSc.

ACKNOWLEDGEMENTS

Foremost, I would like to express my sincere gratitude to my supervisor MUDr. Evžen Křepela, CSc. for his patience, enthusiasm, and immense knowledge. His guidance helped me during the time of research and writing of this thesis.
Besides my advisor, I would like to thank my fellow labmates in Laboratories of Molecular and Cell Biology at Hospital Bulovka, for the stimulating discussions.
Also I thank to laboratory technicians for their excellent technical assistance.
Last but not least, I would like to thank my friends and family for the continuous support during my PhD studies.

I gratefully acknowledge the support of the institutional research projects MZO00064211 and RVO-NNB/2012-00064211 and grants NR/7860-5 and NS/9715-4 from the Ministry of Health, Czech Republic.

LIST OF ABBREVIATIONS

5'-UTR	5'-untranslated region
AA	apoptosome apparatus
ADC	adenocarcinoma
AIF	apoptosis-inducing factor
Apaf-1	apoptotic protease activating factor 1
APIP	Apaf-1 interacting protein
Bcl-2	B cell lymphoma-2 protein
BIR	baculovirus inhibitor of apoptosis protein repeat
CAS	cellular apoptosis susceptibility
CARD	caspase activation and recruitment domain
CDK1	cycline-dependent kinase-1
CpG	cytosine-phospo-guanosine dinucleotide
Cyt-c	cytochrome c
CTL	cytotoxic lymphocyte
DD	death domain
DED	death effector domain
Decitabine	5-aza-2'-deoxycytidine
DFF	DNA fragmentation factor
DNMT	DNA methyltransferase
DISC	death-inducing signaling complex
DTT	D,L-dithiothreitol
DYRK-1A	dual-specificity tyrosine-phosphorylation-regulated kinase A1
E	endogenous caspase-3-like activity
EndoG	endonuclease G
Erk	extracellular signal-regulated kinase
FADD	Fas-associated death domain
FLIP	FLICE-like inhibitory protein
HSP70	heat shock protein 70
I	incremental-induced caspase-3-like activity
IAP	inhibitor of apoptosis protein
IRES	internal ribosome entry segment
LAC	large cell lung carcinoma
Lu	lung
MDM2	murine double minute 2
MOMP	mitochondria outer membrane permeabilization
NF-κB	nuclear factor-B
NBOD	nucleotide binding and oligomerization domain
NK	natural killer
NSCLC	non-small cell lung carcinoma
p38 MAPK	p38 mitogen-activated protein kinase
PHAP	putative HLA-DR associated protein
PI-9	proteinase inhibitor 9
PIDD	p53-induced protein with a death domain
PK	protein kinase
ProT	prothymosin-
RAIDD	RIP associated ICH-1/CED-3-homologous protein with death domain
RING	really interesting new gene
RIP	receptor-interacting serine/threonine-protein kinase
ROS	reactive oxygen species

SeDeS	sequence detection system
SLC	sarcomatoid lung carcinoma
Smac	second mitochondria-derived activator of caspase
SQCLC	squamous cell lung carcinoma
T	total caspase-3-like activity
tBid	truncated Bid
Tu	tumour
UACA	uveal autoantigen with coiled-coil domains and ankyrin repeats
UNDIF	undifferentiated lung carcinoma
XIAP	X-chromosome linked inhibitor of apoptosis protein

Summary

Lung cancer is statistically a leading cause of cancer-related death in Czech Republic and worldwide. Interestingly, more than 85% of all lung cancer patients are diagnosed with non-small cell lung cancer. Although a novel approach in the form of the so-called molecular targeted therapy is combined with the standard cytotoxic therapy to boost cisplatin/carboplatin effectiveness, only a modest progress in the 5-year-survival was achieved so far. Therefore, there is an urgent need to better and deeply understand the molecular mechanisms of lung cancer diseases development to define new powerful and safe strategies and modalities for their effective prevention and treatment.

The apoptosome pathway is interesting as potential therapeutic target because it plays an important role in the cancer chemotherapy- and biological therapy-induced apoptosis as well as in amplifying the death receptor and cytotoxic-granule-induced pathways. The functionality of apoptosome apparatus in non-small cell lung carcinoma (NSCLC) cells and tissues is often impaired due to defects in apoptosome pathway by changes in expression and/or acquired mutations and/or modifications of apoptosome components or its regulators that play a significant role in cancer cell proliferation and treatment unresponsiveness. Therefore, this thesis is aimed at the investigation of the expression status of apoptosome pathway regulators (survivin, HBXIP, XIAP, APIP, and UACA) and of the readiness of apoptosome apparatus activation in non-small cell lung carcinoma cells and tissues.

The results of this work suggest a higher predisposition to apoptosome-mediated apoptosis in NSCLC tumours than in lungs. The higher propensity of NSCLC tumours to apoptosome-mediated apoptosis is due to several factors. First, because of the increased expression of activatable apoptosome pathway core protein components, including Apaf-1 and procaspases-9 and -3. Second, because of the down-regulation of expression of *APIP* and *UACA* genes causing the lack of APIP-mediated apoptosome apparatus suppression and UACA-assisted Apaf-1 nuclear entry, which would lead to the failure of DNA damage checkpoint activation in NSCLC cells leading to their genomic instability and contributing to development and progression of NSCLC tumours. However, the functionality of apoptosome is suppressed in some NSCLC cell lines and in a high proportion of NSCLC tumours. There is evidence, that XIAP-mediated inhibition is not the major suppressor mechanism of apoptosome pathway induction in NSCLC tumours. Although overexpressed survivin together with abundant expression of HBXIP could lead to formation of the antiapoptotic survivin•HBXIP complex, which may be preferentially generated in lung tumours to inhibit the apoptosome pathway, failure of the apoptosome-bound procaspase-9 activation may underlie the malfunction of apoptosome pathway in NSCLC cells.

Contents

1 Introduction

Lung cancer is statistically a leading cause of cancer-related death in Czech Republic and worldwide, comprising 5.2% (5554 cases) of all deaths in Czech Republic in 2010 (Jemal *et al*, 2011; http://data.euro.who.int/dmdb, last accessed 13/9/2012). Incidence and mortality of lung cancer in Czech Republic is one of the highest in the world, slightly decreasing in men but increasing in women (http://www.svod.cz). Interestingly, more than 85% of all lung cancer patients are diagnosed with non-small cell lung cancer, including squamous cell lung carcinoma (SQCLC), lung adenocarcinoma (LAC), large cell lung carcinoma (LCLC), sarcomatoid lung carcinoma (SLC), and undifferentiated lung carcinoma (UNDIF) histopathological subtypes (Fry *et al*, 1996; Travis 2011; American Cancer Society, 2012). Only 20% of diagnosed NSCLC are surgically treatable, because NSCLC tumours are frequently detected at advanced stage. Therefore, the current treatment of non-small cell lung cancer involves to large extent radiotherapy and/or a platinum-based chemotherapy (Molina *et al*, 2008; Moldvay, 2012), which was first introduced into the clinical trials in the seventies. Although a novel approach in the form of the so-called molecular targeted therapy (for instance using tyrosine kinase inhibitors Erlotinib or Gefitinib in the case of activation mutations of the epidermal growth factor receptor gene, monoclonal antibody Bevacizumab that binds and inactivates vascular endothelial growth factor receptor) is combined with the standard cytotoxic therapy to boost cisplatin/carboplatin effectiveness, only a modest progress in the 5-year-survival was achieved so far (http://www.svod.cz, last accessed 3/2/2013; Stinchcombe and Socinski, 2009a and b; Bareschino *et al*, 2011; Vadakara and Borghaei, 2012).

Anticancer therapies such as γ-irradiation and treatment with cytotoxic drugs primarily act, if efficacious, via inducing apoptotic cell death (Lai *et al*, 2000; Brognard *et al*, 2001; Making and Dive, 2001; Reed, 2003; Liu *et al*, 2008a and b). However, dysfunction and suppression of apoptosis mechanisms in cancer cells (Wolf *et al*, 2001; Liu *et al*, 2002; Corvaro *et al*, 2007; Christoph *et al*, 2008; Hanahan and Weinberg 2011; Tan *et al*, 2011) can contribute to development and progression of malignant tumours and their therapy resistance (Brown and Attardi, 2005; Viktorsson and Lewensohn, 2007; Fulda, 2009; Hanahan and Weinberg, 2011). Therefore, there is an urgent need to better and deeply understand the molecular mechanisms of cancer diseases development to define new powerful and safe strategies and modalities for their effective prevention and treatment.

Apoptosis is characterized as a morphologically distinct type of cell death observed in various tissues and cells of multicellular organisms (Kerr *et al*, 1972; Galluzzi *et al*, 2007), by which an organism removes unwanted or harmful cells to maintain its homeostasis (Cecconi *et al*, 1998; Hao *et al*, 2005).

The central role responsible for morphological changes typical for apoptosis is played by caspases, a family of cysteinyl aspartate-specific proteases (Fuentes-Prior and Salvesen, 2004). Signals to activate caspase zymogens involve extrinsic or intrinsic pathways, leading to cell devitalizing and dismantling by specific cleavage of plentiful cellular proteins (Fischer *et al*, 2003; Luthi and Martin, 2007; Timmer and Salvesen, 2007). The inducible extrinsic and intrinsic caspase-dependent apoptotic pathways are described in Figure 1.

Extrinsic induction of caspase-dependent apoptosis Extracellular death ligands, such as TNFα, TRAIL or Fas (in the plasma membrane-bound form on immune cells and some cancer cell types or in a soluble form), bind to their plasma membrane-bound specific death receptors on target cells and causes their conformational change leading to recruitment of protein adaptor molecules containing death domain (DD) to the intracellular DD of the liganded death receptor, followed by the death effector domain (DED)-mediated binding of procaspase-8/-10 monomers to the DED of bound adaptor molecules. The resulting multimolecular proteins assembly forms a death-inducing signaling complex (DISC), serving as an activation platform for the recruited procaspase-8/-10 molecules (Guicciardi and Gores, 2009; Mace and Riedl, 2010; Dickens *et al*, 2012; Schleich *et al*, 2012). Upon DISC-driven dimerization, procaspase-8/-10 undergoes proteolysis between its large and small domains and between large domain and prodomain. Both, dimerization and cleavage are necessary for full activity and stability of caspase-8 (Boatright *et al*, 2003; Donepudi *et al*, 2003; Pop *et al*, 2007; Keller *et al*, 2009; Wachmann *et al*, 2010; Oberst *et al*, 2010; Schleich *et al*, 2013). After release from DISCs, the active caspase-8/-10 heterotetramers cleave the interdomain linkers of the homodimeric executioner caspase zymogens, procaspase-3 and -7, which sterically inhibit the activation loop translocation (Stennicke *et al*, 1998). In some cells (type II cells) caspase-8/-10 must engage the mitochondrial pathway of apoptosis by cleaving the Bcl-2 family proapoptotic regulator of cell death, Bid, to efficiently induce apoptosis (Samraj *et al*, 2006; Wachmann *et al*, 2010; Schug *et al*, 2011).
In the apoptotic pathways initiated by cytotoxic lymphocytes (CTL) or natural killer (NK) cells, secretion of several granzymes, *i.e.* the proapoptotic serine proteinases, plays an important role in host defence against cancerogenesis (Cullen *et al*, 2010; Rousalova and Krepela, 2010). Upon recognition and conjugation of target cells by CTL or NK, secretory granules containing mainly granzyme-B and perforines are released from CTL/NK into the intercellular cleft called immunologic synapse (Tophan and Hewitt, 2009; Jenkins and Griffiths, 2010) and are further transferred into the target cell probably via clathrine-dependent endocytosis (Thiery *et al*, 2010). Granzyme-B is then released from endosomes into the cytosol through a perforin-mediated pore. Once in the cytosol, granzyme-B cleaves multiple proteins leading to activation of procaspases, mitochondrial outer membrane permeabilization (MOMP), activation of endonucleases, *etc.* (Van Damme *et al*, 2009; Rousalova and Krepela, 2010).

Intrinsic induction of caspase-dependent apoptosis Cellular stress, DNA damage, growth factor withdrawal or ionizing- and UV-radiation can induce intrinsic apoptotic pathways

triggered by cytosolic release of intermembrane mitochondrial proteins by partial cytosolic release of lysosomal cathepsins (lysosomal apoptosis), and by activated and processed caspase-2 (Tinel and Tschopp, 2004), which tumour suppressor capacity was proved (Ho *et al*, 2009; Manzl *et al*, 2012). Procaspase-2 can be activated in a complex called PIDDosome, consisting of p53-induced protein with a death domain (PIDD/LRDD) and RIP associated ICH-1/CED-3-homologous protein with death domain (RAIDD/CRADD). Upon DNA damage, PIDD undergoes autoproteolysis resulting in a DD-containing fragment able of translocation from nucleus into the cytosol (Tinel *et al*, 2007), where 5 molecules of PIDD assemble to form a pentameric core of PIDDosome. 7 RAIDD molecules, serving as adaptors, bind above the PIDD pentamer via DD-mediated interactions, while their exposed CARDs recruit monomers of procaspase-2, which are activated by proximity induced dimerization (Park *et al*, 2007). For full caspase-2 activity, removal of prodomain and proteolytic processing between its large and small subunit is needed (Ho *et al*, 2009). However, a PIDDosome-independent procaspase-2 activation was also proved (Manzl *et al*, 2009), which could be dependent on procaspase-8 activation at DISC, as active caspase-8 can cleave and thus activate procaspase-2 (Olsson *et al*, 2009). Conversely, active caspase-2 can process and activate procaspase-8 (Shin *et al*, 2005). Caspase-2 can mediate apoptosis by cleavage of *e.g.* DFFA, procaspase-7, procaspase-8, or proapoptotic Bid protein (Guo *et al*, 2002; Robertson *et al*, 2002; Shin *et al*, 2005; Dahal *et al*, 2007; Vakifahmetoglu *et al*, 2008; Ho *et al*, 2009; Olsson *et al*, 2009). Subsequent translocation of truncated Bid (tBid) into the mitochondria induces mitochondria outer membrane permeabilization (MOMP) leading to release of cytochrome-c (cyt-c) into the cytosol and apoptosome pathway induction. Thereby caspase-2 may act in accelerating apoptosis.

Lysosomes were for long thought to be responsible for nonspecific protein degradation. However, many other functions of lysosomes have been found recently and their participation in apoptotic pathway has been proved. Partial permeabilization of lysosomes induced by various stimuli, such as reactive oxygen species (ROS) or cell death effector Bax (Kagedal *et al*, 2005; Feldstein *et al*, 2006; Terman *et al*, 2006), leads to the cytosolic release of lysosomal proteases, *e.g.* cathepsins (B, D, L) that remain active at neutral cytosolic pH and cause proteolytic fragmentation of vital proteins and/or indirect activation of caspases via Bid protein cleavage, thus initiating/amplifying the MOMP-dependent apoptotic pathway (Boya and Kroemer, 2008; Appelqvist *et al*, 2012; Cesen *et al*, 2012).

All above mentioned events converge at or lead to MOMP and subsequent release of cyt-c from mitochondria into the cytosol, which sets in motion the apoptosome pathway, further described in detail in section 1.1.

The apoptosome pathway is interesting as potential therapeutic target because it plays an important role in the cancer chemotherapy- and biological therapy-induced apoptosis as well as in amplifying the death receptor and cytotoxic-granule-induced pathways (Jiang and Wang, 2004; Liu *et al*, 2008a). The functionality of apoptosome apparatus (AA) in NSCLC cells and tissues is often impaired due to defects in apoptosome pathway by changes in expression and/or acquired mutations and/or modifications of apoptosome components or its regulators

that play a significant role in cancer cell proliferation and treatment unresponsiveness (Krepela *et al*, 2004; Hoffarth *et al*, 2008). Therefore, in my thesis, I aimed at the investigation of the expression status of apoptosome pathway regulators (survivin, HBXIP, XIAP, APIP, and UACA) and of the readiness of apoptosome apparatus activation in non-small cell lung carcinoma (NSCLC) cells and tissues.

1.1 Mechanism of the apoptosome pathway

1.1.1 Assembly and structure of apoptosome apparatus

A classical mechanism to kill the cell by chemo- and radiotherapy is to cause irreparable DNA damage, and promote p53-mediated cell cycle arrest leading to apoptosis (Vazques *et al*, 2008).

The key event in this pathway is the release of holocytochrome-c from the outer-membrane-permeabilized mitochondria through a Bax/Bak pore complex into the cytosol upon stress stimuli. Holocytochrome-c binds to apoptotic protease activating factor 1 (Apaf-1) to induce conformational changes in the presence of (d)ATP. Apaf-1 is a member of AAA+ family of ATPases and in the ground state it exists in the cytosol in an autoinhibited form with N-terminal caspase recruitment domain (CARD) buried between the C-terminal lobes of β-propellers (Acehan *et al*, 2002; Garrido *et al*, 2006). Holocytochrome-c is about the same size as the CARD of Apaf-1 and is able to displace the CARD head from Apaf-1 feet consisting of 13 WD-40 repeats (Hu *et al*. 1999, Martin and Fearnhead, 2002). However, according to a recent structural data of murine Apaf-1 in a closed conformation, CARD is not buried between the WD-40 lobes, but rather the WD-40 conformation itself locks the Apaf-1 in its inactive state (Reubold *et al*, 2011; Reubold and Eschenburg, 2012).

Apaf-1 was found in a complex either with dATP (Kim *et al*, 2005), or ADP buried in Apaf-1 monomer, which strengthens the interactions between the domains in locked Apaf-1 (Riedl *et al*, 2005; Bao *et al*, 2005). However, cyt-c binding not only induces Apaf-1-mediated hydrolysis of dATP or ATP to dADP or ADP but also increases Apaf-1 affinity for dATP or ATP nucleotide. Thus, in both cases, dATP-bound Apaf-1 or ATP-bound Apaf-1, dADP or ADP exchange for dATP or ATP nucleotide is required for full Apaf-1 activation, while dATP has 10 times higher binding affinity for Apaf-1 (Li *et al*, 1997; Jiang and Wang, 2000). Subsequently, Apaf-1 activated monomers assemble via its nucleotide binding and oligomerization domain (NBOD) into ≈700 kDa heptameric circular complex called apoptosome, in which CARD domains form the central hub and are flexibly bound to NBOD which creates a first ring (Yuan *et al*, 2010). Y shaped arm of each Apaf-1 radiates from the hub of the apoptosome and cyt-c creates a bridge between the two β propellers consisting of 13 WD-40 repeats (Acehan *et al*, 2002; Yu *et al*, 2005; Yuan *et al*, 2010). Apoptosome serves as a platform for procaspase-9 recruitment and activation.

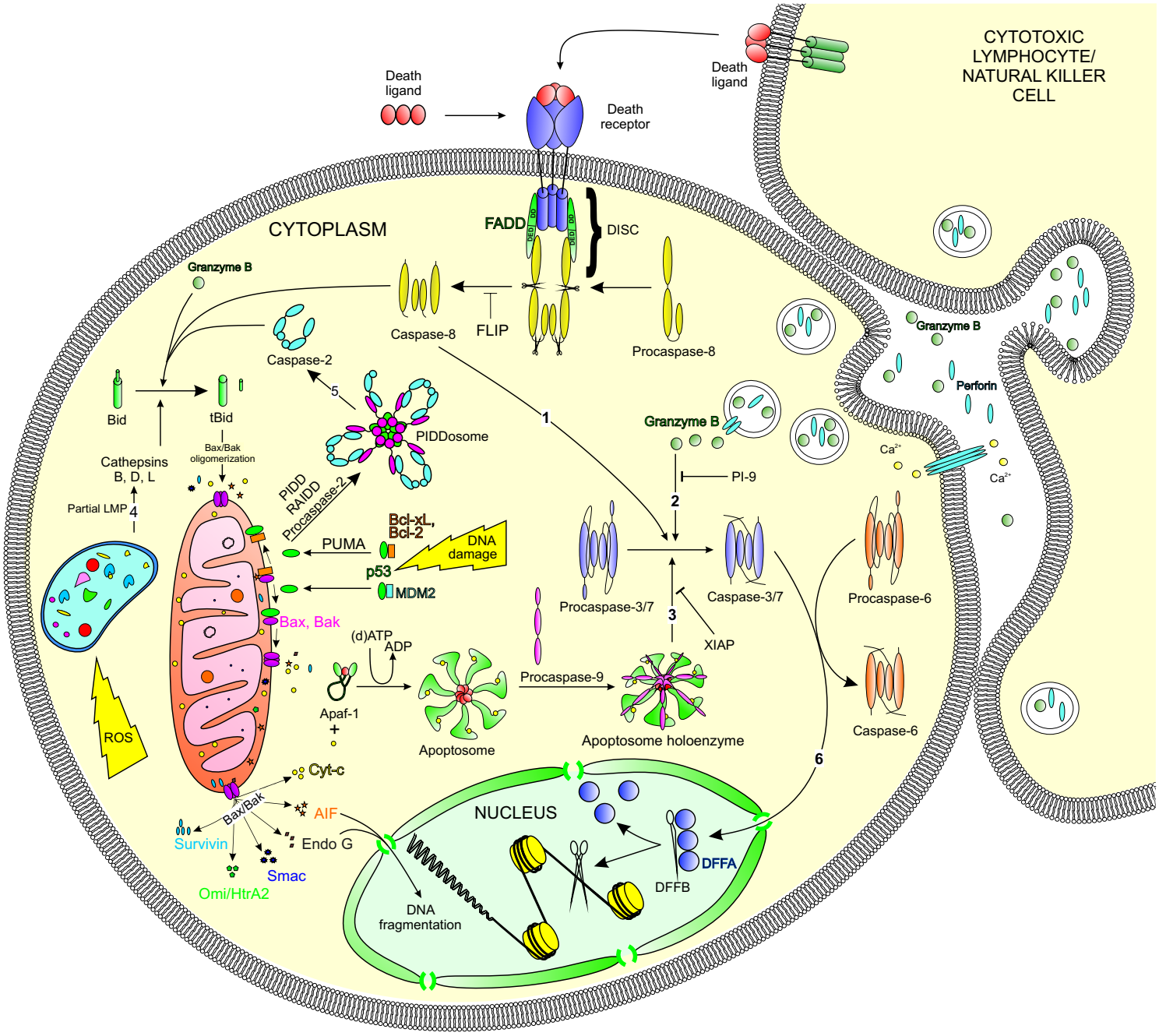

Figure 1: Caspase-dependent apoptotic pathways in cancer cells.
(1) Death ligand induces DISC formation, leading to procaspase-8 activation. Active caspase-8 proteolytically processes and activates executioner procaspase-3 and -7. This pathway can be inhibited by *e.g.* FLIP protein. (2) Cytotoxic lymphocyte or natural killer cell induce secretion of granzyme-B into the host cell, which in cytosol directly cleaves and activates procaspase-3 and -7. This pathway is antagonized by PI-9. [3] DNA damage induces MOMP via p53-mediated Bax/Bak oligomerization and release of antiapoptotic (Survivin) as well as proapoptotic factors (Omi/HtrA2, Smac, EndoG, AIF, cyt-c) from the mitochondrion into the cytosol. Cyt-c and (d)ATP induce Apaf-1 oligomerization following recruitment, processing and activation of procaspase-9. Caspase-9 in turn cleaves and thus activates procaspase-3 and -7. The pathway is suppressed by *e.g.* XIAP. (4) ROS induce partial LMP and release of cathepsins B, D and L, which cleave and thus activate Bid to MOMP-inducing tBid fragment. (5) Genotoxic stress leads to stabilization of p53 protein and p53-mediated expression of procaspase-2, which translocates from nucleus into the cytosol, where is activated in the PIDDosome. Active caspase-2 can induce MOMP by cleavage of Bid protein. (6) All pathways lead to activation of procaspase-3, -7, which when active, proteolytically cleave multiple proteins in the cytoplasm (*e.g.* procaspase-6, actin) or in the nucleus (*e.g.* DFFA subunit of DFF), leading to DNA fragmentation, nuclear pyknosis, karryorhexis, cell shrinkage, plasma membrane blebbing and formation of apoptotic bodies, which are eliminated by phagocytes or neighbouring cells. See the text for a more detailed description.

1.1.2 Recruitment and activation of procaspase-9

The primary function of the apoptosome is the recruitment of procaspase-9 monomers via interaction of its CARD with the Apaf-1 CARDs, forming a disk above the central hub of the apoptosome. Recent structural study has shown, that the interaction of procaspase-9 with apoptosome involves not only CARD domains, but also other parts of the recruited procaspase-9 molecules and NBOD domains of oligomerized Apaf-1 molecules that are required for the caspase-9 zymogen activation (Yuan *et al*, 2011). It was demonstrated that the p20 and p10 domains of procaspase-9 interact with adjacent Apaf-1 molecules in the apoptosome (Yuan *et al*, 2010; Yuan *et al*, 2011). The stoichiometry of Apaf-1: procaspase-9 within the apoptosome complex could range from 7:5 to 7:7. However, the diameter and the acentric position of the CARD disk might limit the binding of the catalytic domains of procaspase-9 on the Apaf-1 central hub and NBOD domain, which seems to be necessary for procaspase-9 activation. Two procaspase-9 activation models have been proposed. In the proximity induced dimerization model, apoptosome facilitates the dimerization of procaspases-9 molecules (Boatright *et al*, 2003; Pop *et al*, 2006). However, within homodimers of caspase-9 molecules, which are active, only one caspase-9 molecule contains the catalytically competent active site (Renatus *et al*, 2001). Moreover, engineered caspase-9 molecules, that form constitutive dimers outside the apoptosome, are much less active than the caspase-9 activated in the apoptosome-dependent manner (Chao *et al*, 2005). In the allosteric model, the binding of procaspase-9 monomer to apoptosome induces a conformational change in the bound procaspase-9 molecule (Rodriguez and Lazebnik, 1999; Shiozaki *et al*, 2002; Chao *et al*, 2005). Furthermore, no proteolytic cleavage is needed for procaspase-9 activation (Rodriguez and Lazebnik, 1999; Renatus *et al*, 2001; Boatright *et al*, 2003). These data together with the recent biochemical (Malladi *et al.*, 2009) and structural data (Yuan *et al.*, 2011) strongly support the apoptosome-dependent allosteric mechanism of procaspase-9 activation.

The apoptosome-activated and -associated procaspase-9 molecule mediates by itself its own proteolytic processing, *i.e.* the cleavage of the interdomain linker at the D315-A316 peptide bond. As a result, two caspase-9 subunits are generated, the large p35 one and the small p12 one (Yin *et al*, 2006). This cleavage not only lowers the Km of caspase-9 for procaspase-3 substrate (Zou *et al*, 2003), but also it activates a molecular cycle, in which the apoptosome bound caspase-9 is replaced by procaspase-9 molecules with higher affinity to the apoptosome (Malladi *et al*, 2009). The purpose of this binding-processing-replacement cycle is to activate procaspase-9 monomers to caspase-9, which only in the association with apoptosome is able to proteolytically process and activate procaspase-3 (Malladi *et al*, 2009). The substrates for the apoptosome-associated caspase-9 are the effector procaspase-3 and -7, which appear to be recruited to the apoptosome by caspase-9 (Srinivasula *et al.*, 1998; Yin *et al.*, 2006; Twiddy *et al*, 2006; Malladi *et al*, 2009; Yuan *et al*, 2011).

1.2 Regulation of the apoptosome pathway in cancer

The negative regulation of apoptosome pathway slows down or suppresses the cell's killing in favour of apoptosis evasion, while its positive regulation enhances the rate and completeness of cell apoptosis. The balance between apoptosis execution and apoptosis suppression is frequently disrupted in cancer cell populations.

Under pathological conditions, a robust induction of apoptosome pathway is essential to kill the cells, otherwise, the apoptotic signaling is vanquished in the presence of a variety of mechanisms that protect the cell from unwanted apoptosis (Schafer and Kornbluth, 2006; Bratton and Salvesen, 2010; Florentin and Arama, 2012). In example, physiological intracellular concentration of potassium and calcium ions inhibits Apaf-1 activation by cyt-c and (d)ATP, therefore only extensive and robust release of cyt-c from mitochondria can overcome the inhibition and successfully initiate the AA-dependent apoptosis (Purring-Koch and McLendon, 2000; Cain *et al*, 2001; Bao *et al*, 2007). Moreover, cell's propensity to apoptosis is set by the level of the key AA components expressed by a cell.

1.2.1 Regulation of expression of the key apoptosome apparatus components

Regulation of Apaf-1 expression

In normal tissue cells, which are permanently exposed to environmental stresses and whose long-term survival is needed, *e.g.* in the lung or brain, it is important to keep Apaf-1 level low to restrict from unwanted apoptosis. On the other hand, upregulation of Apaf-1 expression might be necessary under pathological conditions to undergo AA-mediated apoptosis in these cells. Increased expression of Apaf-1 was observed in certain tumours including NSCLC tumours and brain tumours, compared to normal tissues (Fearnhead *et al*, 1998; Krepela *et al*, 2004; Johnson *et al*, 2007). However, low Apaf-1 expression was found in metastatic tumours and was correlated with malignant tumour progression, chemoresistance and unfavourable prognosis (Soengas *et al*, 2001; Leo *et al*, 2005; Leo *et al*, 2007).

DNA methylation, as an epigenetic regulation mechanism, might be involved in downregulation of apoptosis-associated and tumour suppressor genes in cancer cells with overexpressed DNA methyltransferases as a consequence of carcinogenesis. This could be the case of low level of Apaf-1 in some cancer cells, as the DNA methylation inhibitor 5-aza-2'-deoxycytidine can restore the physiological level of Apaf-1 and increase the sensitivity to apoptosis in melanoma and leukemic cells (Soegans *et al*, 2001; Fu *et al*, 2003; Furukawa *et al*, 2005).

The expression of Apaf-1 mRNA is also regulated by transcriptional factor E2F-1, which is involved in G1/S transition of the cell cycle (Furukawa *et al.* 2005) and by a tumour suppressor p53, which is frequently mutated in cancer cells.

Moreover, five splice variants of Apaf-1 were found expressed in cancer cells: Apaf-1XL, Apaf-1LN, Apaf-1LC, Apaf-1S and Apaf-1ALT (Figure 2). However, only the isoforms containing 13 WD-40 repeats (Apaf-1XL and Apaf-1LC) are activatable by cyt-c to induce apoptosis (Benedict *et al*, 2000; Ogawa *et al*, 2003). Importantly, Apaf-1ALT, lacking the WD-40

regulatory region, but containing the CARD, is able to negatively interfere with Apaf-1XL function (Ogawa *et al*, 2003). It was shown, that Apaf-1 construct containing only the CARD domain interacts with procaspase-9, therefore, Apaf-1 ALT overexpressed in prostate cancer cells could sequester procaspase-9 by CARD interactions and thus could slower the apoptosis. In addition, cap-dependent translation of many mRNAs is inhibited either by eIF4G cleavage by *e.g.* caspase-3 or by translation factors modifications (*e.g.* eIF4 cap-binding protein phosphorylation) during cellular stress (Panniers *et al*, 1994; Clemens *et al*, 1998; Marissen and Lloyd, 1998; Marissen *et al*, 2000; Provot *et al*, 2003; Sherrill *et al*, 2004; Konicek *et al*, 2011; Andreev *et al*, 2012). Therefore, the cell's fate might be determined by proteins, which are continuously synthesised. It was observed, that Apaf-1 mRNA translation inhibition is relatively resistant during apoptosis (Ungureanu *et al*, 2006). One explanation of the Apaf-1 constant synthesis during cellular stress is the presence of an internal ribosomal entry segment (IRES), a stable secondary mRNA structure in the 5'-untranslated region (5'-UTR) of Apaf-1 mRNA (Coldwell *et al*, 2000), that after interaction with trans-acting protein factors allows ribosomes binding to translation start (Mitchell *et al*, 2001). In addition, the level and subcellular localization of cell-specific trans-acting factors that are required for full IRES function (*e.g.* polypyrimidine tract binding proteins and upstream of N-Ras protein) (Mitchell *et al*, 2001) might modulate the Apaf-1 translation and hence the intracellular level of Apaf-1 protein (Markovtsov *et al*, 2000; Mitchell *et al*, 2003; Cammas *et al*, 2007). However, recent study has demonstrated Apaf-1 5'end-dependent scanning by ribosomes, probably mediated by specific structural elements within Apaf-1 mRNA, is also able to recruit the translational machinery leading to eIF4E-independent Apaf-1 continuous synthesis upon cellular stress (Andreev *et al*, 2012).

Regulation of procaspase-9 expression

The cytosolic level of procaspase-9 protein contributes to the cell's sensitivity to stress-induced apoptosis. It was demonstrated that increased expression of caspase-9 could be achieved either by DNA demethylating agent decitabine or E2F-1 transcriptional factor, and that treatments with these compounds can sensitise lung cancer cells to chemotherapy-induced apoptosis (Nahle *et al*, 2002; Gomyo *et al*, 2004).

Increasing evidence shows that alternative splicing of certain pre-mRNAs has functional importance in cancer development. Many alternative splice variants for apoptotic factors have been identified, some having antagonistic function, such as caspase-9 isoform S. To date, three splice variants of human procaspase-9 have been identified, caspase-9-α (Duan *et al*, 1996, Srinivasula *et al*, 1996), caspase-9-β/S/b (Izawa *et al*, 1999; Seol and Billiar, 1999; Srinivasula *et al*, 1999) and caspase-9-γ (Wang *et al*, 2006) (Figure 3). Only the full length caspase-9-α retains the catalytic activity. Caspase-9-β isoform is missing most of the central large subunit domain including the catalytic site, while caspase-9-γ lacks both, the large and the small subunits domains. Containing the CARD domain, but lacking the catalytic domain, procaspase-9-β and procaspase-9-γ can compete with full length procaspase-9-α for

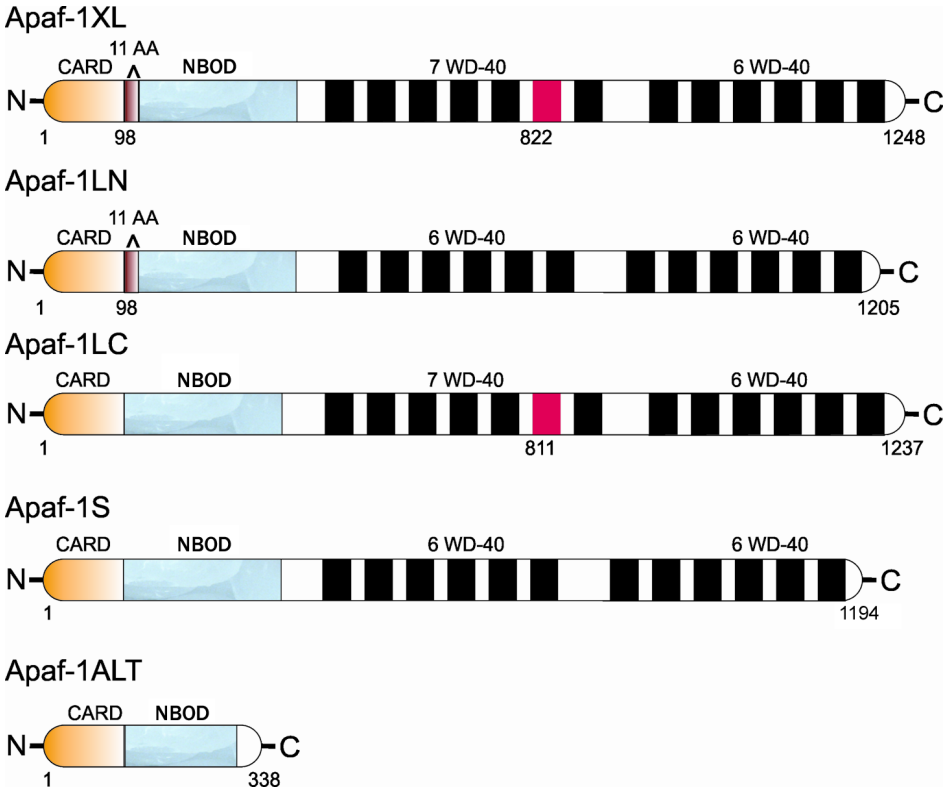

Figure 2: Expression of Apaf-1 protein isoforms.
CARD (orange), NBOD (blue) and WD-40 repeats (black and pink) domains are indicated. Apaf-1XL and -LN contain an additional 11 amino acid sequence (red), while Apaf-1XL and -LC contain an additional WD-40 repeat (pink) after 822nd and 811th amino acid, respectively. Numberings correspond to the UniProt entries (UniProt Consortium, 2012).

binding to Apaf-1 CARD, thus inhibiting apoptosis (Seol and Billiar, 1999; Srinivasula *et al*, 1999; Wang *et al*, 2006). It was shown, using classical RT-PCR, that the ratio of caspase-9-α/caspase-9-β mRNAs is decreased in a high proportion of NSCLCs compared to non-transformed cells (Shultz *et al*, 2010). Protein kinase B (PKB, Akt), which is frequently constitutively active in NSCLC (Brognard *et al*, 2001; Balsara and Mitsuuchi, 2004), phosphorylates the SRp30a splicing factor, which contributes to procaspase-9 pre-mRNA splicing to caspase-9-β mRNA and seems to produce an anti-apoptotic phenotype of NSCLC cell lines (Shultz *et al*, 2010). Interestingly, in some cancer cells, chemotherapeutic agents are able to indirectly change, via the apoptotic inducer ceramide, the caspase-9-α/caspase-9-β ratio in favour of caspase-9-α expression, through regulating the transactivating factors responsible for alternative pre-mRNA splicing (Chalfant *et al*, 2002; Massiello *et al*, 2006, Schultz *et al*, 2011). These results suggest usage of PKB inhibitors next to chemotherapy to treat NSCLC. However, apoptosome pathway dysregulation at the protein level might also play a role in NSCLC chemotherapy resistance.

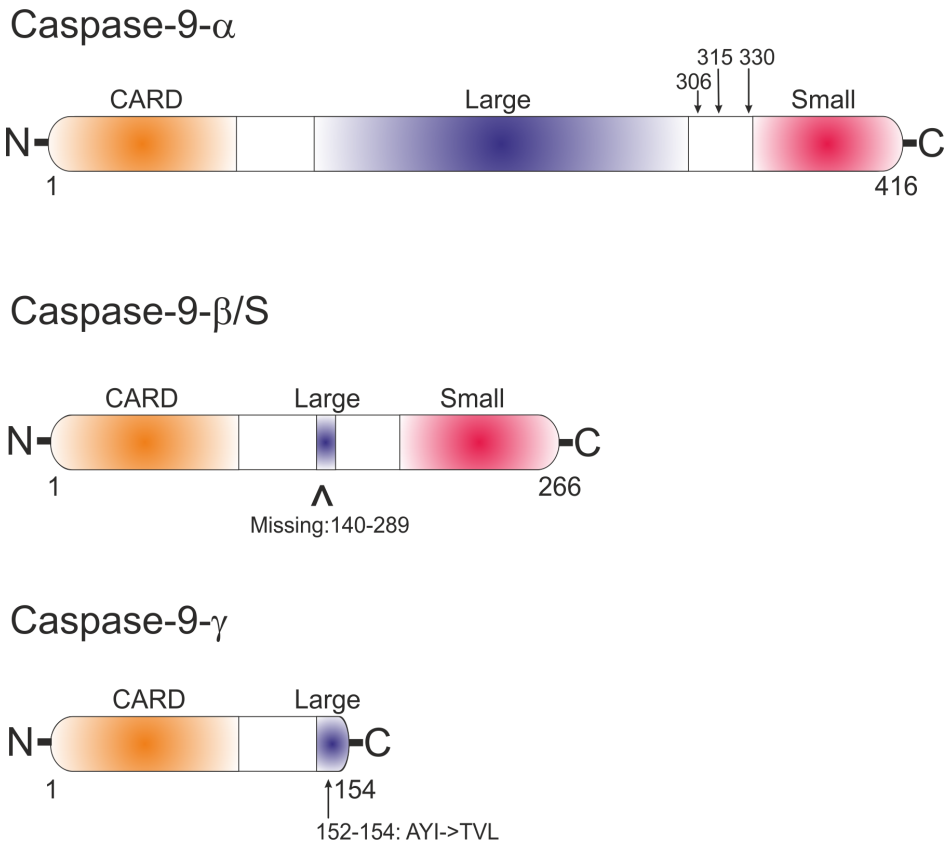

Figure 3: Expression of human caspase-9 protein isoforms.
CARD (orange), large (violet) and small (red) domains are indicated. Arrows show the positions of the cleavage sites in the linker region: autocatalytic (D315) and caspase-3 (D330). The position of the minor autocatalytic cleavage site (G306) is also shown. Caspase-9-α is a full-length procaspase-9 protein consisting of 416 amino acid residues (46 kDa). In caspase-9-β/S, the sequence of 150 amino acids is missing after the 139^{th} amino acid. In caspase-9-γ the 152^{nd}-154^{th} amino acids (AYI) are substituted for TVL and the 155^{th}-416^{th} amino acid sequence is missing. Numberings correspond to the UniProt entries (UniProt Consortium, 2012).

1.2.2 Posttranslational regulation of apoptosome apparatus assembly and function

Localization and covalent modifications of apoptosome apparatus components

The subcellular fractionation and microscopic studies showed, that Apaf-1 is located in the cytoplasm (Hausmann *et al*, 2000). Interestingly, in Burkitt lymphoma cells, Apaf-1 molecules were found anchored in lipid rafts or in cholesterol-rich vesicles near plasma membrane, and the lack of cytosolic Apaf-1 was responsible for chemoresistance of these cells (Sun *et al*, 2005). Although lipid rafts disruption liberated Apaf-1 and sensitised Burkitt lymphoma cells *in vitro*, it remains unclear whether ectopic localization of apoptosome apparatus components contribute to chemoresistance *in vivo* and in other types of cancer cells.
Protein phosphorylation is a common mechanism for posttranslational regulation of variety of apoptotic but also non-apoptotic factors. On one hand, phosphorylation of a particular

protein can activate, or, on the other hand, inhibit its function. Both core apoptosome components were shown to undergo this modification and if phosphorylated at specific site, the activity of AA component is either suppressed, or activated. It was shown, that Apaf-1 can be phosphorylated by the ribosomal S6 kinase which is highly active in some cancer cells. Phosphorylated S268 together with the flanking amino acids on Apaf-1 form a docking site for a small adaptor molecule 14-3-3ϵ which impede the interaction between cyt-c and Apaf-1, thereby inhibiting Apaf-1 oligomerization (Kim *et al*, 2012).

On the other hand, caspase-9 is a target substrate of several protein kinases (PK). The phosphorylation at three single sites, T125, S144 or S196, was shown to suppress procaspase-9 activation at apoptosome. Of note, PKB-α/Akt, which is frequently upregulated in cancer cells (Massion *et al*, 2004), can phosphorylate procaspase-9 at S196 and thereby inhibits its apoptosome-mediated activation (Cardone *et al*, 1998). Interestingly, phosphorylation of the adjacent site, S195, as well as S99 and S183, by PKA, a constitutively active cAMP-dependent PK in some cancer cells, has no effect on procaspase-9 activation (Martin *et al*, 2005).

Likewise, PKC-γ can phosphorylate procaspase-9 at the S144 site (Brady *et al*, 2005). Frutos and colleagues demonstrated, that upon UV-irradiation of HeLa cells, the caspase-3-generated (PKC)- fragment is enzymatically inactive, thus this mechanism serves as prevention of caspase-9 inhibition (Frutos *et al*, 1999).

The major site of caspase-9 that can be phosphorylated is T125. T125 is a target of 4 kinases: CDK1 (cycline-dependent kinase-1), Erk (extracellular signal-regulated kinase), DYRK-1A (dual-specificity tyrosine-phosphorylation-regulated kinase A1) and p38 MAPK (p38 mitogen-activated protein kinase) (Allan *et al*, 2003; Allan and Clarke, 2007; Yoo *et al*, 2007; Seifert and Clarke, 2009).

T125 site of caspase-9 was shown by immunohistochemistry to be phosphorylated in more than half of the 60 studied gastric adenocarcinomas (Yoo *et al*, 2007). However, this finding did not correlate with invasion and metastasis nor stage of the carcinomas, thus suggesting that inhibition of procaspase-9 activation by T125-phosphorylation might play a role in tumour growth.

On the other hand, caspase-9 activity can be positively regulated by c-Abl kinase, which phosphorylates caspase-9 at Y153 upon DNA damage (Raina *et al*, 2005).

Except phosphorylation, proteolytic modification of AA components was shown to affect their function. Once the apoptosome-associated caspase-9 p35/p12 form proteolytically converts procaspase-3 to active caspase-3, the active caspase-3 can cleave both the procaspase-9 monomer at D330 and the N-terminus of the caspase-9 small subunit p12 at D330 as well, thereby removing the intersubunit linker peptide, which results in generation of caspase-9 p37/p10 and caspase-9 p35/p10 forms, respectively (Zou *et al*, 2003). This cleavage removes the ATPF sequence motif from the N-terminus of the caspase-9 small subunit p12 that is needed for caspase-9 inhibition by XIAP (Zou *et al*, 2003; Denault *et al*, 2007). Furthermore, it was shown, that Apaf-1 monomer is also the proteolytic target of the active caspase-3 (Bratton *et al*, 2001a, Lauber *et al*, 2001).

Interestingly, Apaf-1 monomer is cleaved by active caspase-3 resulting in partial removal of

the CARD and WD-40 repeats. The resulted 84 kDa Apaf-1 is able to oligomerize into a 400 kDa Apaf-1 heptamer in the absence of cyt-c due to lacking the WD-40 repeats but cannot associate with procaspase-9 due to the partial removal of CARD. This feedback mechanism of degradation of Apaf-1 may decrease or cease the propagation of the death signal in cancer cells (Lauber *et al*, 2001). Moreover, Apaf-1 can also be cleaved within its NBOD domain. In this case, the resulting p30 fragment can interact with the proteolytically inactive 1.4 MDa apoptosome (Bratton *et al*, 2001a).

APIP

The Apaf-1-interacting protein (APIP) is an endogenous competitive inhibitor of apoptosome-mediated procaspase-9 activation (Cao *et al*, 2004b; Cho *et al*, 2004). It was found, that under ischemic condition, APIP is highly expressed in skeletal muscle, heart and neurons and prevents them from ischemic damage by caspase-9-mediated apoptosis inhibition (Cao *et al*, 2004b, Cho *et al*, 2004). NSCLC tumour microenvironment also contains ischemic regions characterized by hypoxia and acidosis (Graves *et al*, 2010). Therefore, APIP might play a role in suppression of apoptosome pathway in NSCLC tumours.
Cell death suppressing effects of APIP were evident in primary neuronal cultures PC12 or human 293 cell lines when transfected with APIP cDNA. APIP acts only during the action of apoptosis stimuli, downstream of cyt-c release, when Apaf-1 CARD becomes accessible for APIP binding and negatively competes with procaspase-9 recruitment to AA (Cao *et al*, 2004b). Moreover, under ischemic conditions, APIP induces and sustains the activation of Akt and ERK1/2 kinases, which phosphorylate procaspase-9, thus inhibiting its AA-mediated activation (Cho *et al*, 2007). Recently, APIP has been shown to be identical with 5'-methylthioribulose-1-phosphate dehydratase (EC: 4.2.1.109) (Mary *et al*, 2012), an enzyme that is involved in the methionine salvage pathway, and its reduced expression was associated with increased sensitivity to the chemotherapeutic agent carboplatin (Ko *et al*, 2012).

UACA

Uveal autoantigen with coiled-coil domains and ankyrin repeats (UACA) (Yamada *et al*, 2001) or nucling (Sakai *et al*, 2003) is a proapoptotic factor that plays a role in the regulation of proapoptotic and nuclear factor-κB (NF-κB) signaling (Sakai *et al*, 2003; Sakai *et al*, 2004; Liu *et al*, 2009). Proapoptotic stimuli such as treatment with adriamycin or heat shock upregulate nucling expression (Sakai *et al*, 2004). It was shown, that nucling associates with and stabilizes the apoptosome complex components *in vivo* and promotes caspase-dependent cell death (Sakai *et al*, 2004). Moreover, nucling induces Apaf-1 expression and its translocation into the nucleus (Sakai *et al*, 2004). On the other hand, nucling deficient cells are resistant to Apaf-1 upregulation and procaspase activation upon cellular stress from UV radiation (Sakai *et al*, 2004). Apaf-1 and procaspase-9 expressions are down-regulated in nucling-deficient mice after MPTP neurotoxin administration (Teng *et al*, 2006). Moreover, nucling interaction with NF-κB p50 and p65 subunits prevents its nuclear translocation and

thus reduces expression of NF-κB-targeted genes, which products might support cell survival (Liu *et al*, 2004; Liu *et al*, 2009).

PHAP molecules

Putative HLA-DR associated proteins (PHAPs) have a role as tumour suppressors to inhibit cell growth (Bai *et al*, 2001). PHAPI is overexpressed in some cancers (Schafer *et al*, 2006) but decreased expression was observed during cancer progression (Brody *et al*, 2007). Upon apoptosis induction, PHAPI translocates from nucleus into the cytosol (Mazroui *et al*, 2008), where it accelerates caspase-9 activation (Jiang *et al*, 2003; Schafer *et al*, 2006) or restores the resistance to the (cyt-c+dATP)-induced caspase activation (Hoffarth *et al*, 2008). PHAPI, together with the cellular apoptosis susceptibility (CAS) protein and heath shock protein 70 (HSP70), may act as a complex cofactor for the nucleotide exchange that is essential for Apaf-1 activation (Kim *et al*, 2008), or by antagonizing prothymosin-α (ProT), an oncoprotein negatively regulating apoptosome formation and activation of caspase-3 in cancer cells (Jiang *et al*, 2003) by binding to Apaf-1 protein (Qi *et al*, 2010). PHAPI also enhances the activity and stability of active caspase-3 (Hill *et al*, 2004).

Inhibitor of apoptosis proteins

The inhibitor of apoptosis proteins (IAP) family members share a common structural motif, the baculovirus inhibitor of apoptosis protein repeat (BIR), first identified in baculoviruses. The human IAP family includes eight members: NAIP (BIRC1), cIAP1 (BIRC2), cIAP2 (BIRC3), XIAP (BIRC4), survivin (BIRC5), apollon (BIRC6), livin (BIRC7) and ILP-2 (BIRC8). IAPs are involved in various cellular functions, such as apoptosis, cell-division, non-apoptotic signal transduction and copper homeostasis (LaCasse *et al*, 2008; Srinivasula *et al*, 2008). IAPs suppress apoptosis by blocking procaspase-9 and -8 activation (Marusawa *et al*, 2003; Broemer and Meier, 2009), by blocking caspase-9, -3, -7 activity (Srinivasula *et al*, 2001; Shiozaki *et al*, 2003; Scott *et al*, 2005; Dohi *et al*, 2004; Eckelman *et al*, 2006), or by acting as ubiquitin E3 ligases, due to the presence of the really interesting new gene (RING) domain, and thereby promoting caspase-9, -3, and -7 proteosomal degradation (Suzuki *et al*, 2001; Astier *et al*, 2004; Hao *et al*, 2004; Morizane *et al*, 2005; Choi *et al*, 2009; Mace *et al*, 2010). Some members of the IAP family were proved to transfer the ubiquitin molecules to mitochondrial proapoptotic proteins Smac (Martinez-Ruiz *et al*, 2008) and Htra2 (Vande Walle *et al*, 2008), and thus promote their degradation. In addition, cIAP1, cIAP2 and XIAP are involved in activation of NF-κB signaling pathway, which may lead to generation of prosurvival signals in cancer cells (Damgaard *et al*, 2011; Darding and Meier, 2012).
The most studied IAPs are XIAP, for its ability to inhibit caspase activity directly (Eckelman *et al*, 2006), and survivin, which is currently studied as a therapeutic target due to its increased expression in the vast majority of cancers over normal cells (Duffy *et al*, 2007; Altieri, 2012; Chen *et al*, 2012; Khan *et al*, 2012). The overexpression of both, XIAP and survivin is linked with the apoptosis suppression in some cancer cells (Dohi *et al*, 2004; Galban *et*

al, 2009; Chen *et al*, 2012) as well as with chemotherapy- and radiation-induced apoptosis resistance in NSCLC (Hu *et al*, 2003; Cao *et al*, 2004a; Lu *et al*, 2004; Dong *et al*, 2006). These antiapoptotic functions of XIAP and survivin suggest that they might contribute to tumourigenesis and NSCLC progression.

2 Aims of the Thesis

Although non-small cell lung carcinoma (NSCLC) cells express the key cytosolic components of apoptosome apparatus (AA) (Apaf-1, procaspase-9) and its main effector procaspase-3, the activatability or the functionality of the apoptosome apparatus often fails. To date, numerous negative regulators of the assembly or the function of the apoptosome have been described. However, the mechanism of endogenous dysfunction of AA in non-small cell lung carcinoma still remains elusive.

The aims of the thesis were to analyse the expression and activity of molecular factors that might regulate the initiation or the course of the apoptosome cascade in NSCLC cells and tissues of various histopathological types.

The specific aims of this thesis were:

- Analysis of expression status of survivin, HBXIP, APIP - factors blocking the apoptosome assembly, in NSCLC tissues and cells
- Analysis of expression status of XIAP - factor inhibiting the proteolytic activity of the apoptosome apparatus, in NSCLC tissues and cells
- Analysis of expression status of nucling/UACA - factor responsible for translocation of AA and Apaf-1 into the nucleus, in NSCLC tissues and cells
- Analysis of DNA methylation involvement in the expression of Apaf-1, procaspase-9 and procaspase-3 mRNAs in NSCLC cells
- Analysis of expression status of Apaf-1 mRNA variants -XL/-LC and -LN/-S in NSCLC tumours and lungs
- Analysis of expression status of procaspase-9 and caspase-9S mRNAs in NSCLC tumours and lungs
- Analysis of apoptosome functionality in NSCLC tissues and cells
- Analysis of apoptosome assembly in NSCLC cells

3 Materials and Methods

3.1 Reagents

Most reagents used in this study were obtained from suppliers as described previously (Moravcikova *et al*, 2012; Krepela *et al*, 2009; Krepela *et al*, 2004). Sephacryl S300HR, Gel Filtration Molecular Weight Markers (cat. no MW-GF-1000), bovine serum albumin (BSA; cat. no A7030), the affinity purified rabbit anti-caspase-3 and rabbit anti-Apaf-1 antibodies (cat. no C9598 and A8469, respectively), and the goat anti-rabbit IgG horseradish peroxidase (HRP) conjugate (cat. no A4914), used as a secondary antibody, were from Sigma (St. Louis, MO, USA). The rabbit anti-caspase-9 antibody was from Cell Signaling (Danvers, MA, USA, cat. no 9502). The prestained Precision Plus Protein Standards and Blotting-Grade Blocker (BGB) were from Bio-Rad Laboratories, Hercules, CA, USA. The Smac mimetic peptides AVPIAQK (P1) and ATPFQEG (P2) were custom synthesised by Clonestar Peptide Services (Brno, Czech Republic). The gene-specific oligonucleotide primers and TaqMan probes were custom synthesised as indicated below in section 3.10.

3.2 Patients and tissues

NSCLC tissues and matched lung parenchyma were obtained after surgery from 62 lung cancer patients, who did not receive radiotherapy nor chemotherapy before surgery. Tissue samples of approximately 1 g (wet mass) of primary lung tumours and non-tumourous lung parenchyma were excised from non-necrotic part of the tumour and from the lung parenchyma at a site located as distantly as possible from the tumour immediately after resection of the lung or lung lobe containing the tumour. The samples were snap-frozen in liquid nitrogen and stored at -78°C until analysis. The following histopathological types of NSCLC tumours were included into the study: squamous cell lung carcinoma (SQCLC), lung adenocarcinoma (LAC), large cell lung carcinoma (LCLC), sarcomatoid lung carcinoma (SLC), undifferentiated lung carcinoma (UNDIF) and mixed type SQCLC + LAC. The histopathological typing of the tumours was carried out according to the World Health Organization criteria (Travis *et al*, 2004; Beasley *et al*, 2005). Written informed consent was obtained from each NSCLC patient before entry to the study. The study was approved by the local institutional ethical committee and was conducted in accordance with the Declaration of Helsinki.

3.3 Cell lines

NSCLC cell lines investigated in this study included SQCLC-derived cell lines CALU-1, NCI-H520 and SKMES-1, LAC-derived cell lines A549, SKLU-1, LXF-289 and COLO-699, and LCLC-derived cell lines COR-L23, LCLC-103H and NCI-H1299. CALU-1, SKMES-1, A549, SKLU-1 and COR-L23 cells were obtained from the European Collection of Cell Cultures, Salisbury, UK. LXF-289, COLO-699 and LCLC-103H cells were from German Collection of Microorganisms and Cell Cultures, Braunschweg, Germany, and NCI-H520, NCI-H1299 cells, and HeLa S3 and HEK289 cells were from the American Type Culture Collection, Rockville, MD, USA. Cell lines were cultured in humidified atmosphere of 5% CO_2 and air at 37°C in the Eagles minimum essential medium supplemented with 2 mM L-glutamine, 26.2 mM $NaHCO_3$, 1% of a stock solution of non-essential amino acids, 10 mg/l apotransferrin, 0.25 μM $Fe(NO_3)_3$, 5% foetal bovine serum, 10^5 IU/l of penicillin-G and 100 mg/l of streptomycin. After reaching confluence, the cells were harvested and used for preparation of cell-free cytosols or detergent-containing extracts or RNA.

3.4 Preparation of protein extracts and total protein determination

Adherent NSCLC cells growing in monolayer were scraped into the Ca^{2+}- and Mg^{2+}-free Hanks' balanced salt solution and sedimented by centrifugation at 240 g and 4°C for 10 min. The harvested cells were disrupted by sonication, at 0-4°C, in phosphate buffered saline, pH 7.2, containing 0.5% Triton X-100 and a mixture of proteinase inhibitors including 1 mM Na_2EDTA, 50 μM E-64, 200 μM AEBSF and 25 μM pepstatin. The cell homogenates were centrifuged at 40 000 g and 4°C for 30 min. The collected supernatants, *i.e.* protein extracts, were stored in small aliquots at -78°C until analysis. Total protein concentration was determined by the bicinchoninic acid assay using bovine serum albumin (BSA) as a standard (Smith, 1985).

3.5 Preparation of cytosol samples

Unless otherwise indicated, the following preparations of cell-free and tissue cytosols were performed at 0-4°C. Cells at confluence were washed and gently scraped into a Hanks balanced salt solution (HBSS) containing 4.16 mM $NaHCO_3$. Subsequently, cells were centrifuged at 300g for 10 min and the pellets was resuspended in 1/4-1/2 volume of ice-cold 25 mM HEPES/NaOH - 4 mM Na_2EDTA - 1.5 mM $MgCl_2$ - 10 mM KCl buffer, pH 7.4 (HEMK buffer). After 30-minute of gentle shaking, the cells were disrupted using wholeglass Dounce homogenizer fitted with the pestle B. The homogenates were centrifuged at 200000g for 60 minutes and the supernatants, *i.e.* cell-free cytosols, were collected and stored in small aliquots at -78°C until analysis. To prepare tissue cytosols, the samples of NSCLC tissue and lung parenchyma, prefrozen in teflon containers together with a small stainless steel ball using solid CO_2, were deep frozen using three cycles of liquid nitrogen bathing and were

pulverized by horizontal shaking for 30 seconds at 30 s^{-1} on Mixer Mill MM 200 (Retsch, Haan, Germany). The tissue powder was resuspended in HEMK buffer (1.5 ml per 1 g of wet tissue) and shaked on ice for 30 minutes. The suspensions were then homogenized three times for 5 seconds using Ultra-Turrax T25 (IKA, Staufen, Germany) homogenizer at 24000 rpm. The homogenate was centrifuged at 200000g for 60 minutes and the supernatant, *i.e.* tissue cytosol, was collected, aliquoted and stored at -78°C until analysis.

3.6 Apoptosome apparatus activation and assay of caspase-3-like activity

In order to activate AA, cytosol samples (150 μl), containing 2.5 mg of total protein/ml in HEMK buffer with 5 mM D,L-dithiothreitol (DTT), were preincubated with 10 μM of cyt-c and 1 mM of dATP at 37°C for 30 min. When analysing the effect of the Smac mimetic peptides, AVPIAQK and ATPFQEG, each peptide was added to the reaction in a final concentration of 500 μM. Cytosol samples preincubated without cyt-c and dATP were used as controls. Subsequently, aliquots of the preincubation mixtures (20 μl) were used for measurement of the endogenous (in the controls) and the (cyt-c+dATP)-induced caspase-3-like activity, using a continuous assay. The enzyme reactions, carried out in a total volume of 200 μl at 37°C and in duplicate, were done with 100 μM of Ac-DEVD-AFC as a substrate in an assay buffer containing 50 mM HEPES/NaOH, 1.63 mM CHAPS, 1 mM Na2EDTA, 292 mM sucrose, 100 mM NaCl, and 5 mM DTT, pH 7.20. Further control reactions, run in parallel, were performed in the presence of 10 μM of a caspase inhibitor Ac-DEVD-CHO. The fluorescence of the enzymatically released 7-amino-4-trifluoro-methylcoumarin (AFC) was measured on a microplate fluorometer SpectraFluor (TECAN, Salzburg, Austria). The caspase activity was calculated from the progress curves in steady state and was expressed in nkat or pkat per 1 mg of total protein.

3.7 Gel filtration chromatography

For the study of the apoptosome apparatus assembly, samples of cell-free cytosol from COLO-699, CALU-1 and A549 cells (5 mg of total protein/ml) were preincubated in HEMK buffer with 5 mM DTT in the presence or absence of cyt-c (10 μmol/l) and dATP (1 mmol/l) at 37°C for 30 min. Subsequently, the samples were fractionated by gel filtration chromatography on a column (70 x 1.6 cm) of Sephacryl S300HR at 2 - 4°C. The column was equilibrated and eluted with a buffer containing 25 mM HEPES/NaOH, 1 mM Na2EDTA, 1.5 mM $MgCl_2$, 10 mM KCl, 1 mM DTT, and 100 mM NaCl, pH 7.2. The elution rate was 0.5 ml/min and 0.5-ml fractions were collected. Aliquots of collected fractions were denatured in a sample buffer and were subjected to SDS-PAGE followed by Western blot analysis (see below). In some experiments, the samples of cell-free cytosol were not preincubated before loading onto the chromatographic column. The column was calibrated with Blue Dextran 2000, M_r of 2 x 10^6, and six different protein M_r-markers: thyreoglobulin, M_r of 669000, ferritin, M_r

of 440000, β-amylase, M_r of 200000, alcohol dehydrogenase, M_r of 150000, albumin, M_r of 66000, and carbonic anhydrase, M_r of 29000.

3.8 SDS-PAGE and immunoblotting ECL

The assembly of the apoptosome apparatus and the processing of procaspase-9 and -3 in the control and the (cyt-c+dATP)-induced cytosols without or with the caspase inhibitor Ac- DEVD-CHO in the cell-free cytosols were investigated by SDS-polyacrylamide gel electrophoresis (PAGE) and immunoblotting using specific antibodies. Prior loading onto SDS-polyacrylamide gels, the samples for SDS-PAGE were denatured by 5 min boiling in a sample buffer, pH 7.4, containing 2% SDS, 0.01% Serva Blue G, 50 mM Tris/HCl, 100 mM DTT, and 10% glycerol. The samples (50 μg of total protein) were gel-loaded in parallel with prestained protein Mr markers. When the proteolytic processing of procaspase-9 was studied, the samples of cytosols were subjected to the following treatments before boiling in the SDS-PAGE sample buffer. Cytosol samples (5 mg of total protein/ml) were preincubated at 37°C for the indicated times without or with cyt-c + dATP (10 μM and 1 mM, respectively) in HEMK buffer, pH 7.4, with 5 mM DTT. Where indicated, the caspase inhibitor Ac-DEVD-CHO (1 μM) was added into the preincubated sample. For analysis of caspases and Apaf-1, SDS-PAGE was carried out in 16.5% T/3% C and 8% T/3% C SDS-polyacrylamide gels, respectively, using the Tris-Tricine-SDS buffer system (Schgger and von Jagow, 1987). The separated proteins were electrotransferred to Hybond-P PVDF membrane sheets (GE Healthcare, Little Chalfont, UK) using a transfer buffer (48 mM Tris, 39 mM glycine, 1.3 mM SDS, 20% methanol, pH 9.2). The lateral parts of the membrane with Mr-marker proteins were cut off and dried. In order to visualize the protein(s) in question, the central part of the membrane was processed at room temperature by an immunoblotting procedure coupled to an enhanced chemiluminescence (ECL) detection system. Briefly, unless stated otherwise, the treatment steps were carried out at room temperature and included: blocking with 5% BGB and 1% BSA in TBST buffer (20 mM Tris/HCl - 100 mM NaCl - 0.1 v/v% Tween 20, pH 7.6) for 1 h, incubation with anti-Apaf-1 and anti-caspase-3 antibody for 2 h or with anti-caspase-9 antibody overnight at 4°C, extensive washing in TBST buffer, incubation with the secondary HRP-conjugated antibody (at a dilution of 1:10 000 in 5% BSA in TBST buffer) for 1 h, extensive washing in TBST buffer, incubation with the ECL Plus Reagent (GE Healthcare) for 5 min, and capture of the chemiluminiscence signal onto the BioMax Light-1 film (Eastman Kodak, Rochester, NY, USA). The film immunograms and the Hybond-P membrane strips with the transferred Mr-marker proteins were scanned on a desktop scanner and the images were processed with 1D Image Analysis Software (Eastman Kodak). The net intensity data (*i.e.* the sum of the background-subtracted pixel values in the 8-bit grey scale) of specific protein bands were used for the evaluation of relative protein expression.

3.9 Isolation and quantification of total RNA

Total RNA was isolated from tumour and lung tissue samples and cultured NSCLC cell lines using the Trizol Reagent according to the manufacturer's instructions. Spectrophotometric analysis, which was carried out in 10 mM Tris/HCl buffer, pH 7.5, revealed that all samples of total RNA had an A_{260}nm/A_{280}nm ratio >1.8. The concentration of total RNA was determined by fluorometry using the RiboGreen RNA Quantitation Kit (Molecular Probes) according to the manufacturer's protocol. The preparations of total RNA in RNase-free water were stored in small aliquots at -78°C until analysis.

3.10 Real-time RT-PCR analysis

The sequences and final concentrations of the oligonucleotide primers and probes used in real-time RT-PCR assays of expression of the investigated transcripts are indicated in Table 1. The concentrations of primers and TaqMan probes adopted for real-time RT-PCR quantitation of each studied transcript were determined in optimization experiments. The primers and probes were designed with the program Primer Express (Applied Biosystems) and were synthesized at Proligo (Paris, France) or Microsynth (Balgach, Switzerland) and Applied Biosystems (Warrington, Cheshire, UK), respectively. The expression of Apaf-1XL/LC, Apaf-1S/LN, procaspase-9, caspase-9S, survivin and HBXIP mRNAs was quantitated by a two-step (uncoupled) real-time RT-PCR assay as follows. In the first step, 2 μg of total RNA was reverse transcribed in a total volume of 20 μl of 50 mM Tris/acetate buffer, pH 8.4, containing 75 mM of potassium acetate, 8 mM of magnesium acetate, 500 nM of the gene-specific reverse primer (Table 1), 200 nM of each dGTP, dCTP, dATP and dTTP, 5 mM dithiothreitol, 40 units of RNase inhibitor RNAseOUT (Invitrogen) and 15 units of ThermoScript Reverse Transcriptase (Invitrogen). The RT reaction was carried out at 58°C for 30 min and was terminated by heating at 85°C for 10 min. The resulting RT mixes were stored at -25°C until PCR analysis. The PCR step was carried out in a total volume of 50 μl, using 20 mM Tris/HCl buffer, pH 8.4, containing 50 mM of KCl, 1.85 mM of $MgCl_2$, 220 nM of each dGTP, dCTP, dATP and dTTP, the indicated concentrations of gene-specific forward and reverse primers and TaqMan probe (Table 1), 2 units of Platinum Taq DNA polymerase (Invitrogen), and 2 μl of the RT mix (representing an equivalent of an input of 200 ng of total RNA). The PCR amplification included a hot start at 95°C for 3 min and 45 cycles of denaturation at 95°C for 15 sec and of annealing/extension at 58°C for 1 min. The expression of XIAP, APIP and UACA mRNAs was quantitated by a coupled real-time RT-PCR assay. The RT-PCR reaction mixtures of a total volume of 50 μl contained 25 μl of SuperScript Reaction Mix (a buffer with 6 mM $MgSO_4$ and 400 nM of each dGTP, dCTP, dATP and dTTP) or ThermoScript Reaction Mix (a buffer with 3 mM $MgSO_4$ and 200 nM of each dGTP, dCTP, dATP and dTTP) and 1 μl of SuperScript III Reverse Transcriptase/ Platinum Taq DNA Polymerase Mix or ThermoScript Plus Reverse Transcriptase/Platinum Taq DNA Polymerase Mix, the respective primers and TaqMan probe at the indicated final

Table 1: Primers and TaqMan probes used for real-time RT-PCR quantitation of expression of the investigated transcripts.

Human Transcript	GeneBank Accession No.	Sequences of primers and TaqMan probes		Final concentration
Apaf-1-XL and -LC	NM_181861	Forward primer:	5'-CTTCTCCCCACAAAACCATTT-3'	200 nM
	NM_013229	Reverse primer:	5'-GACCTGTTCTTCCATTAATGAGTTG-3'	200 nM
		TaqMan probe:	5'-(6-FAM)ATGGTCAACTGCAAGGACCATCACTTCA(TAMRA)-3'	200 nM
Apaf-1-LN and S	NM_181868	Forward primer:	5'-TAAAATCTTTTTGTGGAATACAGACTCA-3'	200 nM
	NM_001160	Reverse primer:	5'-AGTCAGATAATCAATCTGACCTGTTCT-3'	200 nM
		TaqMan probe:	5'-(6-FAM)ATGGTCAACTGCAAGGACCATCACTTCA(TAMRA)-3'	200 nM
Procaspase-9	NM_001229	Forward primer:	5'-CGTGGTGGTCATTCTCTCTCA-3'	400 nM
		Reverse primer:	5'-CTGTGGTGGGGAGCAGAA-3'	400 nM
		TaqMan probe:	5'-(6-FAM)TCACAATCTTCTCGACCGACACAGGG(TAMRA)-3'	200 nM
Caspase-9S	NM_032996	Forward primer:	5'-ATGCTGGCTTCGTTTCTGC-3'	400 nM
		Reverse primer:	5'-GGTCTTTCTGCTCGACATCAC-3'	400 nM
		TaqMan probe:	5'-(6-FAM)CAGCAAAGTTGTCGAAGCCAACCCTAG(TAMRA)-3'	200 nM
Survivin	NM_001168	Forward primer:	5'-GACGACCCCATAGAGGAACATA-3'	400 nM
		Reverse primer:	5'-TTTCCTTTGCAATTTTGTTCTTG-3'	400 nM
		TaqMan probe:	5'-(6-FAM)CCGGTTGCGCTTTCCTTTCTGTCA(TAMRA)-3'	200 nM
HBXIP	NM_006402	Forward primer:	5'-AGCACTTGGAAGACACAATGAAG-3'	400 nM
		Reverse primer:	5'-GTTTCTGGATCATAATGTTCCCAT-3'	400 nM
		TaqMan probe:	5'-(6-FAM)CCGCGGGACCCTGTCAGATGA(TAMRA)-3'	200 nM
XIAP	U45880	Forward primer:	5'-TCCAGAATGGTCAGTACAAAGTTG-3'	200 nM
		Reverse primer:	5'-TTTGTTGAATTTGGGAAATTCCT-3'	200 nM
		TaqMan probe:	5'-(6-FAM)CACTTCGAATATTAAGATTCCGGCCCA(TAMRA)-3'	200 nM
APIP	NM_015957	Forward primer:	5'-GGAACGAATTCAGCCTGAAG-3'	400 nM
		Reverse primer:	5'-CACCTGCTCCTCTCATTGTGT-3'	400 nM
		TaqMan probe:	5'-(6-FAM)AAGGACATAAGTGGACCTTCGCCATCG(TAMRA)-3'	200 nM
UACA	NM_006402	Forward primer:	5'-CATCCTTATACATGGAGTTGATATTACAA-3'	400 nM
		Reverse primer:	5'-TGTCCGCCCGTCTACATC-3'	400 nM
		TaqMan probe:	5'-(6-FAM)CTGCACTTCACGATGCCGCAATG(TAMRA)-3'	200 nM
β-Actin	NM_001101	Forward primer:	5'-CTGGCACCCAGCACAATG-3'	200 nM
		Reverse primer:	5'-GGGCCGGACTCGTCATAC-3'	200 nM
		TaqMan probe:	5'-(VIC)AGCCGCCGATCCACACGGAGT(TAMRA)-3'	200 nM

concentrations (Table 1), 40 units of an RNase inhibitor RNaseOUT (Invitrogen), and 200 ng of total RNA. The reverse transcription was carried out at 58°C for 30 min and the subsequent PCR amplification included a hot start at 95°C for 5 min, 45 cycles of denaturation at 95°C for 15 sec and of annealing/extension at 58°C for 1 min.
The expression of β-actin mRNA (an internal reference transcript) was quantitated in parallel to the indicated target transcripts either by the two-step or by the coupled real-time RT-PCR assay as described above. The respective gene specific forward and reverse primers and TaqMan probe and their concentrations in the PCR assays were as indicated in Table 1. The real-time RT-PCR assays were run in triplicate or duplicate in MicroAmp Optical 96-well Reaction Plates on the ABI PRISM 7700 Sequence Detection System (SeDeS) operated from within the SeDeS software (all from Applied Biosystems). The threshold cycle (C_T) values of the amplification reactions, represented by the plots of background subtracted fluorescence intensity (ΔFI) of the reporter dye (6-FAM or VIC) against PCR cycle number, were determined with the SeDeS software. The tumour/lung ratio of the β-actin mRNA-normalised target transcript expression was calculated by means of the $2^{-\Delta C_T}$ method (Livak and Smittgen, 2001), and the statistical difference of the β-actin mRNA-normalised target transcript expression in tumours and lungs was calculated from the linearized ΔC_T data (*i.e.* $2^{-\Delta C_T}$) (Krepela *et al*, 2006).

3.11 Effect of treatment of NSCLC cell lines with 5-aza-2'-deoxycytidine on target transcript expression

NSCLC cell lines were cultured with or without 10 μM of 5-aza-2'-deoxycytidine (decitabine) for 72 hours. Cells were then lysed in Trizol reagent and total RNA was isolated. Subsequently, the expression of Apaf-1 (variants XL and L), procaspase-9 and procaspase-3 mRNAs (target transcripts) and β-actin mRNA (an endogenous reference transcript) was quantitated using real-time RT-PCR. The statistical difference of the β-actin mRNA-normalized target transcript expression in the decitabine-treated and -untreated tumour cells was calculated from the linearized ΔC_T data. A two-sided P-value lower than 0.05 was considered as statistical significant difference.

3.12 Statistical analysis

The statistical analysis was performed using the software SigmaStat (Systat Software, Point Richmond, CA, USA) and Stat200 (Biosoft, Cambridge, UK). A two-sided P-value lower than 0.05 was accepted as statistically significant difference.

4 Results

4.1 Expression status of survivin, HBXIP, XIAP, APIP and UACA and their clinicopathological implications

To analyse the expression status of AA regulators, survivin, HBXIP, XIAP, APIP and UACA mRNAs in NSCLC tumours and lungs, we quantitated the level of these transcripts and of an endogenous reference transcript, β-actin mRNA, by means of real-time RT-PCR.

Using the uncoupled (two-step) real-time RT-PCR assay, there was no significant difference between the expression levels of β-actin mRNA (2^{-C_T}data) in NSCLC tumours of different histopathological types and matched lungs ($P > 0.1$; Mann-Whitney test). Using the coupled real-time RT-PCR assay, the expression of β-actin mRNA (2^{-C_T} data) was slightly and significantly higher in SQCLC and LAC tumours as compared to matched lungs ($P < 0.05$, Mann-Whitney test).

Survivin and *XIAP* genes were strongly expressed in the studied NSCLC cell lines at both the mRNA and protein levels (Figure 4).

The expression of survivin mRNA was significantly higher in NSCLC tumours of different histopathological types as compared to matched lungs (Figure 5A). In fact, more than tenfold higher level of survivin mRNA was observed in 96 (64%) of 150 examined NSCLC tumours as compared to the lungs. Importantly, the expression of survivin protein was also highly

Table 2: Immunometric analysis of survivin protein expression in NSCLC tumours and lungs.

Tumour type	n	Survivin protein expression (ng/mg of total protein)[b]		Statistical difference (P) of survivin protein expression in Tu *versus* Lu[c]	Tu/Lu ratio of survivin protein expression[b]	Number of patients with Tu/Lu survivin protein expression ratio ≥ 2 and ≤ 0.5
		Tumours (Tu)	Lungs (Lu)			
NSCLC	88[a]	2.383 (0.107 – 15.901)	0.089 (0.010 – 0.501)	4.7×10^{-29}	23.5 (1.1 – 720)	85 (97%) and 0
SQCLC	39	2.148 (0.107 – 15.901)	0.083 (0.010 – 0.325)	3.2×10^{-13}	27.2 (1.1 – 166.2)	37 (95%) and 0
LAC	38	2.189 (0.224 – 11.365)	0.079 (0.014 – 0.469)	7.8×10^{-14}	24.0 (1.7 – 142.7)	37 (97%) and 0

[a] A total of 88 NSCLC patients was studied including 39 patients with SQCLC, 38 patients with LAC, 3 patients with SQCLC+LAC mixed type tumour, 2 patients with LCLC, 3 patients with SLC, and 3 patients with UNDIF.
[b] Data indicated as median with the range in parentheses.
[c] Statistical difference of survivin protein expression in Tu *versus* Lu was calculated by Mann-Whitney test.

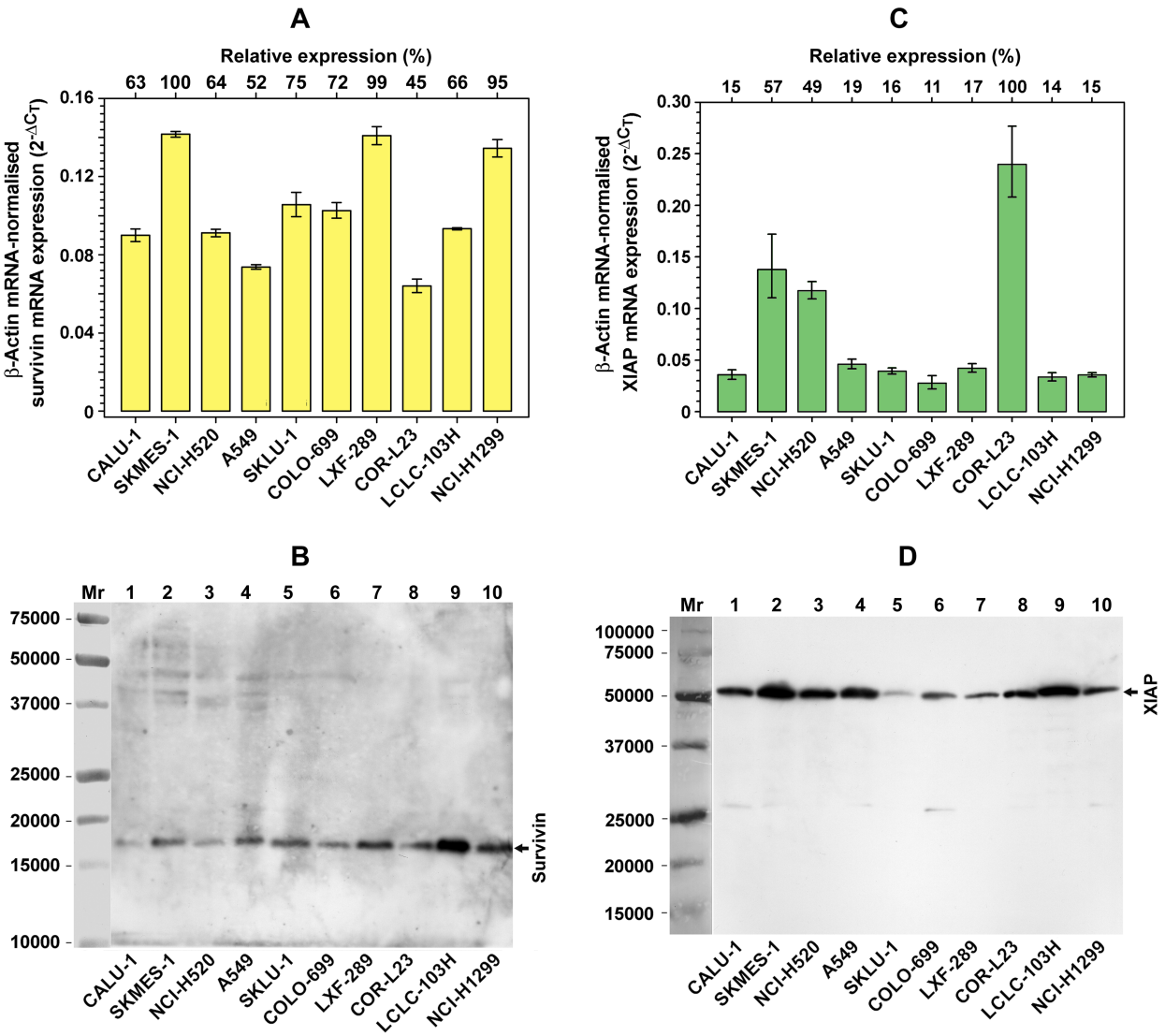

Figure 4: Analysis of survivin and XIAP expression in non-small cell lung carcinoma cell lines. (A and C) Expression of survivin and XIAP mRNAs in the tumour cell lines as quantitated by real time RT-PCR. The data are indicated as mean ± standard error of the mean of three independent experiments. (B and D) Expression of survivin and XIAP proteins in the tumour cell lines as analysed by SDS-PAGE and immunoblotting-ECL.

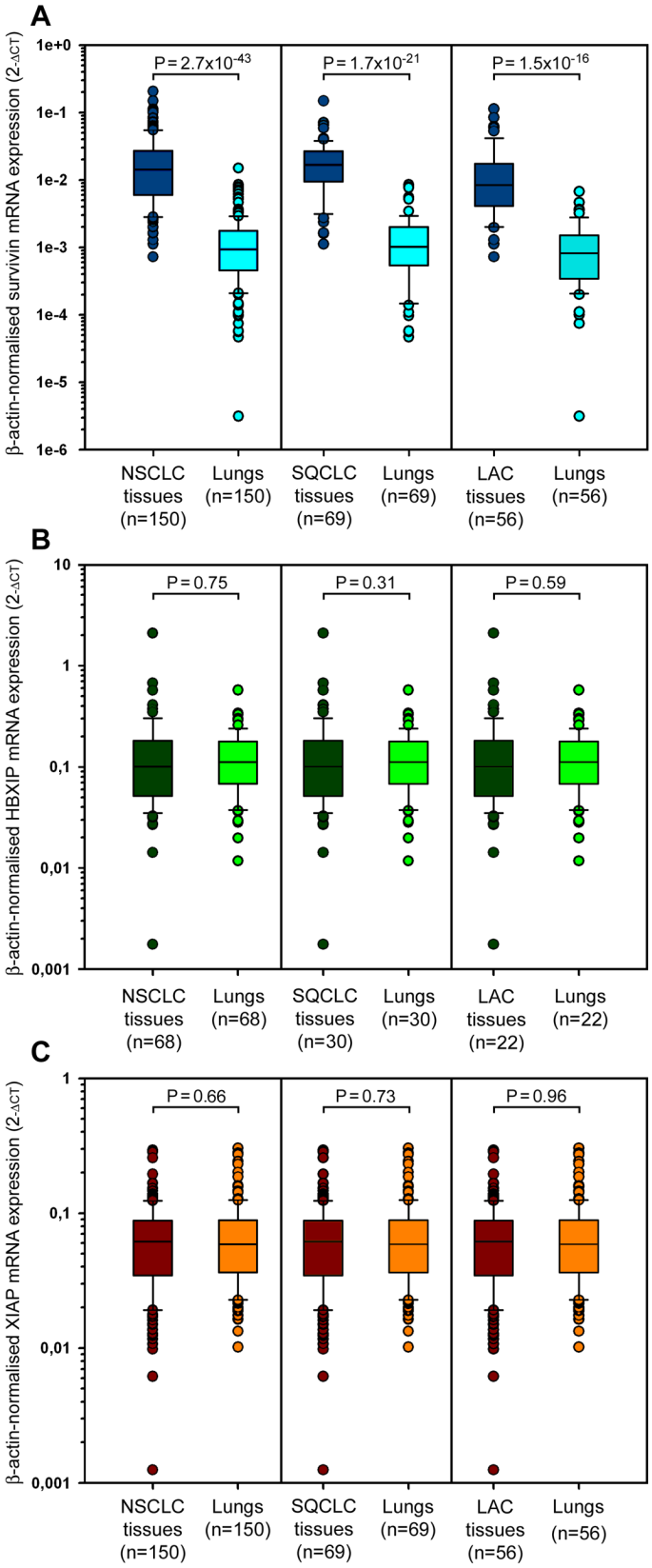

Figure 5: Expression of survivin, HBXIP and XIAP mRNAs in NSCLC tissues and lungs. (A) Survivin, (B) HBXIP and (C) XIAP mRNAs were quantitated by real-time RT-PCR assays, using an input of 200 ng of total RNA, and the expression data were normalized against the expression of β-actin mRNA. The expression data are shown as median (the horizontal line inside the box) with the upper ranges of 75% and 90% and the lower ranges of 25% and 10%. Statistical differences were calculated by Mann-Whitney test.

Table 3: Impact of gender, smoking, tumour grade, and tumour stage on survivin mRNA and survivin protein expression in NSCLC tumours.

Category	n[a]	β-Actin mRNA-normalised expression of survivin mRNA ($2^{-\Delta C_T}$)	Statistical difference (P)[c]	n[a]	Expression of survivin protein (ng/mg of total protein)[b]	Statistical difference (P)[c]
Gender						
Men	110	0.01618 (0.00129 – 0.20590)	0.001	58	2.549 (0.107 – 15.901)	0.529
Women	40	0.00647 (0.00072 – 0.11344)		30	1.638 (0.224 – 11.365)	
Smoking						
Non-smokers	20	0.00625 (0.00072 – 0.05831)	0.011	13	1.276 (0.224 – 11.365)	0.371
Smokers	130	0.01595 (0.00111 – 0.62417)		75	2.465 (0.107 – 15.901)	
Tumour grade						
Grade 1+2	69	0.01060 (0.00072 – 0.11344)	0.007	33	2.333 (0.172 – 10.555)	0.298
Grade 3	54	0.01722 (0.00112 – 0.07081)		42	2.701 (0.107 – 15.901)	
Tumour stage						
Stage IA	21	0.00744 (0.00112 – 0.05872)		13	1.011 (0.172 – 5.944)	
Stage IB	62	0.01505 (0.00111 – 0.20590)	0.054	32	2.474 (0.107 – 11.365)	0.049
Stage II+III	63	0.01584 (0.00072 – 0.14865)	0.122	40	2.099 (0.197 – 15.901)	0.044

[a] The number, n, of examined NSCLC tissues belonging to the particular category is indicated.
[b] Data indicated as median with the range in parentheses.
[c] Statistical difference between NSCLC tissues belonging to the particular category was calculated by Mann-Whitney test. The levels of survivin mRNA and protein expression in stage IB tumours and stage II+III tumours were compared, respectively, with those in stage IA tumours.

upregulated in NSCLC tumours as compared to matched lungs (Table 2). More than tenfold higher level of survivin protein was observed in 72 (82%) of 88 examined NSCLC tumours as compared to the lungs. Moreover, the expression of survivin protein significantly correlated with survivin mRNA in NSCLC tumours ($r = 0.605$, $P = 1.03\text{x}10^{-9}$, $n = 84$; Pearson linear correlation) but not in the lungs ($r = 0.165$, $P = 0.131$, $n = 84$; Pearson linear correlation).

The expression of survivin mRNA, but not of protein, reached a significantly higher level in the tumours of men than women, in the tumours of smokers than non-smokers, and in the less-differentiated tumours than in the well-differentiated ones (Table 3). On the other hand, the expression of survivin protein, but not of mRNA, was significantly higher in stage IB tumours as well as in higher stage tumours as compared to stage IA tumours (Table 3). When SQCLC and LAC tumours were considered separately, the expression of survivin mRNA remained significantly higher in the less-differentiated tumours ($P = 0.035$ and $P = 0.008$, respectively; Mann-Whitney test), but it became statistically insignificantly different in the tumours of men and women and the tumours of smoking and non-smoking LAC patients ($P > 0.07$; Mann-Whitney test).

Regarding HBXIP expression, there was no significant difference in HBXIP mRNA level in NSCLC tumours, except SLC tumours, and matched lungs (Figure 5B and data not shown) and no statistically significant impact of patients gender and smoking habit, tumour grade and tumour stage on the expression of HBXIP mRNA was observed in NSCLC tumours ($P > 0.11$; Mann-Whitney test, data not shown). Likewise, there were comparable levels of XIAP

Table 4: Immunometric analysis of XIAP protein expression in NSCLC tumours and lungs.

Tumour type	n	XIAP protein expression (ng/mg of total protein)[b]		Statistical difference (P) of XIAP protein expression in Tu *versus* Lu[c]	Tu/Lu ratio of XIAP protein expression[b]	Number of patients with Tu/Lu XIAP protein expression ratio ≥ 2 and ≤ 0.5
		Tumours (Tu)	Lungs (Lu)			
NSCLC	88[a]	34.01 (0.24 – 112.70)	29.93 (3.40 – 76.40)	0.017	1.3 (0.01 – 8.3)	14 (16%) and 12(14%)
SQCLC	39	32.86 (0.24 – 86.27)	30.07 (3.40 – 69.46)	0.280	1.1 (0.01 – 8.1)	4(10%) and 5(13%)
LAC	38	41.47 (0.73 – 112.70)	27.73 (14.05 – 76.41)	0.004	1.4 (0.03 – 5.4)	8(21%) and 4(11%)

[a] A total of 88 NSCLC patients was studied including 39 patients with SQCLC, 38 patients with LAC, 3 patients with SQCLC+LAC mixed type tumours, 2 patients with LCLC, 3 patients with SLC and 3 patients with UNDIF.
[b] Data indicated as median with the range in parentheses.
[c] Statistical difference of XIAP protein expression in Tu versus Lu was calculated by Mann-Whitney test.

Table 5: Impact of gender, smoking, tumour grade, and tumour stage on XIAP mRNA and XIAP protein expression in NSCLC tumours.

Category	n[a]	β-Actin mRNA-normalised expression of XIAP mRNA ($2^{-\Delta C_T}$)	Statistical difference (P)[c]	n[a]	Expression of XIAP protein (ng/mg of total protein)[b]	Statistical difference (P)[c]
Gender						
Men	110	0.06315 (0.00617 – 0.28519)	0.553	58	32.85 (0.71 – 86.27)	0.263
Women	40	0.05241 (0.00125 – 0.29321)		30	40.35 (0.24 – 112.70)	
Smoking						
Non-smokers	20	0.06381 (0.00125 – 0.28519)	0.746	13	49.68 (5.91 – 82.39)	0.009
Smokers	130	0.05913 (0.00617 – 0.29321)		75	32.84 (0.24 – 112.70)	
Tumour grade						
Grade 1+2	67	0.05872 (0.01075 – 0.28519)	0.871	36	32.51 (0.71 – 74.53)	0.205
Grade 3	54	0.06655 (0.00617 – 0.29321)		36	42.64 (0.245 – 86.27)	
Tumour stage						
Stage IA	21	0.05441 (0.00137 – 0.12158)		13	45.29 (5.91 – 112.70)	
Stage IB	62	0.06359 (0.00125 – 0.28519)	0.536	32	34.01 (3.50 – 86.27)	0.910
Stage II+III	63	0.06293 (0.01168 – 0.29321)	0.260	40	34.73 (0.24 – 74.53)	0.555

[a] The number, n, of examined NSCLC tissues belonging to the particular category is indicated.
[b] Data indicated as median with the range in parentheses.
[c] Statistical difference between NSCLC tissues belonging to the particular category was calculated by Mann-Whitney test. The levels of survivin mRNA and protein expression in stage IB tumours and stage II+III tumours were compared, respectively, with those in stage IA tumours.

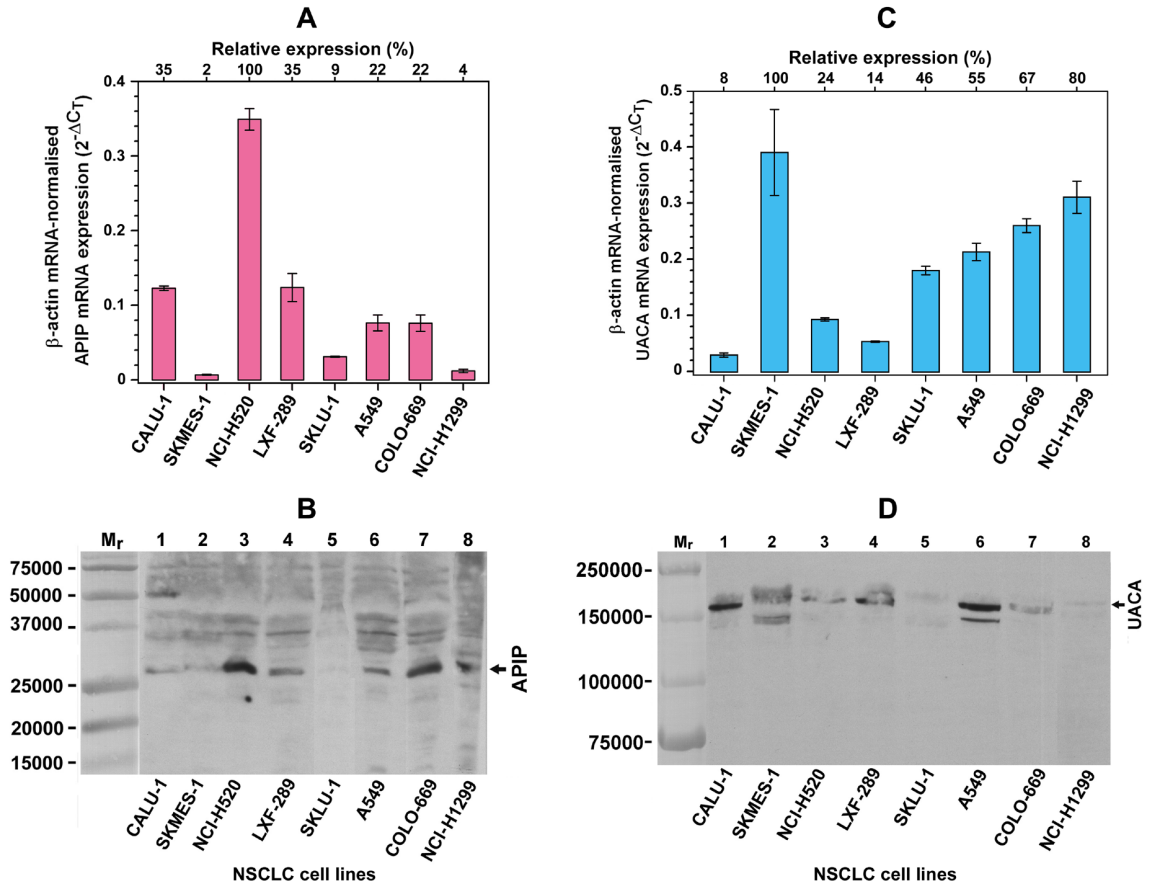

Figure 6: Analysis of APIP and UACA expression in non-small cell lung carcinoma cell lines. (A and C) Expression of APIP and UACA mRNAs in the tumour cell lines as quantitated by real time RT-PCR. The data are indicated as mean ± standard error of the mean of three independent experiments. (B and D) Expression of APIP and UACA proteins in the tumour cell lines as analysed by SDS-PAGE and immunoblotting-ECL.

mRNA in NSCLC tumours and lungs (Figure 5C), but the expression of XIAP protein in NSCLC tumours, and particularly in LAC tumours, was significantly higher as compared to matched lungs (Table 4). Nevertheless, the number of patients with the tumour/lung XIAP mRNA and XIAP protein expression ratio greater than 2 was relatively low in the groups of all examined NSCLC patients (Table 4; Krepela *et al*, 2009). There was no correlation between XIAP mRNA and protein expression in the tumours and the lungs (data not shown). The expression of both XIAP mRNA and protein in the studied NSCLC tumours and NSCLC cell lines was not significantly different ($P > 0.78$; Mann-Whitney test). Patient's gender, tumour grade and tumour stage did not have any significant impact on the expression of XIAP mRNA and protein in NSCLC tumours. The tumours of smokers showed a significantly lower expression of XIAP protein, but not of mRNA, as compared to the tumours of non-smokers (Table 5). However, when LAC tumours were considered separately the expression of XIAP protein in the tumours of smoking and non-smoking LAC patients was not statistically significant ($P > 0.12$; Mann-Whitney test).

Table 6: Impact of gender, smoking, tumour grade, and tumour stage on APIP mRNA expression in non-small cell lung carcinomas.

Category	n[a]	β-Actin mRNA-normalised expression of APIP mRNA ($2^{-\Delta C_T}$)	Statistical difference (P)[c]
Gender			
Men	72	0.0327 (0.0042 – 0.1321)	0.577
Women	30	0.0269 (0.0087 – 0.1216)	
Smoking			
Non-smokers	13	0.0302 (0.0173 – 0.0708)	0.523
Smokers	89	0.0304 (0.0046 – 0.1119)	
Tumour grade			
Grade 1+2	33	0.0259 (0.0064 – 0.1119)	0.847
Grade 3	39	0.0268 (0.0046 – 0.1008)	
Tumour stage			
Stage IA	15	0.0280 (0.0123 – 0.0866)	
Stage IB	42	0.0333 (0.0046 – 0.1119)	0.379
Stage II+III	41	0.0268 (0.0104 – 0.1119)	0.579

[a] The number, n, of examined NSCLC tissues belonging to the particular category is indicated.
[b] Data indicated as median with the range in parentheses.
[c] Statistical difference between NSCLC tissues belonging to the particular category was calculated by Mann-Whitney test. The levels of survivin mRNA and protein expression in stage IB tumours and stage II+III tumours were compared, respectively, with those in stage IA tumours.

The analyses of APIP and UACA mRNAs and proteins expression revealed, that APIP and UACA genes were expressed in all tested NSCLC cell lines on the level of both mRNA and protein, but the levels of their expression were quite variable (Figure 6). Moreover, in the case of APIP, but not UACA, the expression of mRNA and protein showed a significant positive Pearson linear correlation (r = 0.854, P = 0.0069) in NSCLC cell lines.

To test whether DNA methylation is involved in the transcriptional regulation of APIP and UACA expression in NSCLC cell lines, we cultured the tumour cells in the presence and the absence of 5-aza-2'-deoxycytidine (decitabine), a DNA demethylating agent. Although we detected statistically significant increase of APIP and UACA mRNAs expression in several NSCLC cell lines cultured in the presence of decitabine (Figure 7), the decitabine-induced up-regulation of transcript expression higher than 2-fold was observed only for UACA mRNA in CALU-1 cells (3.9-fold increase; Figure 7B).

There was a significant downregulation of both APIP and UACA mRNAs and proteins in NSCLC tumours including the major histopathological types of NSCLC (SQCLC and LAC) as compared to matched lungs (Figures 8 and 9). In fact, APIP mRNA expression was two- or more-fold downregulated in 33 (34%), while UACA mRNA expression in 72 (70%) of 102 studied NSCLC patients. Although the tumour stage did not have significant impact on the expression of APIP mRNA in NSCLC tumours (Table 6), the expression of UACA mRNA was significantly lower in stage IA tumours as compared to stage IB tumours and higher stage tumours (Table 7). Moreover, the down-regulation of UACA mRNA expression was relatively more frequent in stage IA tumours (in 14 of 15 patients, 93%) than in stage IB

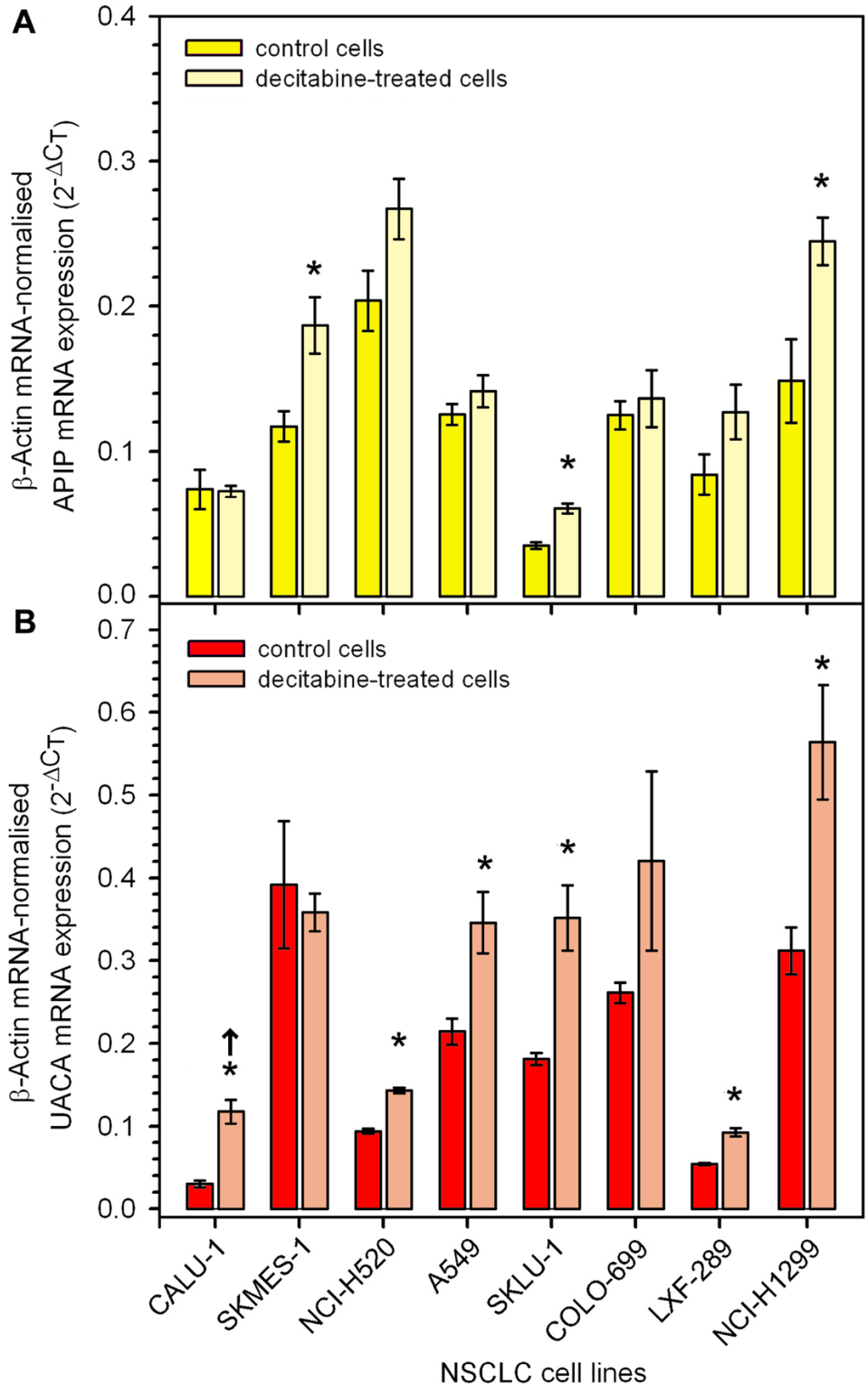

Figure 7: Effect of 5-aza-2'-deoxycytidine (decitabine) in cultured NSCLC cell lines. (A) APIP and (B) UACA mRNAs expression in NSCLC cells treated or untreated with 1μM decitabine. Data are indicated as the mean ± SEM from three independent experiments. Statistically significant (*: P<0.05, t-test) and more than two-fold (↑) up-regulation of transcripts expression in the decitabine-treated compared to -untreated cells are indicated.

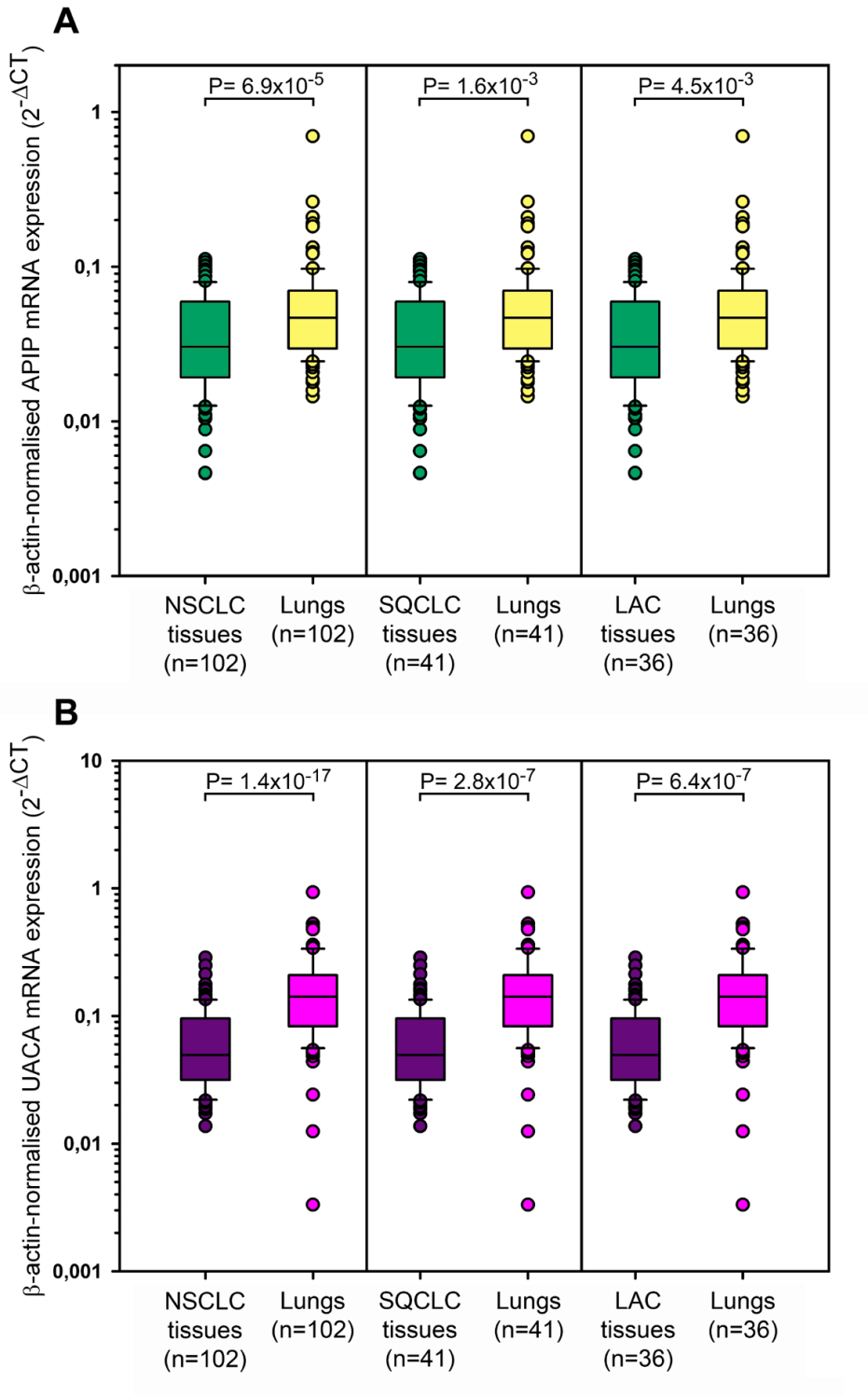

Figure 8: Expression of APIP and UACA mRNAs in NSCLC tumours and lungs. (A) APIP and (B) UACA mRNAs were quantitated by real-time RT-PCR assays, using an input of 200 ng of total RNA, and the expression data were normalized against the expression of β-actin mRNA. The expression data are shown as median (the horizontal line inside the box) with the upper ranges of 75% and 90% and the lower ranges of 25% and 10%. Statistical differences were calculated by Mann-Whitney test.

Table 7: Impact of gender, smoking, tumour grade, and tumour stage on UACA mRNA expression in non-small cell lung carcinomas.

Category	n[a]	β-Actin mRNA-normalised expression of UACA mRNA ($2^{-\Delta C_T}$)	Statistical difference (P)[c]
Gender			
Men	72	0.0475 (0.0137 – 0.1406)	0.436
Women	30	0.0492 (0.0172 – 0.2872)	
Smoking			
Non-smokers	13	0.0421 (0.0186 – 0.2872)	0.485
Smokers	89	0.0508 (0.0137 – 0.2483)	
Tumour grade			
Grade 1+2	33	0.0412 (0.0186 – 0.2483)	0.075
Grade 3	39	0.0559 (0.0172 – 0.2872)	
Tumour stage			
Stage IA	15	0.0317 (0.0137 – 0.1088)	
Stage IB	42	0.0531 (0.0194 – 0.2132)	0.025
Stage II+III	41	0.0518 (0.0186 – 0.2872)	0.014

[a] The number, n, of examined NSCLC tissues belonging to the particular category is indicated.
[b] Data indicated as median with the range in parentheses.
[c] Statistical difference between NSCLC tissues belonging to the particular category was calculated by Mann-Whitney test. The levels of survivin mRNA and protein expression in stage IB tumours and stage II+III tumours were compared, respectively, with those in stage IA tumours.

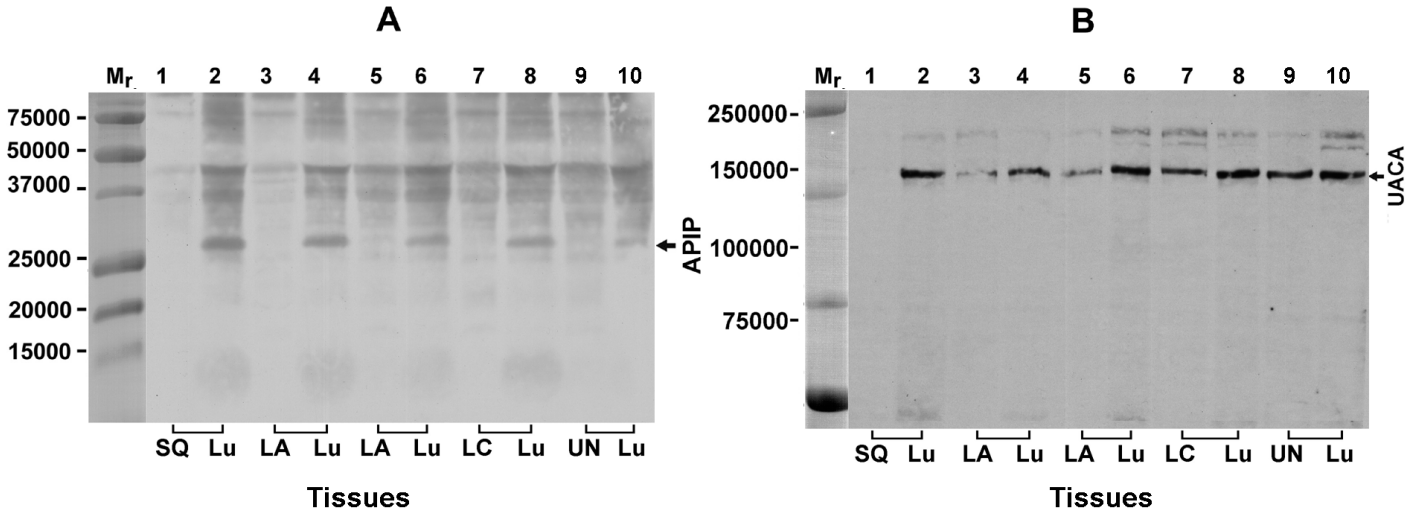

Figure 9: Expression of APIP and UACA proteins in NSCLC tumours and lungs. Expression of APIP and UACA proteins in NSCLC tissues and lungs as analysed by SDS-PAGE and immunoblotting-ECL.

tumours (in 29 of 42 patients, 69%) and stage II + III tumours (in 28 of 41 patients, 68%). Patients gender, smoking status and tumour grade did not significantly affect the expression neither of APIP nor UACA mRNAs (Table 6 and Table 7).

4.2 Involvement of DNA methylation in the regulation of transcriptional expression of APAF1, CASP9 and CASP3 genes in NSCLC cells

Transcriptional silencing of a gene is tightly associated with gene promoter methylation by DNA methyltransferases (DNMTs), which can methylate cytosines in cytosine-phosphoguanosine dinucleotide (CpG) dense regions. Importantly, methylation in CpG islands within the first exon might also play a significant role in gene silencing (Brenet *et al*, 2011). Therefore, we used a DNA sequence of promoter region proximal to the transcription start site extending to the first exon to predict the possible methylation sites of genes encoding the key components of the apoptosome pathway. Using the software MethPrimer (Li and Dahiya, 2002), we found five CpG islands in the input sequence of *APAF1* gene and one CpG island in the input sequences of each, *CASP-9* and *CASP-3* genes (Figure 10). These *in silico* results prompted us to investigate whether DNA methylation is involved in the transcriptional regulation of *APAF1*, *CASP9* and *CASP3* genes expression. We cultured NSCLC cells in the presence and the absence of a DNA methyltransferase inhibitor and demethylating agent, 5-aza-2'-deoxycytidine (decitabine) (Nguyen *et al*, 2010) and quantitated the expression of Apaf-1, procaspase-9 and procaspase-3 mRNAs using real-time RT-PCR analysis. The results of these experiments showed, that the expression of Apaf-1, procaspase-9 and procaspase-3 mRNAs was significantly upregulated in 3, 5 and 5 of 7 decitabine-treated NSCLC cell lines, respectively (Figure 11). In fact, the decitabine-induced up-regulation of transcript expression higher than two-fold was observed for procaspase-9 mRNA in SKMES-1, NCI-H520 and SKLU-1 cells and for procaspase-3 mRNA in CALU-1, SKMES-1 and NCI-H520 cells. Nonetheless, the highest upregulation of mRNA expression was only 3.2-fold, which was achieved for procaspase-9 mRNA in SKLU-1 cells. Furthermore, there was no significant difference between the β-actin mRNA expression in the decitabine-treated and -untreated NSCLC cell lines (data not shown).

4.3 Expression status of Apaf-1 and caspase-9 mRNA splice variants in NSCLC tumours and lungs

We further investigated the expression status of Apaf-1 mRNA variants -XL/-LC and LN/-S, encoding the (cyt-c+dATP)-activatable and the (cyt-c+dATP)-non-activatable Apaf-1 protein isoforms, respectively, in 50 NSCLC tumours of 5 histopathological types and matched lung parenchyma from surgically treated lung cancer patients. We found that the expression of Apaf1-XL/-LC mRNAs was significantly higher compared to the expression of Apaf-1-LN/-S mRNAs in NSCLC tumours ($P = 1.7 \times 10^{-14}$; Mann-Whitney test), including 22 SQCLC tumours ($P = 3.8 \times 10^{-6}$; Mann-Whitney test) and 20 LAC tumours ($P = 1.9 \times 10^{-9}$; Mann-Whitney test), as well as in the lungs ($P = 1.3 \times 10^{-15}$; Mann-Whitney test) (Figure 12A). Importantly, caspase-9S as the dominant negative inhibitor of the apoptosome

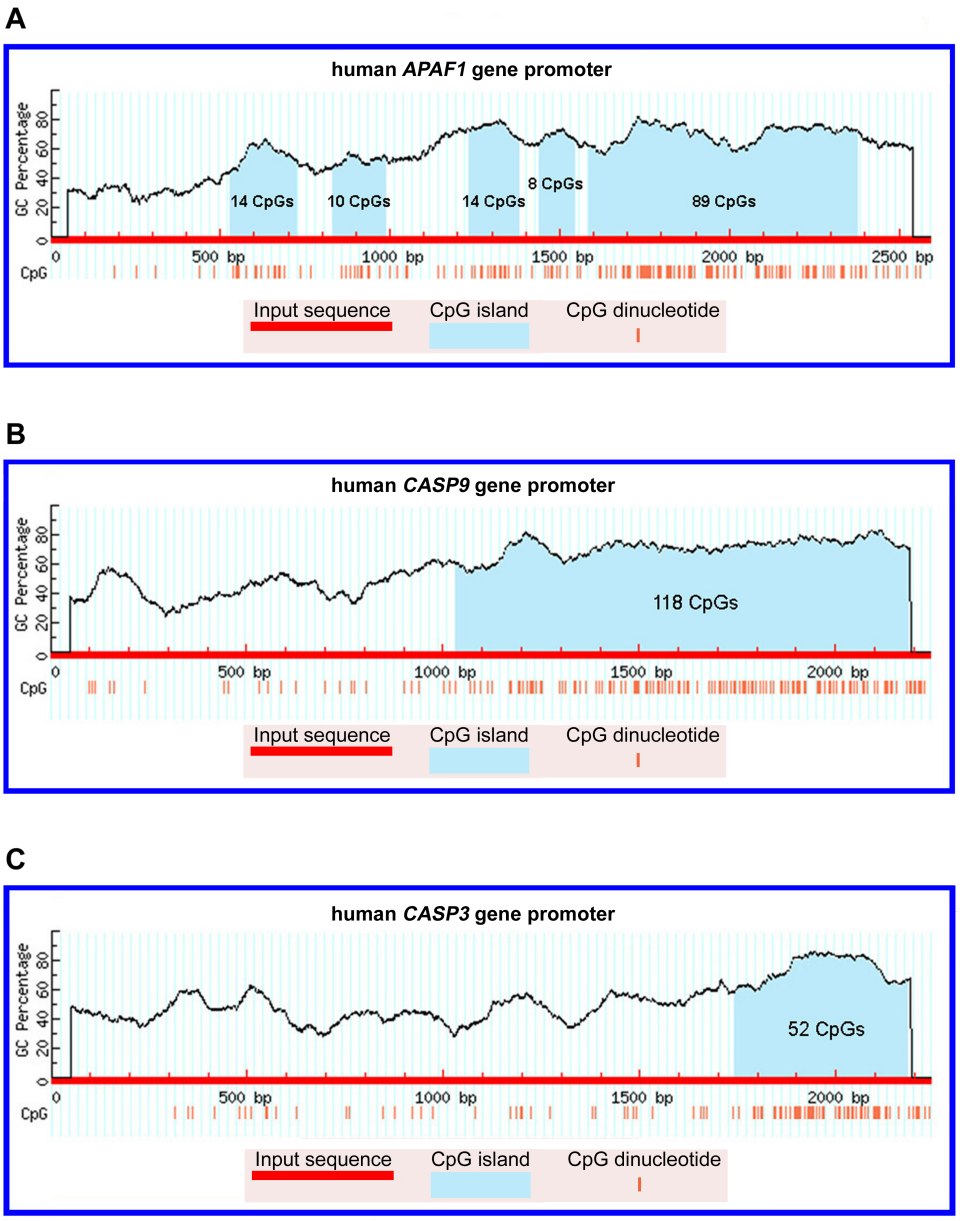

Figure 10: Prediction of possible CpG islands and the methylation sites in proximal promoter and the first exon of genes encoding the core components of apoptosome pathway. The bioinformatic analyses were performed using the on-line program MethPrimer. Criteria for CpG island prediction were: a DNA region greater than 100 bp with a GC content above 0.5 and observed/expected CpG ratio above 0.6. (A) Human *APAF1* gene: in the searched 2590-base long DNA sequence input 5 CpG islands with the indicated numbers of CpG dinucleotides as putative methylation sites were found. (B) Human *CASP9* gene: in the searched 2240-base long DNA input 1 CpG island with 118 CpG dinucleotides as putative methylation sites were found. (C) Human *CASP3* gene: in the searched 2240-base long DNA input 1 CpG island with 52 CpG dinucleotides as putative methylation sites were found.

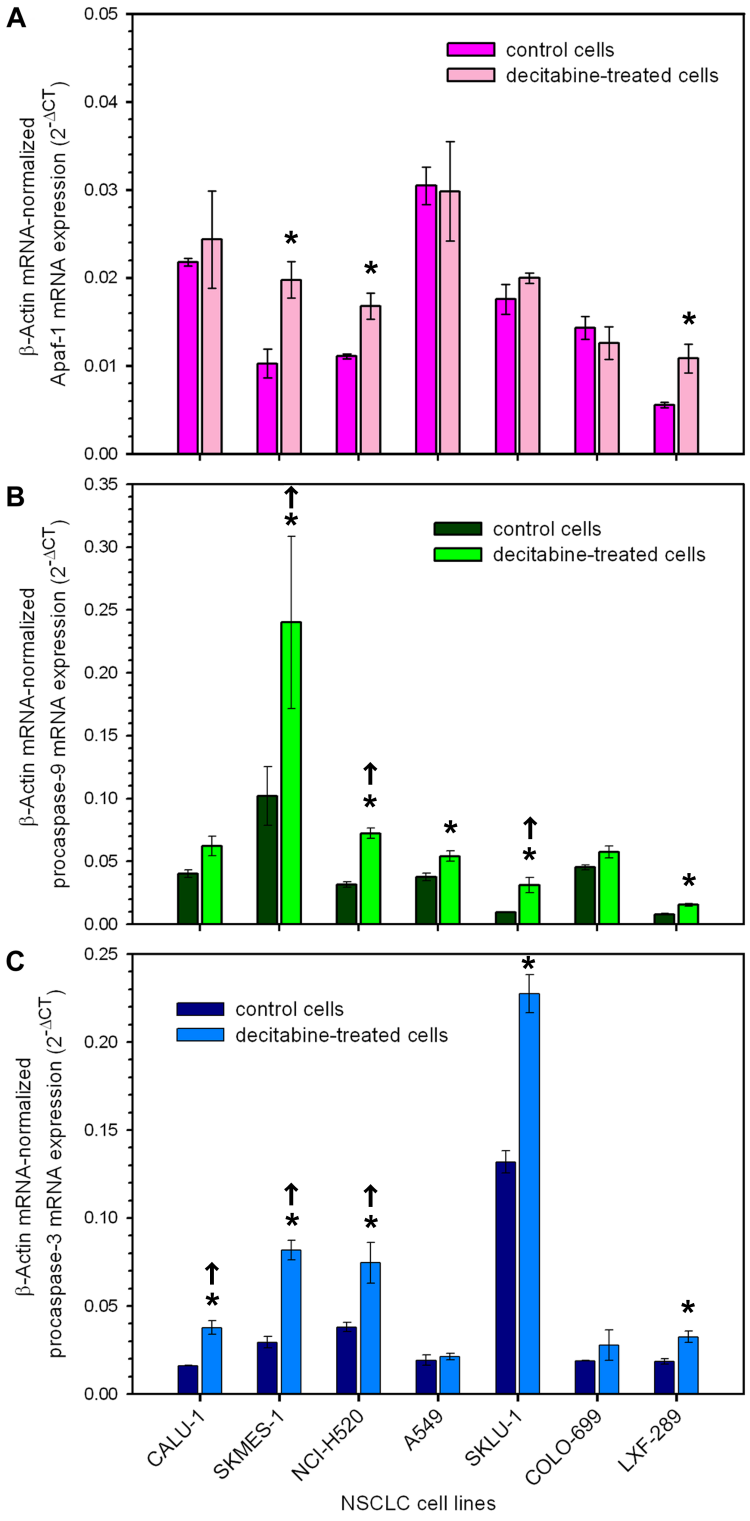

Figure 11: Effect of 5-aza-2'-deoxycytidine (decitabine) in cultured NSCLC cell lines. (A) Apaf-1, (B) procaspase-9 and (C) procaspase-3 mRNAs expression in NSCLC cells treated and untreated with 1μM decitabine. Data are indicated as the mean ± standard error of the mean from three independent experiments. Statistically significant (*: P<0.05, t-test) and more than two-fold (↑) up-regulation of transcript expression in the decitabine-treated compared to -untreated cells are indicated.

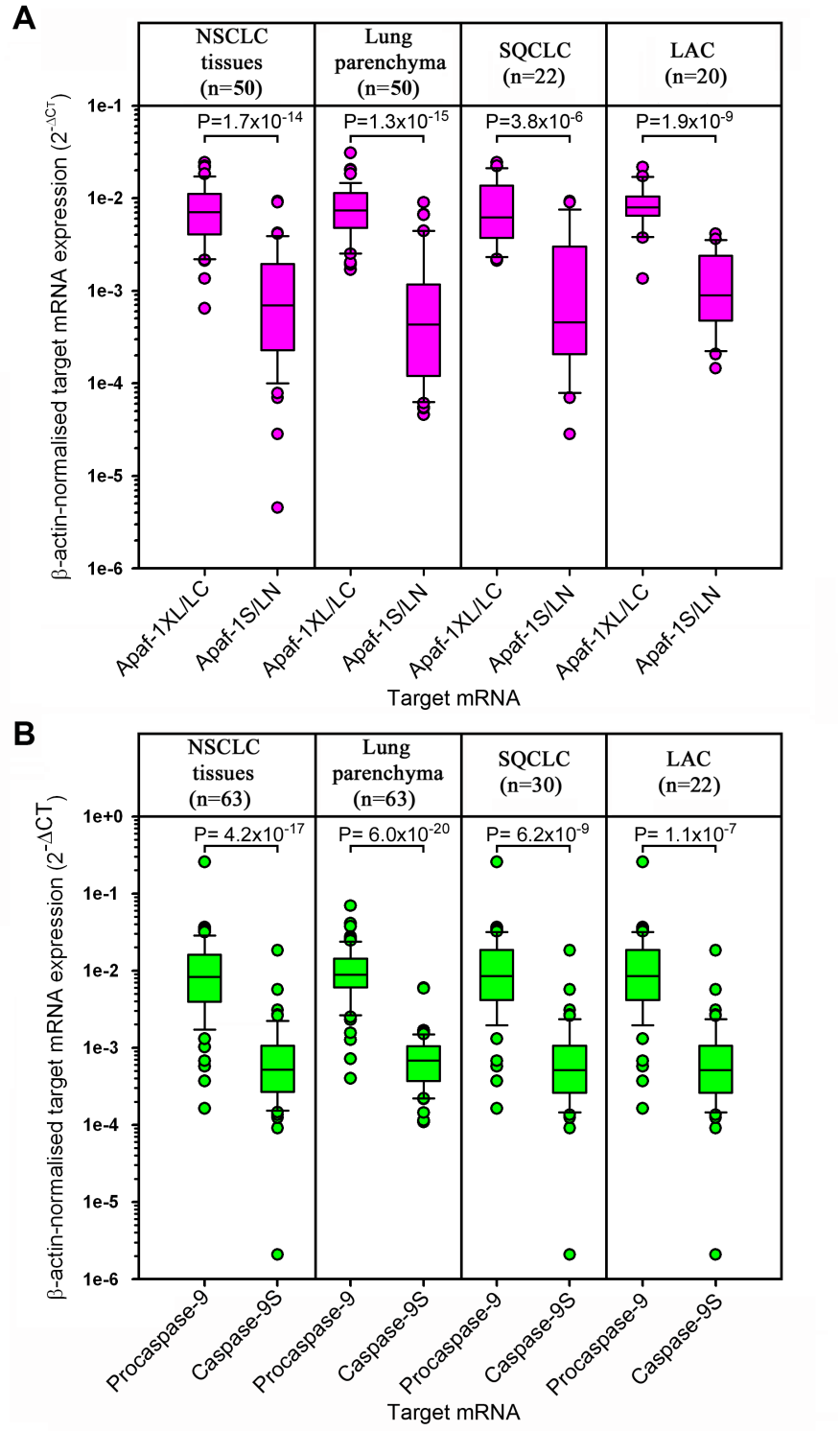

Figure 12: Expression of Apaf-1 and procaspase-9 mRNA variants in NSCLC tissues and lungs. (A) The expression of Apaf-1XL/-LC and Apaf-1LN/-S mRNA variants was quantitated by uncoupled real-time RT-PCR assays, using an input of 200 ng of total RNA, and the expression data were normalized against the expression of β-actin mRNA (an internal reference transcript). (B) The expression of procaspase-9 and caspase-9S mRNA variants was quantitated by uncoupled real-time RT-PCR assays, using an input of 200 ng of total RNA, and the expression data were normalized against the expression of β-actin mRNA. The expression data are shown as median (the horizontal line inside the box) with the upper ranges of 75% and 90% and the lower ranges of 25% and 10%. Statistical differences were calculated by Mann-Whitney test.

pathway initiation might significantly suppress the apoptosome-mediated procaspase-9 activation due to competing with procaspase-9 recruitment to Apaf-1 oligomer. Therefore, we investigated the expression levels of procaspase-9 and caspase-9S mRNAs in NSCLC tumours and matched lung parenchyma. Uncoupled real-time RT-PCR analysis showed that the expression of procaspase-9 mRNA was significantly higher compared to caspase-9S mRNA in 63 NSCLC tumours ($P = 4.2 \times 10^{-17}$; Mann-Whitney test) as well as in matched lungs ($P = 6.0 \times 10^{-20}$; Mann-Whitney test) (Figure 12B).

4.4 Activatability of apoptosome apparatus in NSCLC cell lines

To assess the functionality of apoptosome apparatus (AA) in NSCLC cell lines, we studied its activatability by monitoring the generation of caspase-3-like activity upon preincubation of cell-free cytosols with cyt-c and dATP. The (cyt-c+dATP)-dependent caspase-3-like activity was induced in 5 (CALU-1, NCI-H520, SKMES-1, LXF-289 and COLO-699) of 7 studied NSCLC cell lines (Figure 13A). The samples of cell-free cytosol from A549 and SKLU-1 cell lines were resistant to the (cyt-c+dATP)-mediated induction of caspase-3-like activity. Interestingly, a high level of caspase-3-like activity was already present in the (cyt-c+dATP)-untreated cell-free cytosol from SKLU-1 cells (Figure 13A). Both, the endogenous and the (cyt-c+dATP)-induced caspase-3-like activities were completely inhibited by the caspase inhibitor Ac-DEVD-CHO at 10 μM (data not shown).
SDS-PAGE and immunoblotting analysis of NSCLC cell-free cytosols confirmed the presence of procaspase-3 protein in all studied NSCLC cells. Furthermore, a putative processed form of caspase-3 containing a p24 subunit was detected in cell-free cytosol from SKLU-1 cells (Figure 13B).

4.5 Apoptosome complexes assembly in cell-free cytosol from NSCLC cell lines

To gain an insight into apoptosome dysfunction, we analysed the capability of Apaf-1 and procaspase-9 to assemble into apoptosome complexes using gel filtration chromatography (GFC) followed by SDS-PAGE and immunoblotting-ECL. As an unincubated control, we used cell-free cytosol from COLO-669 cells which did not receive exogenous cyt-c and dATP and was not incubated prior to GFC. Using this material, Apaf-1 and procaspase-9 eluted in a M_r-region corresponding to their unoligomerized forms (Figure 14A). Surprisingly, if cell-free cytosol from COLO-669 cells was incubated alone at 37°C for 30 min, procaspase-9 eluted in the same M_r-region as in non-incubated control, but Apaf-1 eluted in two M_r-regions, one corresponding to its high-M_r complexes or aggregates and the other one to its unoligomerized forms (Figure 14B). By contrast, if the cell-free cytosol from COLO-669 cells was incubated with cyt-c and dATP at 37°C for 30 min, procaspase-9 was completely converted to caspase-9, which coeluted with Apaf-1 in two M_r-regions, one corresponding to their high-M_r complexes and the other one to their unoligomerized forms (Figure 14C). In order to verify these results,

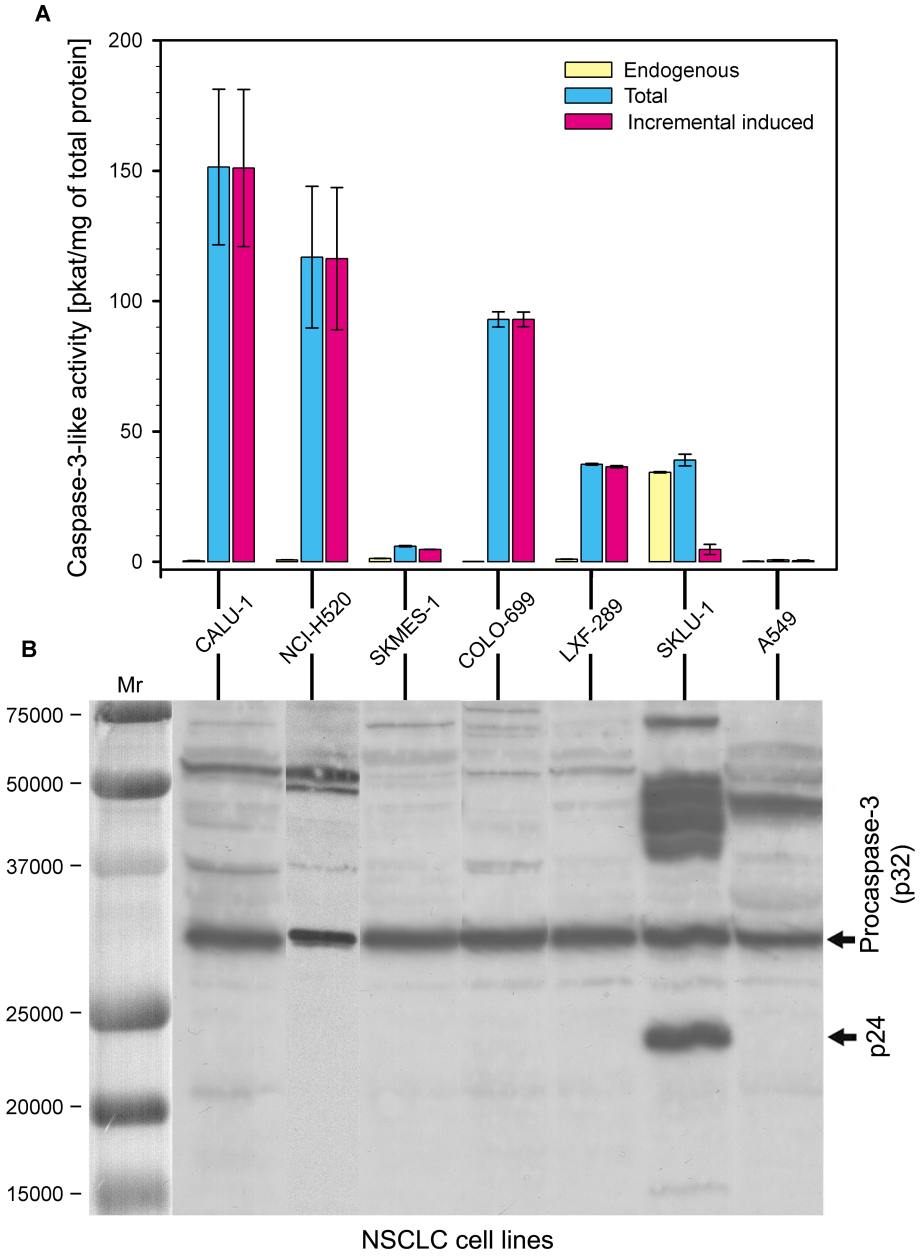

Figure 13: Analysis of the endogenous and the (cyt-c+dATP)-induced caspase-3-like activity in cell-free cytosol samples from NSCLC cells and immunodetection of procaspase-3 expression in NSCLC cells. (A) Cell-free cytosol samples were preincubated without (endogenous caspase-3-like activity) or with 10 μM cyt-c and 1 mM dATP (total caspase-3-like activity) at 37°C for 30 min. The concentration of total cytosolic protein in the preincubation reaction was 2.5 mg/ml. Samples of the preincubated cytosol were then added into the reaction with Ac-DEVD-AFC as substrate and the fluorescence of enzymatically released 7-amino-4-trifluoro-methylcoumarin (AFC) was measured. The incremental-induced caspase-3-like activity was calculated by subtracting the endogenous caspase-3-like activity from the total caspase-3-like activity. (B) Cell-free cytosol samples (50μg of total protein) were analysed for expression of procaspase-3 by SDS-PAGE followed by immunoblotting-ECL. The caspase-3 zymogen of 32kD (p32) and its putative processed form containing a 24kDa subunit (p24) are indicated.

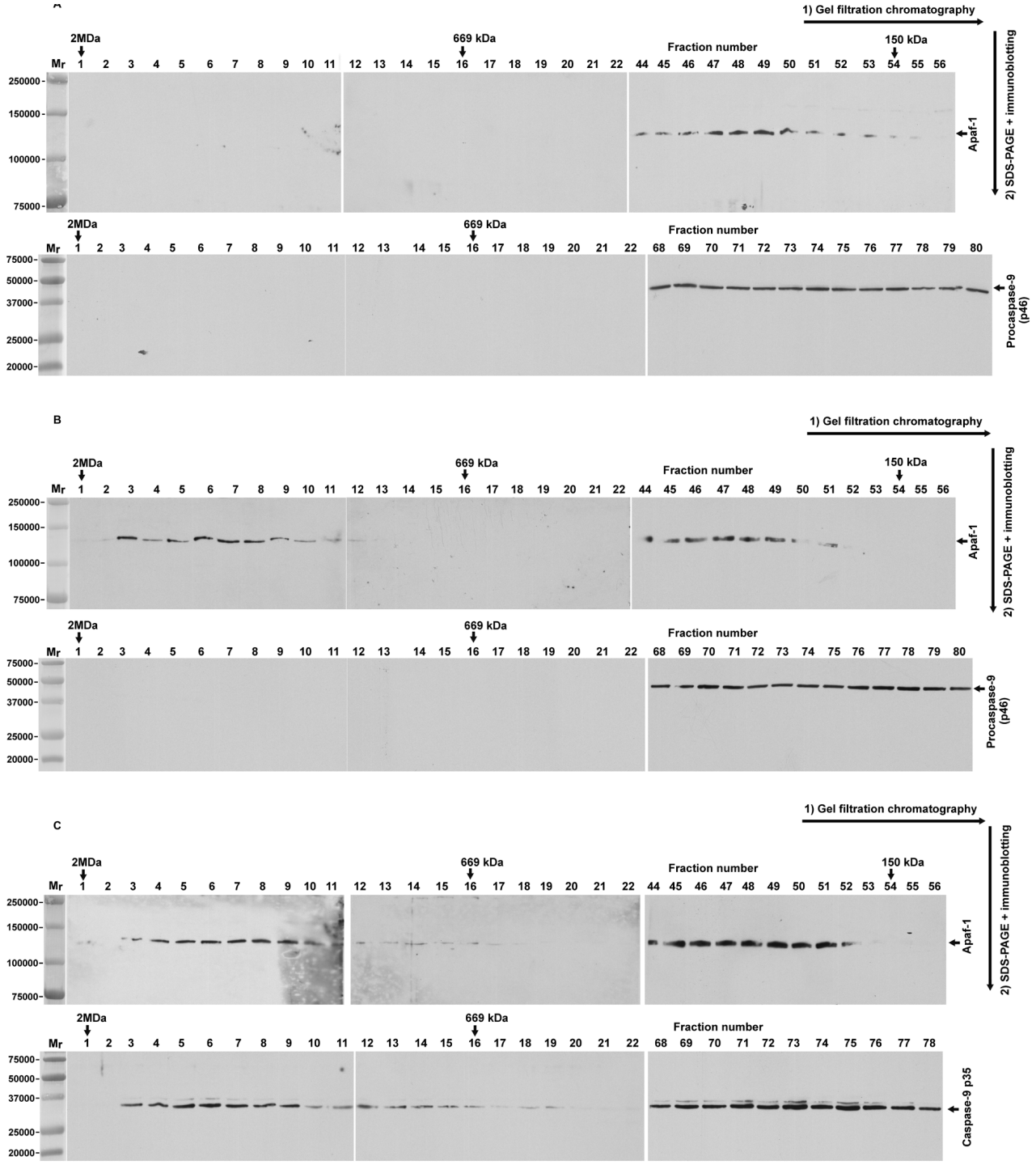

Figure 14: Analysis of apoptosome complexes formation in COLO-699 cell-free cytosol. COLO-699 cell-free cytosol (5 mg of total protein/ml) was either kept unincubated at $0 - 4°C$ or it was incubated at 37°C for 30 min in the absence or the presence of exogenous cyt-c (10μM) + dATP (1mM) prior to its separation by gel filtration chromatography on a column of Sephacryl S300HR. Selected fractions were subjected to analysis by SDS-PAGE and immunoblotting-ECL as described in Materials and Methods. (A) Unincubated control cell-free cytosol: Apaf-1 and unprocessed procaspase-9 eluted in low M_r-fractions. (B) Cell-free cytosol after incubation without of exogenous cyt-c and dATP: Apaf-1 eluted in both high and low M_r-fractions, while procaspase-9 eluted in low M_r-fractions only. (C) Cell-free cytosol after incubation with exogenous cyt-c and dATP: Apaf-1 eluted in both high and low M_r-fractions, while procaspase-9 was completely converted to caspase-9 p35 form which coeluted with Apaf-1 in high M_r-fractions and also eluted in low M_r-fractions. The positions of M_r markers are indicated with arrows.

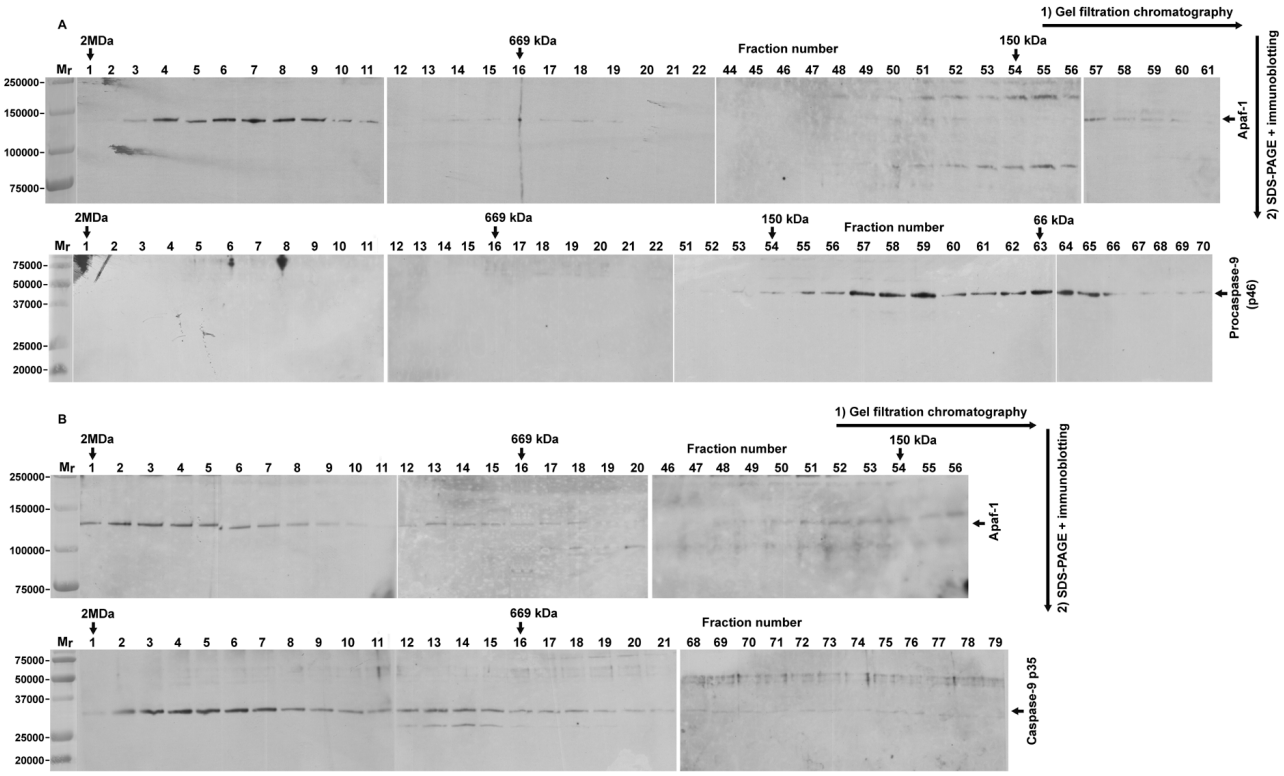

Figure 15: Analysis of apoptosome complexes formation in CALU-1 cell-free cytosol. CALU-1 cell-free cytosol (5 mg/ml) was incubated without or with exogenously added cyt-c and dATP at 37°C for 30 min and fractionated on Sephacryl S300HR column. Selected fractions were subjected to analysis by SDS-PAGE and immunoblotting-ECL as described in Materials and Methods. (A) Cell-free cytosol after incubation without of exogenous cyt-c and dATP: Apaf-1 eluted predominantly in high M_r-fractions, while procaspase-9 eluted in low M_r-fractions only. (B) Cell-free cytosol after incubation with exogenous cyt-c and dATP: Apaf-1 eluted predominantly in high M_r-fractions, while procaspase-9 was completely converted to caspase-9 p35 form which predominantly coeluted with Apaf-1 in high M_r-fractions. The positions of M_r markers are indicated with arrows.

we tested cell-free cytosol from another NSCLC cells for apoptosome assembly and function, *i.e.* for Apaf-1 oligomerization and procaspase-9 proteolytic processing to caspase-9, and its association with Apaf-1 oligomers. The mere incubation of the cell-free cytosol from CALU-1 cells at 37°C for 30 min also resulted in the formation of high-M_r Apaf-1 complexes/aggregates which did not co-elute with procaspase-9 (Figure 15A). On the other hand, the incubation of CALU-1 cell-free cytosol with cyt-c and dATP led to full conversion of procaspase-9 to caspase-9, which elution shifted to high-M_r fractions along with Apaf-1 protein (Figure 15B). In addition, a portion of unoligomerized Apaf-1 eluted together with caspase-9 in a low-M_r region (Figure 15B).

By contrast, the incubation of A549 cell-free cytosol with cyt-c and dATP induced a shift of a portion of both Apaf-1 and procaspase-9 proteins to high-M_r fractions. These fraction coeluted and contained predominantly procaspase-9 while the caspase-9 p35 and p37 forms were detectable in the high-M_r fractions only in trace amounts. However, the majority of

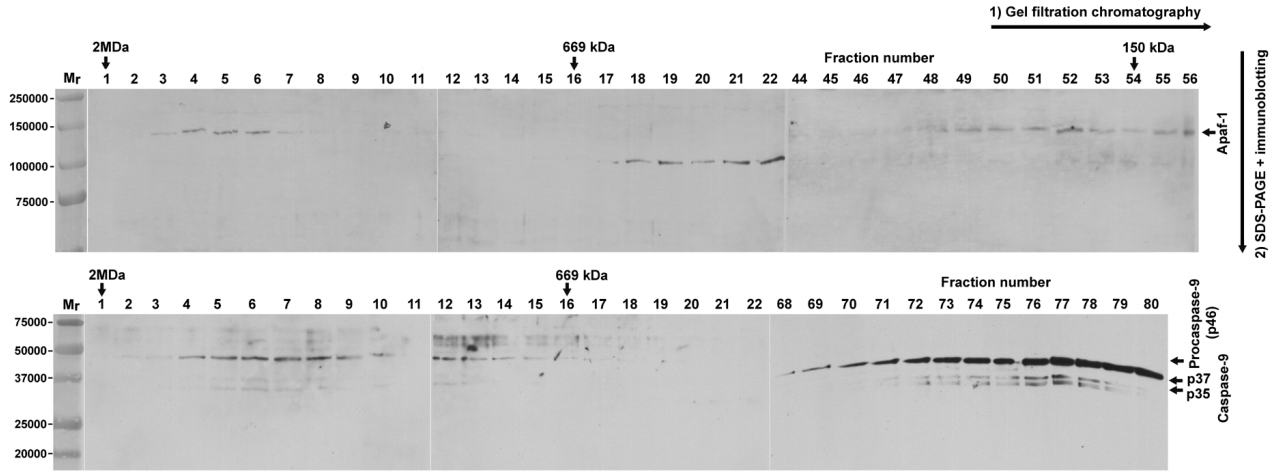

Figure 16: Analysis of apoptosome complexes formation in A549 cell-free cytosol. A549 cell-free cytosol was incubated with cyt-c and dATP at 37°C for 30 min. The sample (5 mg of total protein/ml) was fractionated on a column of Sephacryl S300HR and selected fractions were subjected to SDS-PAGE and immunoblotting-ECL analysis as described in Materials and Methods. Apaf-1 and procaspase-9 eluted in high-M_r fractions as well as low-M_r fractions. Trace amounts of p35 and p37 forms of caspase-9 were found in low-molecular fractions. The positions of M_r markers are indicated with arrows.

procaspase-9 and some caspase-9 eluted in the low-M_r fractions (Figure 16).

4.6 Apoptosome-dependent procaspase-9 proteolytic processing and caspase-9 activity

The functional assembly of activated Apaf-1 monomers to an Apaf-1 oligomeric complex is followed by recruitment of procaspase-9 molecules to this complex and eventually by activation and proteolytic processing of the bound procaspase-9 to the caspase-9 p35/p12 form (Malladi *et al*, 2009). Once the apoptosome-associated p35/p12 form of caspase-9 converts procaspase-3 to active caspase-3, the active caspase-3 can proteolytically process both caspase-9 p35/p12 and procaspase-9, resulting in generation of caspase-9 p35/p10 and caspase-9 p37/p10 forms, respectively (Zou *et al*, 2003). Therefore, we analysed the formation of caspase-9 p35 and p37 forms upon the (cyt-c+dATP)-mediated induction of AA assembly in cell-free cytosols prepared from NSCLC cell lines, in the absence and the presence of the caspase inhibitor Ac-DEVD-CHO.

In cell-free cytosols from CALU-1 and SKMES-1 cells, we detected the generation of the p35 caspase-9 subunit already within 5 min after the addition of cyt-c and dATP into cell-free cytosol, while the p37 caspase-9 subunit appeared later, usually in 10 min after the addition of cyt-c and dATP into cell-free cytosol (Figure 17A). Surprisingly, in the (cyt-c+dATP)-activated cell-free cytosol from COLO-699 and LXF-289 cells the p35 caspase-9 subunit, detected in 10^{th} min of activation, became undetectable later (Figure 17B). In cell-free cytosol from A549 incubated with cyt-c and dATP, the generation of p35 and p37 caspase-9 subunits was not detected and only a protein band corresponding to proscaspase-9 (p46)

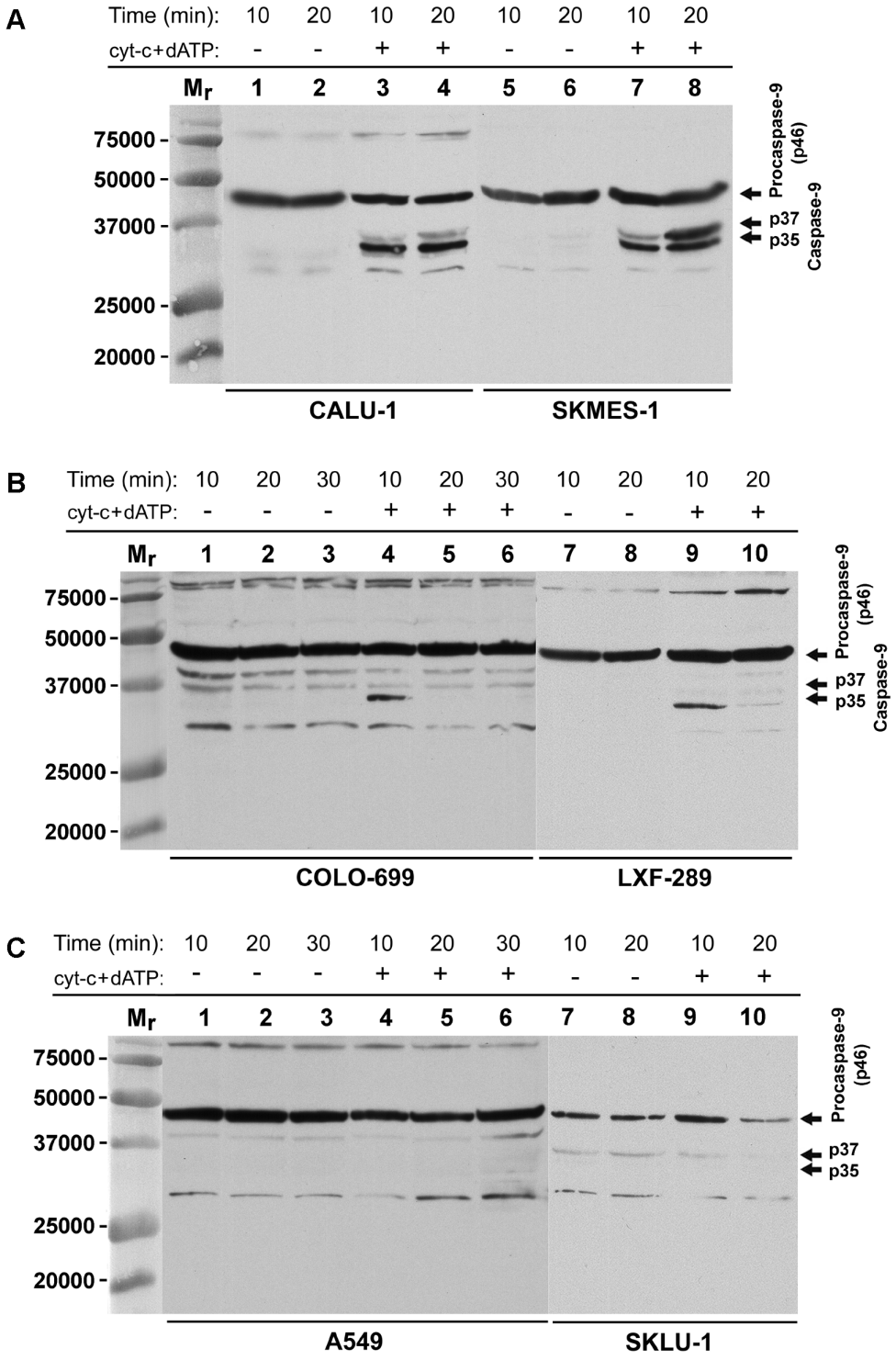

Figure 17: Analysis of procaspase-9 processing in cell-free cytosols from NSCLC cell lines. Aliquots of cytosols from (A) CALU-1 and SKMES-1 (B) COLO-699 and LXF-289 (C) A549 and SKLU-1 cells were preincubated with (+) or without (-) cyt-c and dATP at 37°C for indicated times. The reactions were stopped on ice by adding the SDS-PAGE sample buffer. After denaturation, the samples were subjected to SDS-PAGE and were immunoblotted with an anti-caspase-9 antibody. The arrows indicate the full length procaspase-9 precursor (p46) and the subunits p35 and p37 of two caspase-9 forms resulting from the proteolytic processing of procaspase-9.

was found (Figure 17C). Finally, in SKLU-1 cell-free cytosol, which was proved to exhibit a significant endogenous level of caspase-3-like activity (Figure 13A), the p35 caspase-9 subunit was not generated by exogenously added cyt-c and dATP, while the p37 caspase-9 subunit was detected in both the control and the (cyt-c+dATP)-treated samples (Figure 17C). This indicates that procaspase-9 from SKLU-1 cells is resistant to the apoptosome-dependent activation and that the caspase-3-like enzyme in viable SKLU-1 cells may be involved in extra-apoptosome procaspase-9 processing.

To study further the procaspase-9 processing, we incubated cell-free cytosol from NCI-H520 cells for different times with cyt-c and dATP and in the absence or the presence of the caspase inhibitor Ac-DEVD-CHO. The Western blot analysis showed that in the absence of the caspase inhibitor, procaspase-9 was processed into two caspase-9 forms, one containing the p35 subunit and other one containing the p37 subunit (Figure 18A, left panel). The formation of the p35 caspase-9 form preceded the generation of the p37 caspase-9 form (Figure 18A, lanes 1 and 2). The time-dependent loss of procaspase-9 was faster in samples without Ac-DEVD-CHO compared to the samples with Ac-DEVD-CHO (Figure 18A, the left and right panel). In addition, the formation of the caspase-9 p37 form correlated with the generation of the p20 and p17 forms of the large subunit of active caspase-3 (Figure 18A and B, left panels), since both the processing of procaspase-9 to the p37 form of caspase-9 and the generation of active caspase-3 p20/p17 forms were completely blocked in the presence of Ac-DEVD-CHO (Figure 18A and B, right panels). These results indicate that Ac-DEVD-CHO, a typical caspase-3 inhibitor, does not inhibit the apoptosome-dependent procaspase-9 activity, which manifests itself by the autoproteolytic formation of caspase-9 p35 form, but it does inhibit the active, *i.e.* the apoptosome associated, caspase-9 p35 form, which initiates the proteolytic activation of procaspase-3. The result of these experiments shed light on the target of the Ac-DEVD-CHO- mediated inhibition of the (cyt-c+dATP)-induced caspase-3-like activity, we observed in control reaction done in studies of apoptosome activation (data not shown). During these control enzyme reactions, Ac-DEVD-CHO (10 μM) inhibited the activity of the apoptosome-associated caspase-9 but not the activity of caspase-3/-7, because the later enzymes could not be generated due to preceding caspase-9 inhibition.

4.7 Thermal effect on the (cyt-c + dATP)- induced apoptosome apparatus activation

During initial experiments, the cell-free cytosol samples preincubated at 37°C for 30 min with Smac mimetic peptides failed in induction of AA activation by cyt-c and dATP, although they showed previously good activation response to cyt-c and dATP (data not shown). To assess the effect of the thermal pretreatment on the (cyt-c + dATP)-induced caspase-3-like activity, we preincubated cell-free cytosol from NCI-H520 cells without cyt-c and dATP at different temperatures and for different times, following the standard incubation with exogenously added cyt-c and dATP at 37°C for 30 min. As shown in Figure 19, the (cyt-

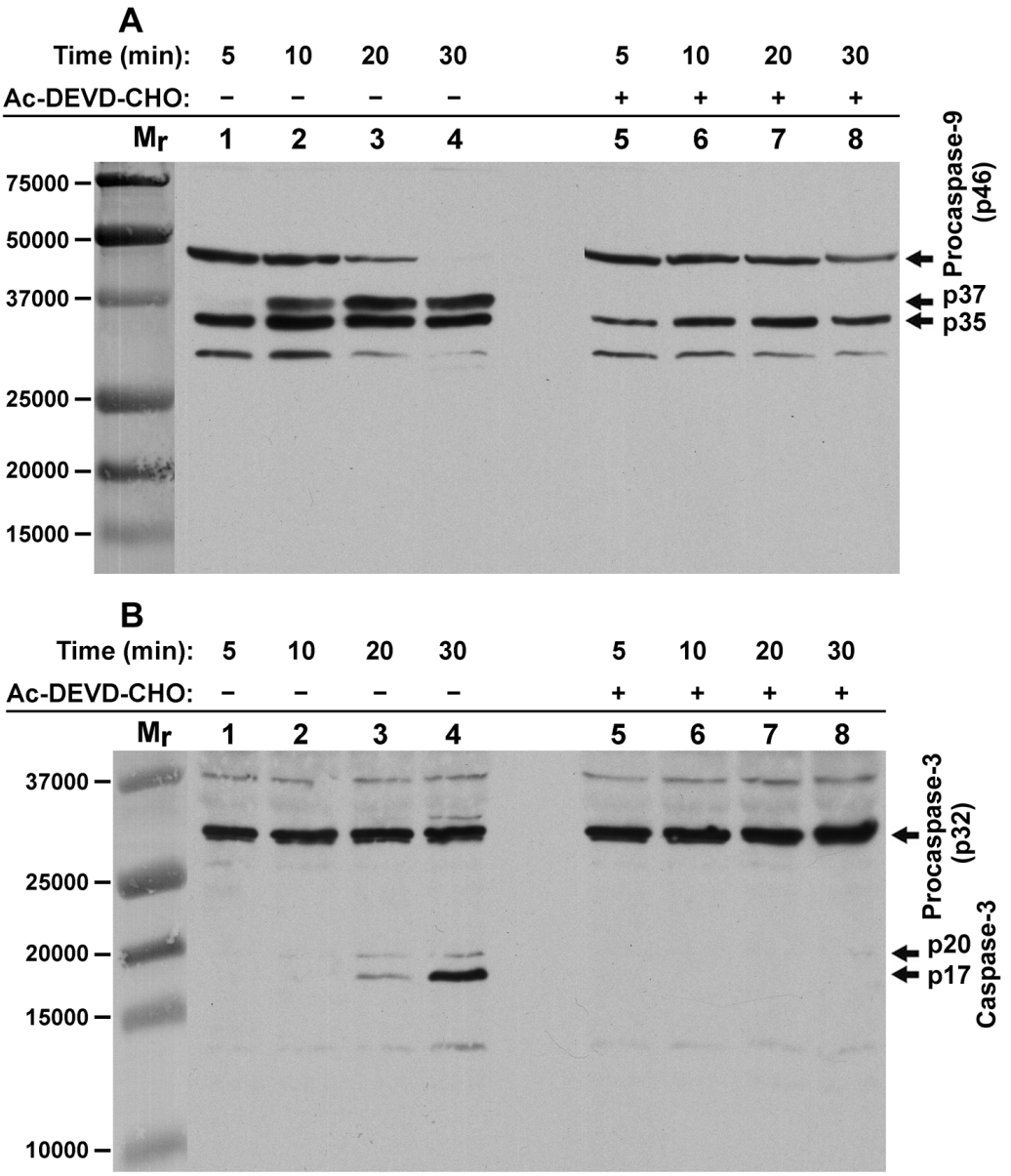

Figure 18: Analysis of procaspase-9 proteolytic processing and caspase-9 activity in NCI-H520 cytosol. NCI-H520 cell-free cytosol was incubated with cyt-c and dATP and without or with the caspase inhibitor Ac-DEVD-CHO for indicated times. Samples were subjected to SDS-PAGE and were immunoblotted with specific antibodies. (A) The arrows point to procaspase-9 (p46) and the caspase-9 p35 and p37 forms. (B) The arrows indicate procaspase-3 (p32) and the active caspase-3 p20 and p17 forms.

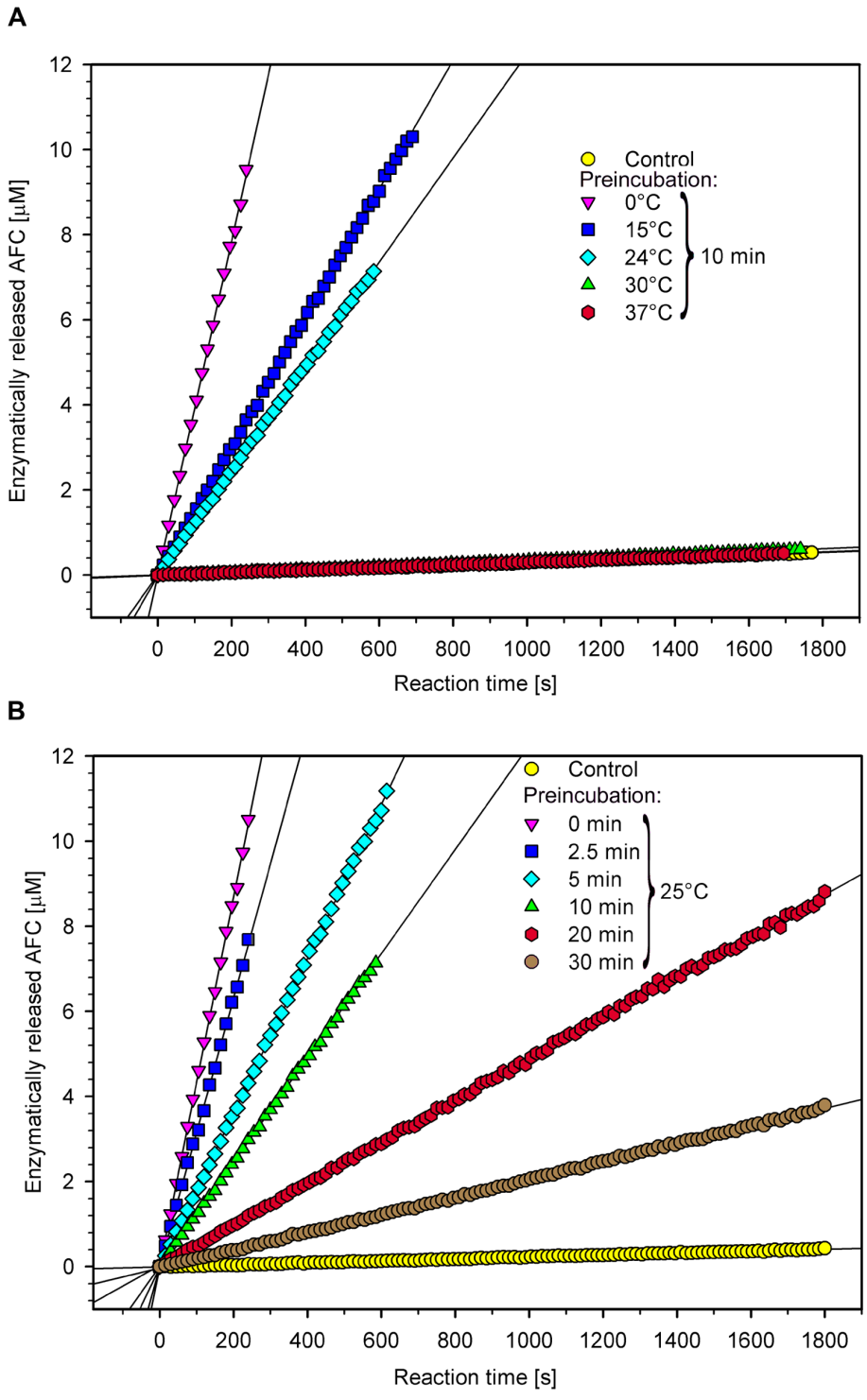

Figure 19: Effect of thermal pretreatment of NCI-H520 cell-free cytosol on the (cyt-c + dATP)-induced caspase-3-like activity. NCI-H520 cell-free cytosol was preincubated without cyt-c and dATP at (A) different temperatures and for (B) different times, following incubation with exogenously added cyt-c and dATP at 37°C for 30 min. Enzymatically released AFC was measured fluorometrically as described in Matherials and Methods. One representative data set of three independent experiments is shown.

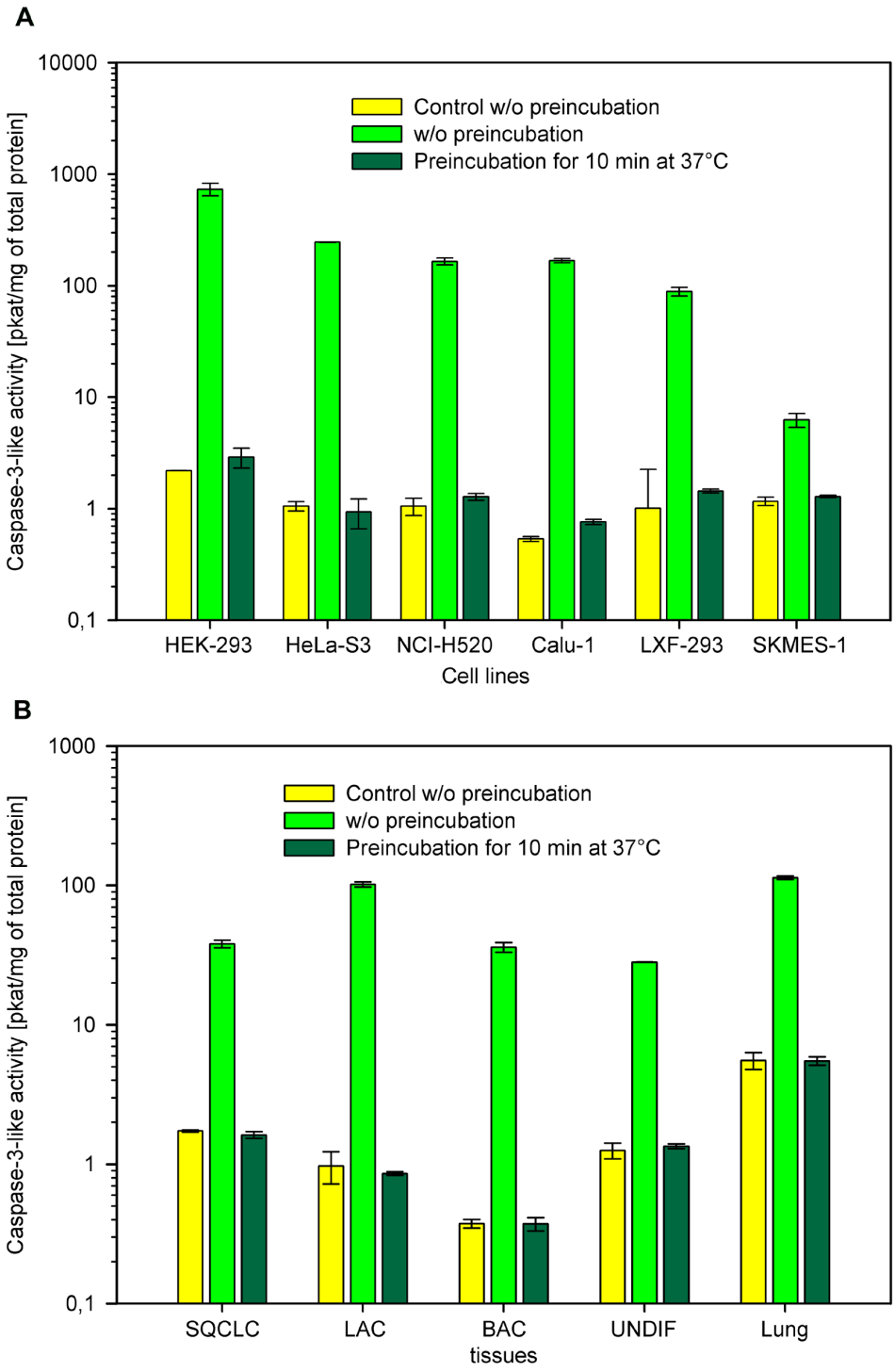

Figure 20: Effect of thermal pretreatment of cell-free cytosols from cell lines, NSCLC tumours and lung parenchyma on the (cyt-c + dATP)-induced caspase-3-like activity. Cell-free cytosols were incubated without (yellow) or with (light green) cyt-c and dATP or were preincubated without cyt-c and dATP at 37°C for 10 min following addition of cyt-c and dATP and incubation at 37°C for 30 min (dark green). Enzymatically released AFC was measured fluorometrically as described in Matherials and Methods. Data represents means ± standard error of the mean from three independent experiments.

Table 8: Analysis of the (cyt-c + dATP)-induced activation of apoptosome apparatus in cytosol from non-small cell lung carcinoma and lung tissues via measurement of increase of the endogenous caspase-3-like activity.

Category of caspase-3-like activity	Caspase-3-like activity[a,b] (pkat/mg of total protein)		Statistical difference (P) of caspase-3-like activity in Tu *versus* Lu[c]
	Tumours (Tu)	Lungs (Lu)	
Endogenous (E)	0.717 (0-7.710)	0.019 (0.1.351)	9.2×10^{-11}
Total (T)	1.428 (0-88.706)	0.064 (0-5.645)	9.8×10^{-11}
Incremental induced (I)[d]	0.289 (0-88.429)	0.004 (0-5.245)	1.3×10^{-5}
Activity ratio I/E[e]	1.068 (0.032-536.343)	0.488 (0.001-28.396)	

[a] A total of 62 NSCLC patients was studied including 29 patients with SQCLC, 26 patients with LAC, 1 patient with SQCLC+LAC mixed type tumour, 1 patient with LCLC, 3 patients with SLC, and 2 patients with UNDIF.
[b] Data are represented as the median with the range in parentheses.
[c] Statistical difference of caspase-3-like activity in Tumour versus Lungs was calculated using Mann-Whitney test.
[d] Incremental induced activity was calculated as follows: total activity - endogenous activity.
[e] The positive ratio I/E could be calculated in 47 tumours and 29 lungs. Chi-square test showed that the apoptosome apparatus was more frequently activated in tumour cytosols than in lung cytosols (P = 0.0017).

c+dATP)-dependent activatability of AA was rapidly lost by thermal pretreatment of cell-free cytosol. Moreover, the preincubation at 37°C for 10 min lead to irreversible loss of the AA activatability in all cell-free cytosol samples tested, including cytosols from six cell lines, four NSCLC tumours of different histopathological types as well as lung parenchyma (Figure 20). These results provide evidence that the loss of AA activatability by thermal treatment of the *ex-vivo* cell-free cytosol is a general phenomenon and must be considered as a critical drawback condition for biochemical experiments analysing mechanisms of AA regulation.

4.8 Apoptosome apparatus in cytosol from NSCLC tumours and its relationship to XIAP

In order to analyse the capability of AA to be activated in NSCLC tumours, we studied the activatability of AA by cyt-c and dATP in cytosol samples prepared from NSCLC and lung tissues using the fluorometric Ac-DEVD-AFC cleavage assay, which measures the AA-generated caspase-3-like activity. The endogenous (E) as well as the total (T; T = E + I) and the (cyt-c + dATP)-induced incremental (I; I =T - E) caspase-3-like activities were significantly higher in NSCLC tumours as compared to the lungs (Table 8). When only the robust activation (R) of the (cyt-c+dATP)-induced caspase-3-like activity over the endoge-

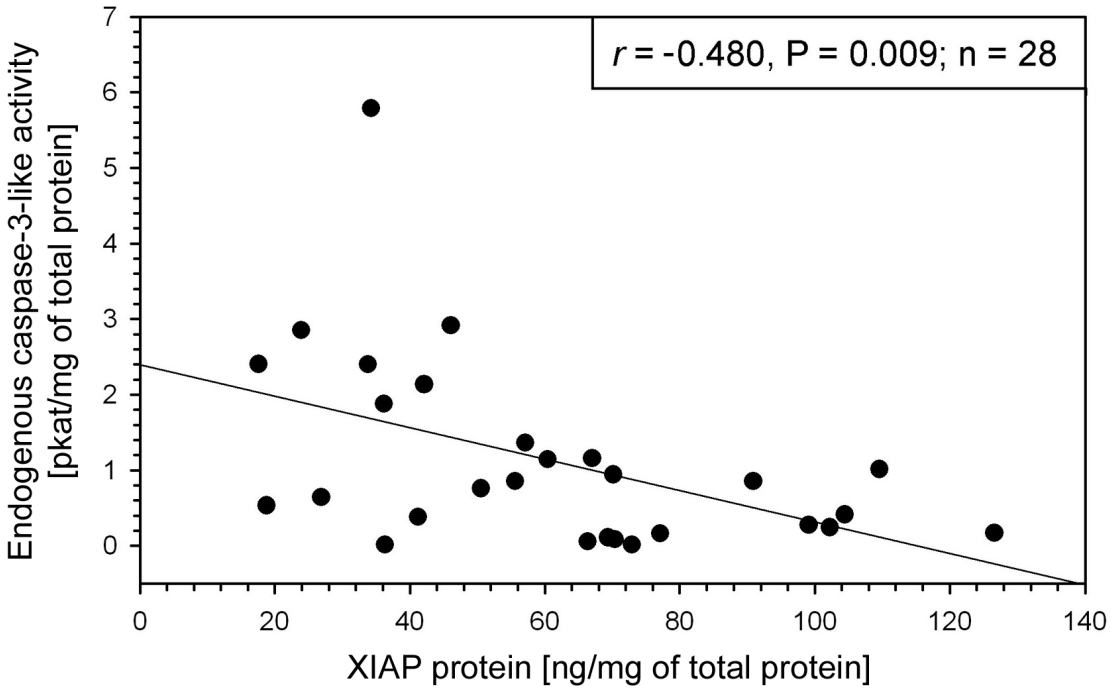

Figure 21: Correlation analysis of the XIAP protein level and the endogenous caspase-3-like activity. The correlation was evaluated between the XIAP protein level and the endogenous caspase-3-like activity in 28 selected NSCLC tumour cytosols. Pearson linear correlation coefficient r and its P-value are indicated.

nous caspase-3-like activity (*i.e.* R $\geq$ 2) was considered, it was found in 19 (31%) of 62 examined tumours and in 5 (8%) of 62 examined lungs (P = 0.0031; Chi-square test). When we considered the robust and the weak degrees of AA activation together (*i.e.* I/E > 0), then the AA activation was found in 47 (76%) tumours and 29 (47%) lungs (P = 0.0017; Chi-square test). These data indicate that AA is more frequently activated in the cytosol from NSCLC tumours compared to the cytosol from lungs. We could not determine caspase-3-like activity increase in 15 (24%) tumours and in 33 (53%) lungs.

We further tested whether XIAP, the direct inhibitor of caspase-9 (Bratton *et al*, 2002; Eckelman *et al*, 2006; Shiozaki *et al*, 2003), played a role in inhibition of AA activity in the cytosol from NSCLC tumours which showed activation response to exogenous cyt-c and dATP. Although there was no inverse correlation between the XIAP protein level and the (cyt-c+dATP)-induced caspase-3-like activity in cytosols from NSCLC tumours (data not shown), we found a significant negative linear correlation between the XIAP protein level and the endogenous caspase-3-like activity in NSCLC tumour cytosols (Figure 21). The inhibition of the apoptosome-associated caspase-9 by XIAP can be reverted by the antiapoptotic protein Smac, which sequesters XIAP and relieves the caspase-9 to activate procaspase-3 to caspase-3, which in turn removes the IAP binding motif (a pentadecapeptide) (Denault *et al*, 2007). To test whether the failure to activate the AA in cytosol from NSCLC tumours involves

inhibition by XIAP, we used XIAP-neutralizing peptides AVPIAQK (P1, a Smac-mimetic peptide) and ATPFQEG (P2, a caspase-9-mimetic peptide), which displayed similar binding affinities toward their target XIAP-BIR3 recombinant polypeptide (Denault *et al*, 2007). Shorter peptides, AVPIA and ATPFQ, were previously shown to be effective derepressors of AA (Srinivasula *et al*, 2001). Using cytosol samples from NSCLC tumours (n = 21), in which AA was activatable by cyt-c and dATP, the endogenous caspase-3-like activity (E) was slightly but significantly increased in the presence of peptide P1, whereas its increase by the peptide P2 was not significant ($P = 7.0 \times 10^{-4}$ and P = 0.082, respectively; Wilcoxon matched-pair test). On the other hand, the (cyt-c+dATP)-induced caspase-3-like activity (I) was significantly increased by the peptide P2 (IP2), while its increase by the peptide P1 (IP1) was not significant (P = 0.012 and P = 0.418, respectively; Wilcoxon matched pair test). In the cytosol from NSCLC tumours, the caspase-3-like activity ratios IP1/I and IP2/I higher than 1.5 were found in 4 (21%) and 9 (47%) of 19 examined NSCLC tumours, respectively (Figure 22). Although the (cyt-c+dATP)-induced caspase-3-like activity was more frequently increased by the peptide P2 compared to the peptide P1, this difference was not statistically significant (P = 0.171, Chi-square test).

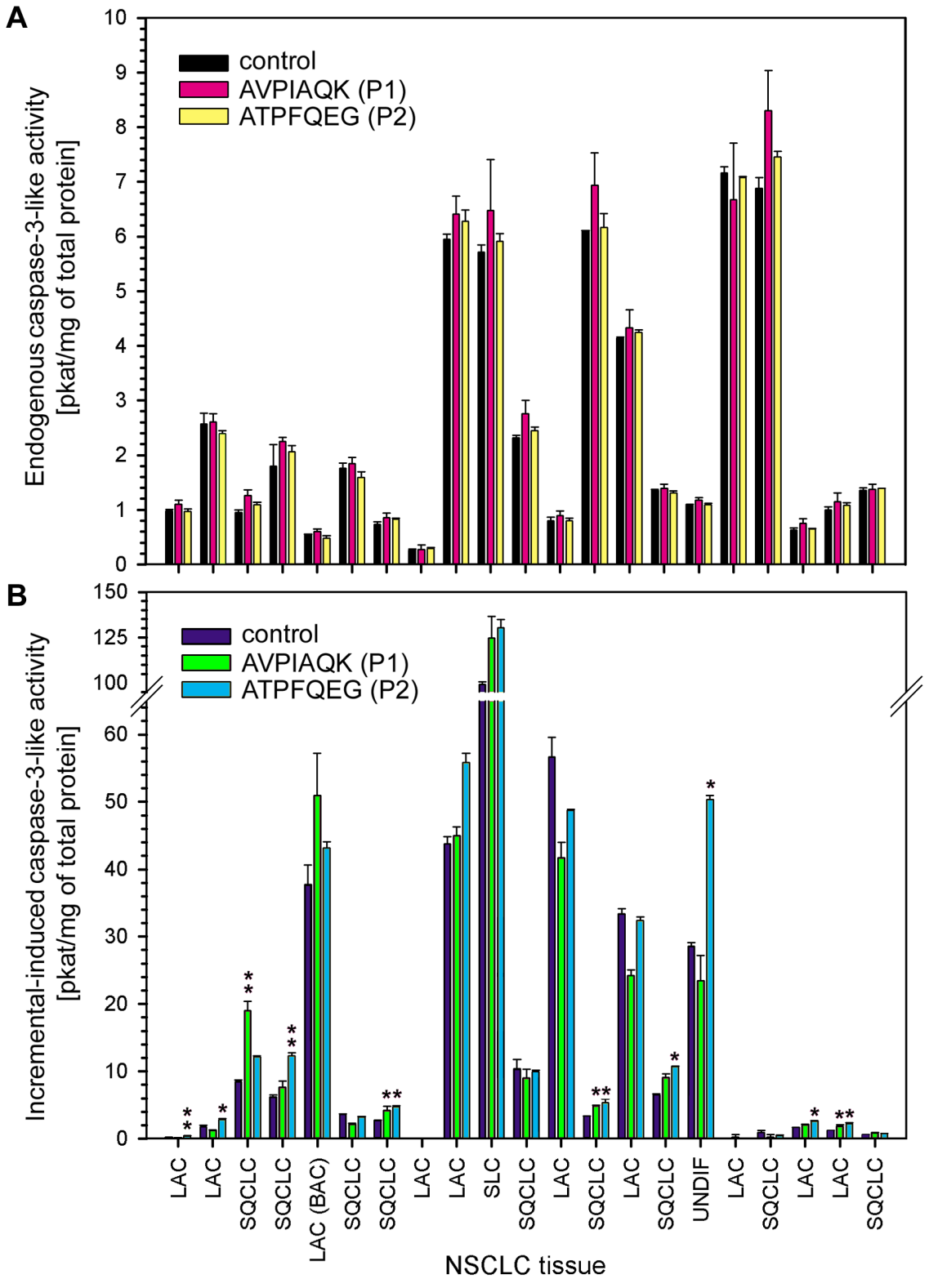

Figure 22: Effect of XIAP-neutralizing peptides on the endogenous and the (cyt-c + dATP)-induced caspase-3-like activity in cell-free cytosols from NSCLC tumours. Cell-free cytosol samples from 21 selected NSCLC tumours were incubated at 37°C for 30 min (A) alone (black), with P1 (purple), with P2 (yellow), and (B) with cyt-c+dATP (violet), with cyt-c+dATP+P1 (green) and with cyt-c+dATP+P2 (blue). The incremental-induced caspase-3-like activities were calculated as described in Materials and Methods. Data indicate mean ± standard error of the mean from three independent experiments. The caspase-3-like activity ratios ((I-P1)/I and (I-P2)/I) higher than 2 (**), and >1.5 but <2 (*) are indicated.

5 Discussion

One of the most interesting protein that regulate the apoptosome pathway is survivin, a member of the IAPs family. Since its discovery by Ambrosini and colleagues in 1997, it was found that this 17 kDa protein is overexpressed in most cancer types. Consistent with previously reported and recent studies (Falleni *et al*, 2003; Nakano *et al*, 2005; Rosato *et al*, 2013), we found that both survivin mRNA and protein are overexpressed in NSCLC cell lines and NSCLC tissues of different histopathological subtypes, while survivin mRNA was significantly higher in SQCLCs as compared to LACs. Concerning the differentiation and the stage of the tumours, survivin mRNA expression was significantly higher in the less-differentiated than in the well-differentiated SQCLCs and LACs, and was also higher in stage IB and stage II+III tumours than in stage IA tumours. Our published immunometric data together with the previously reported immunohistochemical findings (Falleni *et al*, 2003) suggest that survivin may play a role in tumourigenesis and growth of NSCLC neoplasms. This notion is further substantiated by the immunohistochemical detection of increased survivin protein expression in premalignant stages of lung cancerogenesis including squamous metaplasia, dysplasia and atypical adenomatous hyperplasia (Falleni *et al*, 2003; Nakanishi *et al*, 2003; Akyurek *et al*, 2006). The expression of survivin mRNA and protein showed a high positive correlation in NSCLC tumours, but there was lack of correlation of their expression in the lungs. The latter result points to the possibility that there may be an accelerated degradation of the weakly expressed survivin protein in normal lung cells, such as bronchial epithelia (Jin *et al*, 2007), which can be promoted by the XIAP•XAF1 protein complex (Arora *et al*, 2007). This view is supported by ubiquitous expression of XAF1, an antagonist of XIAP, in normal cells and tissues including lung (Chen *et al*, 2011) as well as by high expression of XIAP in normal cells including bronchial epithelia (Vischioni *et al*, 2006).

On the other hand, increased co-expression of several *BIRC5* gene-targeting transcription factors including E2F-1 (Huang *et al*, 2007), Stat3 (Zhang *et al*, 2007), NF-κB (Gradilone *et al*, 2007), and HIF-1α (Chen *et al*, 2009) and low or absent expression of XAF1 (Arora *et al*, 2007; Chen *et al*, 2011a) can contribute to survivin mRNA and protein overexpression in NSCLC cells and tissues. It was shown, that survivin only in complex with HBXIP binds procaspase-9 and prevents its recruitment to apoptosome (Marusawa *et al*, 2003). We found that HBXIP mRNA is abundantly expressed in NSCLC cells and tumours as well as in the lungs. This result together with the differential expression of survivin in lung tumours and lungs indicates that survivin is the limiting factor for the formation of the antiapoptotic survivin•HBXIP complex, which may be preferentially generated in lung tumours to inhibit the apoptosome pathway of apoptosis.

XIAP, a member of the IAPs family, which can inhibit the apoptosome pathway on both the initiation and the execution levels (Scott *et al*, 2005; Twiddy *et al*, 2006; Denault *et al*, 2007), showed a slightly but significantly increased expression in NSCLC tumours compared to the lungs in a group of 34 NSCLC patients (Hofmann *et al*, 2002). In a larger subsequent study, we found that the expression of XIAP mRNA in NSCLC cell lines (n = 10) and matched pairs (n = 150) of NSCLC tumours and lungs was not significantly different. However, we demonstrated a significantly increased level of XIAP protein in LAC tumours, as compared to the lungs. The latter results and the lack of correlation between the levels of XIAP mRNA and protein in the tumours suggest that the expression of XIAP may be translationally upregulated and/or post-translationally stabilised in the tumours. In fact, the translation initiation of XIAP mRNA is internal ribosome entry segment (IRES)-dependent and can be enhanced by several IRES trans-acting factors such as La autoantigen, hnRNP C1/C2 and MDM2 protein (Holcik *et al*, 2000 and 2003; Gu *et al*, 2009). Furthermore, the level of XIAP in cancer cells can be upregulated through protection against the proteasomal degradation-promoting ubiquitination. Such stabilization involves phosphorylation of XIAP by the Akt kinase (Dan *et al*, 2004) or interaction of XIAP with survivin (Dohi *et al*, 2004), Notch receptor (Liu *et al*, 2007) or p34SEI-1 protein (Hong *et al*, 2009). The upregulated expression of XIAP in cancer cells that occurs in response to DNA damage is due to the Che-1 protein- (Bruno *et al*, 2008) and/or MDM2 protein-mediated (Gu *et al*, 2009) activation of XIAP NF-κB-dependent transcription and XIAP IRES-dependent translation, respectively. The expression of XIAP mRNA and protein in NSCLC tumours did not show any significant relationship to clinicopathological factors such as gender, tumour histology, differentiation, and stage. These results are in line with the previously reported data on XIAP expression in NSCLC tumours (Hofmann *et al*, 2002; Ferreira *et al*, 2001a and 2001b).

Although the expression of XIAP and cIAPs in NSCLC tumours does not predict response to classical chemotherapy in patients with advanced NSCLC (Ferreira *et al*, 2001b; Chen *et al*, 2010; Seeger *et al*, 2010), treatment of NSCLC cells as well as other cancer cells with novel synthetic Smac-mimetic antagonists of XIAP and cIAPs induces apoptosis in these cells (Lu *et al*, 2008; Galban *et al*, 2009; Petersen *et al*, 2008; Sun *et al*, 2008; Darding *et al*, 2011) or sensitises them against apoptosis inducers such as nonsteroidal anti-inflammatory drugs and TRAIL (Bank *et al*, 2008; Vogler *et al*, 2009). We found, that a peptide inhibitor of XIAP (ATPFQEG, a caspase-9 p12-mimetic peptide) slightly but significantly increased the (cyt-c+dATP)-induced caspase-3-like activity in NSCLC tumour cytosols. Furthermore, in NSCLC tumour cytosols, XIAP protein levels positively correlated with the endogenous caspase-3-like activity, which itself was slightly but significantly increased in the presence of a Smac-mimetic peptide AVPIAQK.

Surprisingly, NSCLC tumours of different histopathological types showed significantly lower expression of both APIP and UACA mRNAs and proteins as compared to matched lungs. In particular, the expression of UACA mRNA was down-regulated with a high frequency in NSCLC tumours. The lower level of UACA mRNA in stage IA tumours as compared to higher stage tumours suggests that the down-regulation of UACA gene expression is of

particular importance during the earlier period of NSCLC development. The weak increase of expression of both APIP and UACA mRNAs in the decitabine-treated NSCLC cell lines indicates that mechanisms other than DNA methylation are involved in regulation of APIP and UACA genes expression in these cancer cells.

It has been reported that ischemia/hypoxia up-regulates the expression of APIP in some tissues and tumour cells (Cao *et al*, 2004b; Cho *et al*, 2004 and 2007). Although there is evidence that the microenvironment of NSCLC tumours contains many ischemic regions characterized by hypoxia and acidosis (Graves *et al*, 2010), we frequently observed decreased expression of APIP mRNA and protein in NSCLC tumours. The downregulation of APIP gene expression in NSCLC cells and tissues suggests that APIP is probably not involved in suppression of the apoptosome apparatus in these cancer cells. However, APIP may have antiapoptotic effect in other tumour cells such as head and neck squamous cell carcinoma of tongue and larynx where its expression is upregulated and associates with increased copy number of *APIP* gene (Jarvinen *et al*, 2008).

Immunohistochemical studies of stage I NSCLC tumours demonstrated cytoplasmic localization of Apaf-1 (Apaf-1^{Cyt}) in most examined tumours and marked nuclear localization of Apaf-1 (Apaf-1^{Nuc}) in a small subset (24%) of the tumours (Besse *et al*, 2004). Interestingly, the Apaf-1^{Nuc} group of NSCLC patients had significantly better overall survival rate as compared to the Apaf-1^{Cyt} group (Besse *et al*, 2004). Recently, a non-apoptotic role for the intranuclear Apaf-1 in the DNA damage checkpoint activation has been demonstrated (Zermati *et al*, 2007). As increased expression of UACA/nucling has been implicated in promoting Apaf-1 nuclear translocation after proapoptotic stress (Sakai *et al*, 2004), the nuclear translocation of Apaf-1 may be impaired in the majority of NSCLC tumours due to downregulation of UACA expression.

UACA/nucling has been shown to interact with the transcription factor NF-κB and to prevent its nuclear translocation thus reducing expression of the NF-κB-targeted genes (Liu *et al*, 2009). Under the conditions of downregulated expression of UACA in NSCLC cells, we may expect increased nuclear translocation of NF-κB and upregulation of NF-κB-targeted genes, which were shown to mediate cancer cells survival (Chaturvedi *et al*, 2011; Chen *et al*, 2011b).

It was demonstrated, that DNA methylation is involved in downregulated or silenced transcription of Apaf-1 and caspases in some cancer cells and that decitabine-mediated increase of Apaf-1 or caspases levels enhance chemosensitivity of the tumour cells (Soengas *et al*, 2001; Gomyo *et al*, 2004; Christoph *et al*, 2007). Although our *in silico* prediction of possible methylation sites in proximal promoter and first exon regions of *APAF1*, *CASP9* and *CASP3* revealed CpG islands, the treatment with decitabine did not upregulate the mRNA expression of these genes more than 3.2 times. This suggests, that DNA methylation is not heavily involved in regulation of the transcriptional expression of *APAF1*, *CASP9* and *CASP3* genes in NSCLC cells. Furthemore, Apaf-1LN/S splice variants were shown to be incapable of oligomerization due to a missing WD-40 repeat in their regulatory domain (Benedict *et al*, 2000) and were linked with chemotherapy resistance in leukemia cells (Benites *et al*, 2008), while expression of caspase-9S splice variant, a dominant negative inhibitor of procaspase-9,

was linked to various apoptosis stimuli resistance (Seol and Billar, 1999). Nonetheless, we found a significant upregulation of Apaf-1XL/LC activatable variants, as well as procaspase-9 variant in NSCLC tumours and lungs. These results, together with the previous reports demonstrating that NSCLC cells and tumours express increased or sufficient levels of Apaf-1, procaspase-9 and procaspase-3 mRNAs and proteins compared to lungs (Krepela *et al*, 2004 and 2006), predicts that NSCLC tissues are advantageously equipped with the key apoptosome components for inducing apoptosis. However, the induction of functional AA in terms of its capability to generate robust caspase-3-like activity was missing in 3 of 7 investigated NSCLC cell lines and 43 (69%) of 62 examined NSCLC tumours. This suggests that certain NSCLC cell populations possess mechanisms that avoid or suppress the functional AA. It was reported, that two size-different apoptosome complexes are formed in the dATP activated lysates from human tumour cells (THP1, MCF-7, Jurkat). However, only the ∼700-kDa apoptosome complex, but not the ∼1400-kDa one, could activate the zymogens of effector caspases (Cain *et al*, 2000; Almond *et al*, 2001; Twiddy *et al*, 2004 and 2006). We confirmed abundant formation of a high-Mr AA complex of ∼1400 kDa in the (cyt-c+dATP)-activated cell-free cytosol from COLO-699 and CALU-1 cells, however, the ∼700 kDa complex was also detected. Interestingly, procaspase-9 was completely processed to caspase-9, containing the p35 subunit, which coeluted with both apoptosome complexes. However, in COLO-699 cytosol, most caspase-9 was present in low-M_r fractions corresponding to its monomer size. This could be explained by the function of the AA as molecular timer, where procaspase-9 has higher affinity to AA and displaces already processed caspase-9 (Malladi *et al*, 2009). Thus, in CALU-1 and COLO-699 cytosols, apparently all procaspase-9 molecules can be processed within 30 min of the AA activation. By contrast, analysis of the (cyt-c+dATP)-activated cell-free cytosol from A549 cells failed to detect the caspase-9 p35 the p37 subunits in the high-Mr fractions where Apaf-1 protein and procaspase-9 coeluted, thus forming a non-functional AA complex of ∼1400 kDa. Similar results were reported in A549 cells by Hoffarth *et al*(2008). However, we could detect the p35 and p37 caspase-9 subunits in A549 cell-free cytosol regardless of the addition of cyt-c and dATP, when much higher concentration of the anti-caspase-9 antibody was used. Although the origin of the caspase-9 p35 and p37 forms in A549 cells cytosol is not known, for instance, calpains are capable of procaspase-9 cleavage to p35 and p37 caspase-9 forms (Chua *et al*, 2000). In the (cyt-c+dATP)-activated A549 cells cytosol, Apaf-1 monomer was able to oligomerize and bind procaspase-9, but the processing of the apoptosome-associated procaspase-9 was blocked. Moreover, most of the procaspase-9 was present outside the apoptosome. The trace amounts of p35 and p37 caspase-9 forms detected in the apoptosome did not have to be generated by the apoptosome itself, but as extra-apoptosome generated caspase-9 forms they could merely be recruited to the apoptosome via their CARD domains. It was already demonstrated that the p35 and p37 caspase-9 forms could be recruited to apoptosome (Zou *et al*, 2003).

The reason(s) for the blocked processing of the apoptosome-associated procaspase-9 in A549 cells are not known yet. The involvement of caspase-9S can be ruled out, since this caspase-9 spliced isoform, when overexpressed, blocks primarily the recruitment of procaspase-9 to

Apaf-1 oligomer (Srinivasula *et al*, 1999). The possible candidate mechanisms for suppression of the apoptosome-associated procaspase-9 activation might involve the inhibitory phosphorylations of procaspase-9 (Kurokawa and Kornbluth, 2009; Allan and Clarke, 2009). However, this seems also to be unlikely, because APIP protein, the activator of Akt and Erk1/2 protein kinases that can introduce the inhibitory phosphorylations into procaspase-9 (Cho *et al*, 2007), is strongly downregulated in NSCLC cells and tumours (Moravcikova *et al*, 2012).
Importantly, in the (cyt-c+dATP)-activatable cell-free cytosols from NSCLC cell lines two distinct mechanisms can be seen in procaspase-9 processing. The first one involves procaspase-9 monomer autoprocessing to a caspase-9 form having the p35 and p12 subunits. The second one is a feedback processing mediated by caspase-3 that cleaves procaspase-9 monomer to a caspase-9 form containing the p37 and p10 subunits. Generation of the p35 caspase-9 form precedes the formation of the p37 caspase-9 form, which starts to be produced once the apoptosome-associated caspase-9 p35/p12 form proteolytically converts procaspase-3 to active caspase-3 (Zou *et al*, 2003; Denault *et al*, 2007).
Interestingly, both, the processing of procaspase-9 to its p37 form and the generation of active caspase-3 were completely blocked by the caspase aldehyde inhibitor Ac-DEVD-CHO. Thus, the inhibitor does not inhibit the apoptosome-dependent procaspase-9 activation to caspase-9 p35 form, but it inhibits the apoptosome-associated caspase-9 p35 form. This finding is consistent with a study by Srinivasula and colleagues (Srinivasula *et al*, 1998).
Furthermore, we provided evidence that mere incubation of cell-free cytosol from COLO-699 cells without cyt-c and dATP leads to formation of an aggregate of Apaf-1 monomers, which is not able to recruit and activate procaspase-9. However, formation of Apaf-1 aggregates is an irreversible process, which extent increases with time and temperature of incubation in all studied cell and tissue cytosols including cytosols prepared from NSCLC tumours and lungs. The irreversible inactivation of Apaf-1 in the absence of dATP was also observed by Kim *et al*, 2005. Therefore, preincubation of cell-free cytosol intended to reactivate modified AA component without simultaneous addition of cyt-c+dATP certainly leads to irreversible loss of AA activatability, unless the temperature is kept at 4°C or below (Cardone *et al*, 1998; Kim *et al*, 2008). The aggregation and hence inactivation of Apaf-1 at 37°C does not occur *in vivo*. Although the reason for this event is still not clear yet, it probably involves sustained (d)ATP sufficiency in the living cell. It seems that (d)ATP might play an important role in maintaining Apaf-1 in a cyt-c-activatable state (Zhang *et al*, 2011). By contrast, procaspase-2 activation platform, called PIDDosome, can assemble from monomeric components, such as PIDD-1 and RAIDD/CRADD, into a functional complex spontaneously at 37°C (Tinel and Tschopp, 2004).
Taken together, our results suggest a higher predisposition to AA-mediated apoptosis in NSCLC tumours than in lungs (Moravcikova *et al*, submitted). Similar findings were reported for breast carcinomas and brain tumours compared to their counterpart normal tissues (Schafer *et al*, 2006; Johnson *et al*, 2007). The higher propensity of NSCLC tumours to apoptosome-mediated apoptosis is due to several factors. First, because of increased expression of activatable apoptosome pathway core protein components in NSCLC tumours, includ-

ing Apaf-1 and procaspases-9 and -3. Second, because of the down-regulation of expression of APIP and UACA genes causing the lack of APIP-mediated AA suppression and UACA-assisted Apaf-1 nuclear entry, which would lead to the failure of DNA damage checkpoint activation in NSCLC cells leading to their genomic instability and contributing to development and progression of NSCLC tumours. However, the functionality of AA is suppressed in some NSCLC cell lines and in a high proportion of NSCLC tumours. In conclusion, our results indicate that the XIAP-mediated inhibition is not the major suppressor mechanism of apoptosome pathway induction in NSCLC tumours and that failure of the apoptosome-bound procaspase-9 activation may underlie the malfunction of apoptosome pathway in NSCLC cells.

List of Figures

List of Tables

List of publications

Papers related to the thesis

E.Moravcikova, E. Krepela, J. Prochazka, Cermak, and K. Benkova. Apoptosome apparatus in non-small cell lung carcinoma. Submitted to Br. J. Cancer.

E.Moravcikova, E. Krepela, J. Prochazka, I. Rousalova, J. Cermak, and K. Benkova. Downregulated expression of apoptosis-associated genes APIP and UACA in non-small cell lung carcinoma. Int.J.Oncol. 40 (6):2111-2121, 2012. (IF = 2.399)

E. Krepela, P. Dankova, **E.Moravcikova**, A. Krepelova, J. Prochazka, J. Cermak, J. Schutzner, P. Zatloukal, and K. Benkova. Increased expression of inhibitor of apoptosis proteins, survivin and XIAP, in non-small cell lung carcinoma. Int.J.Oncol. 35 (6):1449-1462, 2009. (IF = 2.399)

Published papers

L. Janovec, D. Sabolova, M. Kozurkova, H. Paulikova, P. Kristian, **E.Moravcikova**, M. Bajdichova, D. Podhradsky, J. Imrich. Synthesis, DNA interaction, and cytotoxic activity of a novel proflavine-dithiazolidinone pharmacophore. Bioconjug.Chem. 18(1):93-100, 2007. (IF = 4.930)

Published abstracts

E.Moravcikova, E. Krepela, J. Prochazka, J. Cermak, and K. Benkova. Expression and activation of the appoptosome apparatus core components in non-small cell lung carcinoma. 22nd IUBMB and 37th FEBS Congress, Sevilla, Spain. FEBS J. 279(s1):52, 2012.

E. Krepela, I. Rousalova, **E.Moravcikova**, J. Prochazka. DNA methylation downregulates expression of several apoptosis-associated and tumor suppressor genes in non-small cell lung carcinoma cells. 13th Central European Lung Cancer Conference, Prague, Czech Republic. Lung Cancer. 77(s1):8-9, 2012.

E. Krepela and **E.Moravcikova**. Inhibition of apoptosome apparatus in non-small cell lung cancer. 16th World Congress on Advances in Oncology and 14th International Symposium on Molecular Medicine. Int. J. Mol. Medicine. 28(s):14, 2011.

E.Moravcikova, E. Krepela, J. Prochazka, J. Cermak, and K. Benkova. Frequent dysfunction of apoptosome apparatus in human non-small cell lung cancer cells and tissues. 36th FEBS Congress, Torino, Italy. FEBS J. 278(s1):349, 2011.

E.Moravcikova, E. Krepela, J. Prochazka, J. Cermak, and K. Benkova. The functionality of apoptosome apparatus and the expression of its regulators in non-small cell lung carcinoma. XXII. Biochemicky zjazd CSBMB A SSBMB Martin, Zbornik abstraktov:187, 2010.

E.Moravcikova, E. Krepela, J. Cermak, and K. Benkova. Apoptosome pathway activation in non-small cell lung cancer cells a tissues. 34th FEBS Congress, Prague, Czech Republic. FEBS J. 254(s1):265, 2009.

E.Moravcikova, E. Krepela, J. Cermak, and K. Benkova. Functional status of apoptosome apparatus in non-small cell lung cancer cells and tissues. 21st IUBMB International Congress and 12th FAOBMB Congress of Biochemistry and Molecular Biology, Schanghai, China. Abstracts:156, 2009.

E.Moravcikova, E. Krepela, J. Prochazka, J. Cermak, and K. Benkova. Malfunction of apoptosome pathway in non-small cell lung cancer cells. XXI. Biochemicky sjezd CSBMB A SSBMB Ceske Budejovice, Sbornik prednasek a posteru:123, 2008.

Bibliography

D. Acehan, X. Jiang, D. G. Morgan, J. E. Heuser, X. Wang, and C. W. Akey. Three-dimensional structure of the apoptosome: implications for assembly, procaspase-9 binding, and activation. Mol.Cell 9 (2):423-432, 2002.

N. Akyurek, L. Memis, O. Ekinci, N. Kokturk, and C. Ozturk. Survivin expression in pre-invasive lesions and non-small cell lung carcinoma. Virchows Arch. 449 (2):164-170, 2006.

L. A. Allan and P. R. Clarke. Apoptosis and autophagy: Regulation of caspase-9 by phosphorylation. FEBS J. 276 (21):6063-6073, 2009.

L. A. Allan and P. R. Clarke. Phosphorylation of caspase-9 by CDK1/cyclin B1 protects mitotic cells against apoptosis. Mol.Cell 26 (2):301-310, 2007.

L. A. Allan, N. Morrice, S. Brady, G. Magee, S. Pathak, and P. R. Clarke. Inhibition of caspase-9 through phosphorylation at Thr 125 by ERK MAPK. Nat.Cell Biol. 5 (7):647-654, 2003.

J. B. Almond, R. T. Snowden, A. Hunter, D. Dinsdale, K. Cain, and G. M. Cohen. Proteasome inhibitor-induced apoptosis of B-chronic lymphocytic leukaemia cells involves cytochrome c release and caspase activation, accompanied by formation of an approximately 700 kDa Apaf-1 containing apoptosome complex. Leukemia 15 (9):1388-1397, 2001.

D. C. Altieri. Targeting survivin in cancer. Cancer Lett., 2012.

American Cancer Society. Cancer Facts and Figures 2012, Atlanta. American Cancer Society, 2012

D. E. Andreev, S. E. Dmitriev, R. Zinovkin, I. M. Terenin, and I. N. Shatsky. The 5' untranslated region of Apaf-1 mRNA directs translation under apoptosis conditions via a 5' end-dependent scanning mechanism. FEBS Lett. 586 (23):4139-4143, 2012.

H. Appelqvist, A. C. Johansson, E. Linderoth, U. Johansson, B. Antonsson, R. Steinfeld, K. Kagedal, and K. Ollinger. Lysosome-mediated apoptosis is associated with cathepsin D-specific processing of bid at Phe24, Trp48, and Phe183. Ann.Clin.Lab Sci. 42 (3):231-242, 2012.

R. Arora, M. Shuda, A. Guastafierro, H. Feng, T. Toptan, Y. Tolstov, D. Normolle, L. L. Vollmer, A. Vogt, A. Domling, J. L. Brodsky, Y. Chang, and P. S. Moore. Survivin is a therapeutic target in Merkel cell carcinoma. Sci.Transl.Med. 4 (133):133ra56, 2012.

V. Arora, H. H. Cheung, S. Plenchette, O. C. Micali, P. Liston, and R. G. Korneluk. Degradation of survivin by the X-linked inhibitor of apoptosis (XIAP)-XAF1 complex. J.Biol.Chem. 282 (36):26202-26209, 2007.

A. L. Astier, M. Svoboda, E. Hinds, R. De Beaumont, O. Munoz, and A. S. Freedman. Integrins regulate survival of pre-B-ALL cells through differential IAP and caspase-7 ubiquitination and degradation. Leukemia 18 (4):873-875, 2004.

J. Bai, J. R. Brody, S. H. S. Kadkol, and G. R. Pasternack. Tumor suppression and potentiation by manipulation of pp32 expression. Oncogene 20 (17):2153, 2001.

B. R. Balsara, J. Pei, Y. Mitsuuchi, R. Page, A. Klein-Szanto, H. Wang, M. Unger, and J. R. Testa. Frequent activation of AKT in non-small cell lung carcinomas and preneoplastic bronchial lesions. Carcinogenesis 25 (11):2053-2059, 2004.

A. Bank, P. Wang, C. Du, J. Yu, and L. Zhang. SMAC mimetics sensitize nonsteroidal anti-inflammatory drug-induced apoptosis by promoting caspase-3-mediated cytochrome c release. Cancer Res 68 (1):276-284, 2008.

Q. Bao, W. Lu, J. D. Rabinowitz, and Y. Shi. Calcium blocks formation of apoptosome by preventing nucleotide exchange in Apaf-1. Mol.Cell 25 (2):181-192, 2007.

Q. Bao, S. J. Riedl, and Y. Shi. Structure of Apaf-1 in the auto-inhibited form: a critical role for ADP. Cell Cycle 4 (8):1001-1003, 2005.

M. A. Bareschino, C. Schettino, A. Rossi, P. Maione, P. C. Sacco, R. Zeppa, and C. Gridelli. Treatment of advanced non small cell lung cancer. J.Thorac.Dis. 3 (2):122-133, 2011.

M. B. Beasley, E. Brambilla, and W. D. Travis. The 2004 World Health Organization classification of lung tumors. Semin.Roentgenol. 40 (2):90-97, 2005.

M. A. Benedict, Y. Hu, N. Inohara, and G. Nunez. Expression and functional analysis of Apaf-1 isoforms. Extra Wd-40 repeat is required for cytochrome c binding and regulated activation of procaspase-9. J.Biol.Chem. 275 (12):8461-8468, 2000.

B. D. Benites, A. Fattori, C. Hackel, I. Lorand-Metze, C. A. De Souza, E. Schulz, F. F. Costa, and S. T. Saad. Low expression of APAF-1XL in acute myeloid leukemia may be associated with the failure of remission induction therapy. Braz.J.Med.Biol.Res. 41 (7):571-578, 2008.

B. Besse, C. Cande, J. P. Spano, A. Martin, D. Khayat, T. Le Chevalier, T. Tursz, L. Sabatier, J. C. Soria, and G. Kroemer. Nuclear localization of apoptosis protease activating factor-1 predicts survival after tumor resection in early-stage non-small cell lung cancer. Clin.Cancer Res 10 (17):5665-5669, 2004.

K. M. Boatright, M. Renatus, F. L. Scott, S. Sperandio, H. Shin, I. M. Pedersen, J. E. Ricci, W. A. Edris, D. P. Sutherlin, and D. R. Green. A unified model for apical caspase activation. Molecular cell 11 (2):529-541, 2003.

P. Boya and G. Kroemer. Lysosomal membrane permeabilization in cell death. Oncogene 27 (50):6434-6451, 2008.

S. C. Brady, L. A. Allan, and P. R. Clarke. Regulation of caspase 9 through phosphorylation by protein kinase C zeta in response to hyperosmotic stress. Mol.Cell Biol. 25 (23):10543-10555, 2005.

S. B. Bratton and G. S. Salvesen. Regulation of the Apaf-1-caspase-9 apoptosome. J.Cell Sci. 123 (Pt 19):3209-3214, 2010.

S. B. Bratton, J. Lewis, M. Butterworth, C. S. Duckett, and G. M. Cohen. XIAP inhibition of caspase-3 preserves its association with the Apaf-1 apoptosome and prevents. Cell Death.Differ. 9 (9):881-892, 2002.

S. B. Bratton, G. Walker, D. L. Roberts, K. Cain, and G. M. Cohen. Caspase-3 cleaves Apaf-1 into an approximately 30 kDa fragment that associates with an inappropriately oligomerized and biologically inactive approximately 1.4 MDa apoptosome complex. Cell Death.Differ. 8 (4):425-433, 2001a.

S. B. Bratton, G. Walker, S. M. Srinivasula, X. M. Sun, M. Butterworth, E. S. Alnemri, and G. M. Cohen. Recruitment, activation and retention of caspases-9 and -3 by Apaf-1 apoptosome and associated XIAP complexes. EMBO J. 20 (5):998-1009, 2001b.

J. R. Brody, A. Witkiewicz, T. K. Williams, S. S. Kadkol, J. Cozzitorto, B. Durkan, G. R. Pasternack, and C. J. Yeo. Reduction of pp32 expression in poorly differentiated pancreatic ductal adenocarcinomas and intraductal papillary mucinous neoplasms with moderate dysplasia. Mod.Pathol. 20 (12):1238-1244, 2007.

M. Broemer and P. Meier. Ubiquitin-mediated regulation of apoptosis. Trends Cell Biol. 19 (3):130-140, 2009.

J. Brognard, A. S. Clark, Y. Ni, and P. A. Dennis. Akt/protein kinase B is constitutively active in non-small cell lung cancer cells and promotes cellular survival and resistance to chemotherapy and radiation. Cancer Res. 61 (10):3986-3997, 2001.

J. M. Brown and L. D. Attardi. The role of apoptosis in cancer development and treatment response. Nat.Rev.Cancer 5 (3):231-237, 2005.

T. Bruno, S. Iezzi, F. De Nicola, M. Di Padova, A. Desantis, M. Scarsella, M. G. Di Certo, C. Leonetti, A. Floridi, C. Passananti, and M. Fanciulli. Che-1 activates XIAP expression in response to DNA damage. Cell Death.Differ. 15 (3):515-520, 2008.

K. Cain, C. Langlais, X. M. Sun, D. G. Brown, and G. M. Cohen. Physiological concentrations of K+ inhibit cytochrome c-dependent formation of the apoptosome. J.Biol.Chem. 276 (45):41985-41990, 2001.

K. Cain, S. B. Bratton, C. Langlais, G. Walker, D. G. Brown, X. M. Sun, and G. M. Cohen. Apaf-1 oligomerizes into biologically active approximately 700-kDa and inactive approximately 1.4-MDa apoptosome complexes. J.Biol.Chem. 275 (9):6067-6070, 2000.

A. Cammas, F. Pileur, S. Bonnal, S. M. Lewis, N. Leveque, M. Holcik, and S. Vagner. Cytoplasmic relocalization of heterogeneous nuclear ribonucleoprotein A1 controls translation initiation of specific mRNAs. Mol.Biol.Cell 18 (12):5048-5059, 2007.

C. Cao, Y. Mu, D. E. Hallahan, and B. Lu. XIAP and survivin as therapeutic targets for radiation sensitization in preclinical models of lung cancer. Oncogene 23 (42):7047-7052, 2004a.

G. Cao, M. Xiao, F. Sun, X. Xiao, W. Pei, J. Li, S. H. Graham, R. P. Simon, and J. Chen. Cloning of a novel Apaf-1-interacting protein: a potent suppressor of apoptosis and ischemic neuronal cell death. J.Neurosci. 24 (27):6189-6201, 2004b.

M. H. Cardone, N. Roy, H. R. Stennicke, G. S. Salvesen, T. F. Franke, E. Stanbridge, S. Frisch, and J. C. Reed. Regulation of cell death protease caspase-9 by phosphorylation. Science 282 (5392):1318-1321, 1998.

F. Cecconi, G. Alvarez-Bolado, B. I. Meyer, K. A. Roth, and P. Gruss. Apaf1 (CED-4 homolog) regulates programmed cell death in mammalian development. Cell 94 (6):727, 1998.

M. H. Cesen, K. Pegan, A. Spes, and B. Turk. Lysosomal pathways to cell death and their therapeutic applications. Exp.Cell Res. 318 (11):1245-1251, 2012.

C. E. Chalfant, K. Rathman, R. L. Pinkerman, R. E. Wood, L. M. Obeid, B. Ogretmen, and Y. A. Hannun. De novo ceramide regulates the alternative splicing of caspase 9 and Bcl-x in A549 lung adenocarcinoma cells. Dependence on protein phosphatase-1. J.Biol.Chem. 277 (15):12587-12595, 2002.

Y. Chao, E. N. Shiozaki, S. M. Srinivasula, D. J. Rigotti, R. Fairman, and Y. Shi. Engineering a dimeric caspase-9: a re-evaluation of the induced proximity model for caspase activation. PLoS.Biol. 3 (6):e183, 2005.

M. M. Chaturvedi, B. Sung, V. R. Yadav, R. Kannappan, and B. B. Aggarwal. NF-kappaB addiction and its role in cancer: 'one size does not fit all'. Oncogene 30 (14):1615-1630, 2011.

X. Q. Chen, S. Yang, Z. Y. Li, H. S. Lu, M. Q. Kang, and T. Y. Lin. Effects and mechanism of downregulation of survivin expression by RNA interference on proliferation and apoptosis of lung cancer cells. Mol.Med.Report. 5 (4):917-922, 2012.

Y. B. Chen, J. Shu, W. T. Yang, L. Shi, X. F. Guo, F. G. Wang, and Y. Y. Qian. XAF1 as a prognostic biomarker and therapeutic target in squamous cell lung cancer. Chin Med.J.(Engl.) 124 (20):3238-3243, 2011 a.

W. Chen, Z. Li, L. Bai, and Y. Lin. NF-kappaB in lung cancer, a carcinogenesis mediator and a prevention and therapy target. Front Biosci. 16:1172-1185, 2011 b.

P. Chen, J. Li, L. P. Ge, C. H. Dai, and X. Q. Li. Prognostic value of survivin, X-linked inhibitor of apoptosis protein and second mitochondria-derived activator of caspases expression in advanced non-small-cell lung cancer patients. Respirology. 15 (3):501-509, 2010.

Y. Q. Chen, C. L. Zhao, and W. Li. Effect of hypoxia-inducible factor-1alpha on transcription of survivin in non-small cell lung cancer. J.Exp.Clin.Cancer Res. 28:29, 2009.

D. H. Cho, H. J. Lee, H. J. Kim, S. H. Hong, J. O. Pyo, C. Cho, and Y. K. Jung. Suppression of hypoxic cell death by APIP-induced sustained activation of AKT and ERK1/2. Oncogene 26 (19):2809-2814, 2007.

D. H. Cho, Y. M. Hong, H. J. Lee, H. N. Woo, J. O. Pyo, T. W. Mak, and Y. K. Jung. Induced inhibition of ischemic/hypoxic injury by APIP, a novel Apaf-1-interacting protein. J.Biol.Chem. 279 (38):39942-39950, 2004.

Y. E. Choi, M. Butterworth, S. Malladi, C. S. Duckett, G. M. Cohen, and S. B. Bratton. The E3 ubiquitin ligase cIAP1 binds and ubiquitinates caspase-3 and -7 via unique mechanisms at distinct steps in their processing. J.Biol.Chem. 284 (19):12772-12782, 2009.

F. Christoph, S. Hinz, S. Weikert, C. Kempkensteffen, M. Schostak, K. Miller, and M. Schrader. Comparative promoter methylation analysis of p53 target genes in urogenital cancers. Urol.Int. 80 (4):398-404, 2008.

F. Christoph, S. Hinz, C. Kempkensteffen, M. Schostak, M. Schrader, and K. Miller. mRNA expression profiles of methylated APAF-1 and DAPK-1 tumor suppressor genes uncover clear cell renal cell carcinomas with aggressive phenotype. J.Urol. 178 (6):2655-2659, 2007.

B. T. Chua, K. Guo, and P. Li. Direct cleavage by the calcium-activated protease calpain can lead to inactivation of caspases. J.Biol.Chem. 275 (7):5131-5135, 2000.

M. J. Clemens, M. Bushell, and S. J. Morley. Degradation of eukaryotic polypeptide chain initiation factor (eIF) 4G in response to induction of apoptosis in human lymphoma cell lines. Oncogene 17 (22):2921-2931, 1998.

M. Corvaro, C. Fuoco, M. Wagner, and F. Cecconi. Analysis of apoptosome dysregulation in pancreatic cancer and of its role in chemoresistance. Cancer Biol.Ther. 6 (2):209-217, 2007.

S. P. Cullen, M. Brunet, and S. J. Martin. Granzymes in cancer and immunity. Cell Death & Differentiation 17 (4):616-623, 2010.

G. R. Dahal, P. Karki, A. Thapa, M. Shahnawaz, S. Y. Shin, J. S. Lee, B. Cho, and I. S. Park. Caspase-2 cleaves DNA fragmentation factor (DFF45)/inhibitor of caspase-activated DNase (ICAD). Arch.Biochem.Biophys. 468 (1):134-139, 2007.

R. B. Damgaard and M. Gyrd-Hansen. Inhibitor of apoptosis (IAP) proteins in regulation of inflammation and innate immunity. Discov.Med. 11 (58):221-231, 2011.

H. C. Dan, M. Sun, S. Kaneko, R. I. Feldman, S. V. Nicosia, H. G. Wang, B. K. Tsang, and J. Q. Cheng. Akt phosphorylation and stabilization of X-linked inhibitor of apoptosis protein (XIAP). J.Biol.Chem. 279 (7):5405-5412, 2004.

M. Darding and P. Meier. IAPs: guardians of RIPK1. Cell Death.Differ. 19 (1):58-66, 2012.

M. Darding, R. Feltham, T. Tenev, K. Bianchi, C. Benetatos, J. Silke, and P. Meier. Molecular determinants of Smac mimetic induced degradation of cIAP1 and cIAP2. Cell Death.Differ. 18 (8):1376-1386, 2011.

P. B. Deming, Z. T. Schafer, J. S. Tashker, M. B. Potts, M. Deshmukh, and S. Kornbluth. Bcr-Abl-mediated protection from apoptosis downstream of mitochondrial cytochrome c release. Mol.Cell Biol. 24 (23):10289-10299, 2004.

J. B. Denault, B. P. Eckelman, H. Shin, C. Pop, and G. S. Salvesen. Caspase 3 attenuates XIAP (X-linked inhibitor of apoptosis protein)-mediated inhibition of caspase 9. Biochem.J. 405 (1):11-19, 2007.

L. S. Dickens, R. S. Boyd, R. Jukes-Jones, M. A. Hughes, G. L. Robinson, L. Fairall, J. W. Schwabe, K. Cain, and M. Macfarlane. A death effector domain chain DISC model reveals a crucial role for caspase-8 chain assembly in mediating apoptotic cell death. Mol.Cell 47 (2):291-305, 2012.

T. Dohi, K. Okada, F. Xia, C. E. Wilford, T. Samuel, K. Welsh, H. Marusawa, H. Zou, R. Armstrong, S. Matsuzawa, G. S. Salvesen, J. C. Reed, and D. C. Altieri. An IAP-IAP complex inhibits apoptosis. J.Biol.Chem. 279 (33):34087-34090, 2004.

M. Donepudi, A. M. Sweeney, C. Briand, and M. G. Gr+-tter. Insights into the regulatory mechanism for caspase-8 activation. Molecular cell 11 (2):543-549, 2003.

F. Dong, W. Guo, L. Zhang, S. Wu, F. Teraishi, J. J. Davis, and B. Fang. Downregulation of XIAP and induction of apoptosis by the synthetic cyclin-dependent kinase inhibitor GW8510 in non-small cell lung cancer cells. Cancer Biol.Ther. 5 (2):165-170, 2006.

H. Duan, K. Orth, A. M. Chinnaiyan, G. G. Poirier, C. J. Froelich, W. W. He, and V. M. Dixit. ICE-LAP6, a novel member of the ICE/Ced-3 gene family, is activated by the cytotoxic T cell protease granzyme B. J.Biol.Chem. 271 (28):16720-16724, 1996.

M. J. Duffy, N. O'Donovan, D. J. Brennan, W. M. Gallagher, and B. M. Ryan. Survivin: a promising tumor biomarker. Cancer Lett. 249 (1):49-60, 2007.

B. P. Eckelman, G. S. Salvesen, and F. L. Scott. Human inhibitor of apoptosis proteins: why XIAP is the black sheep of the family. EMBO Rep. 7 (10):988-994, 2006.

M. Falleni, C. Pellegrini, A. Marchetti, B. Oprandi, F. Buttitta, F. Barassi, L. Santambrogio, G. Coggi, and S. Bosari. Survivin gene expression in early-stage non-small cell lung cancer. J.Pathol. 200 (5):620-626, 2003.

H. O. Fearnhead, J. Rodriguez, E. E. Govek, W. Guo, R. Kobayashi, G. Hannon, and Y. A. Lazebnik. Oncogene-dependent apoptosis is mediated by caspase-9. Proc.Natl.Acad.Sci.U.S.A 95 (23):13664-13669, 1998.

A. E. Feldstein, N. W. Werneburg, Z. Z. Li, S. F. Bronk, and G. J. Gores. Bax inhibition protects against free fatty acid-induced lysosomal permeabilization. American Journal of Physiology-Gastrointestinal and Liver Physiology 290 (6):G1339-G1346, 2006.

C. G. Ferreira, der van, V, S. W. Span, I. Ludwig, E. F. Smit, F. A. Kruyt, H. M. Pinedo, H. van Tinteren, and G. Giaccone. Expression of X-linked inhibitor of apoptosis as a novel prognostic marker in radically resected non-small cell lung cancer patients. Clin.Cancer Res 7 (8):2468-2474, 2001 a.

C. G. Ferreira, der van, V, S. W. Span, J. M. Jonker, P. E. Postmus, F. A. Kruyt, and G. Giaccone. Assessment of IAP (inhibitor of apoptosis) proteins as predictors of response to chemotherapy in advanced non-small-cell lung cancer patients. Ann.Oncol. 12 (6):799-805, 2001 b.

U. Fischer, R. U. Janicke, and K. Schulze-Osthoff. Many cuts to ruin: a comprehensive update of caspase substrates. Cell Death.Differ. 10 (1):76-100, 2003.

A. Florentin and E. Arama. Caspase levels and execution efficiencies determine the apoptotic potential of the cell. J.Cell Biol. 196 (4):513-527, 2012.

S. Frutos, J. Moscat, and M. T. Diaz-Meco. Cleavage of zetaPKC but not lambda/iotaPKC by caspase-3 during UV-induced apoptosis. J.Biol.Chem. 274 (16):10765-10770, 1999.

W. A. Fry, H. R. Menck, and D. P. Winchester. The National Cancer Data Base report on lung cancer. Cancer 77 (9):1947-1955, 1996.

W. N. Fu, F. Bertoni, S. M. Kelsey, S. M. McElwaine, F. E. Cotter, A. C. Newland, and L. Jia. Role of DNA methylation in the suppression of Apaf-1 protein in human leukaemia. Oncogene 22 (3):451-455, 2003.

P. Fuentes-Prior and G. S. Salvesen. The protein structures that shape caspase activity, specificity, activation and inhibition. Biochem.J. 384 (Pt 2):201-232, 2004.

S. Fulda. Apoptosis pathways and their therapeutic exploitation in pancreatic cancer. J.Cell Mol.Med. 13 (7):1221-1227, 2009.

Y. Furukawa, K. Sutheesophon, T. Wada, M. Nishimura, Y. Saito, H. Ishii, and Y. Furukawa. Methylation silencing of the Apaf-1 gene in acute leukemia. Mol.Cancer Res. 3 (6):325-334, 2005.

S. Galban, C. Hwang, J. M. Rumble, K. A. Oetjen, C. W. Wright, A. Boudreault, J. Durkin, J. W. Gillard, J. B. Jaquith, S. J. Morris, and C. S. Duckett. Cytoprotective effects of IAPs revealed by a small molecule antagonist. Biochem.J. 417 (3):765-771, 2009.

L. Galluzzi, M. C. Maiuri, I. Vitale, H. Zischka, M. Castedo, L. Zitvogel, and G. Kroemer. Cell death modalities: classification and pathophysiological implications. Cell Death.Differ. 14 (7):1237-1243, 2007.

C. Garrido, L. Galluzzi, M. Brunet, P. E. Puig, C. Didelot, and G. Kroemer. Mechanisms of cytochrome c release from mitochondria. Cell Death.Differ. 13 (9):1423-1433, 2006.

Y. Gomyo, J. Sasaki, C. Branch, J. A. Roth, and T. Mukhopadhyay. 5-aza-2'-deoxycytidine upregulates caspase-9 expression cooperating with p53-induced apoptosis in human lung cancer cells. Oncogene 23 (40):6779-6787, 2004.

A. Gradilone, I. Silvestri, S. Scarpa, S. Morrone, O. Gandini, F. M. Pulcinelli, W. Gianni, L. Frati, A. M. Agliano, and P. Gazzaniga. Failure of apoptosis and activation on NFkappaB by celecoxib and aspirin in lung cancer cell lines. Oncol.Rep. 17 (4):823-828, 2007.

E. E. Graves, A. Maity, and Q. T. Le. The tumor microenvironment in non-small-cell lung cancer. Semin.Radiat.Oncol. 20 (3):156-163, 2010.

L. Gu, N. Zhu, H. Zhang, D. L. Durden, Y. Feng, and M. Zhou. Regulation of XIAP translation and induction by MDM2 following irradiation. Cancer cell 15 (5):363-375, 2009.

M. E. Guicciardi and G. J. Gores. Life and death by death receptors. FASEB J. 23 (6):1625-1637, 2009.

Y. Guo, S. M. Srinivasula, A. Druilhe, T. Fernandes-Alnemri, and E. S. Alnemri. Caspase-2 induces apoptosis by releasing proapoptotic proteins from mitochondria. J.Biol.Chem. 277 (16):13430-13437, 2002.

D. Hanahan and R. A. Weinberg. Hallmarks of cancer: the next generation. Cell 144 (5):646-674, 2011.

Y. Hao, K. Sekine, A. Kawabata, H. Nakamura, T. Ishioka, H. Ohata, R. Katayama, C. Hashimoto, X. Zhang, T. Noda, T. Tsuruo, and M. Naito. Apollon ubiquitinates SMAC and caspase-9, and has an essential cytoprotection function. Nat.Cell Biol. 6 (9):849-860, 2004.

Z. Hao, G. S. Duncan, C. C. Chang, A. Elia, M. Fang, A. Wakeham, H. Okada, T. Calzascia, Y. Jang, A. You-Ten, W. C. Yeh, P. Ohashi, X. Wang, and T. W. Mak. Specific ablation of the apoptotic functions of cytochrome C reveals a differential requirement for cytochrome C and Apaf-1 in apoptosis. Cell 121 (4):579-591, 2005.

G. Hausmann, L. A. O'Reilly, R. van Driel, J. G. Beaumont, A. Strasser, J. M. Adams, and D. C. Huang. Pro-apoptotic apoptosis protease-activating factor 1 (Apaf-1) has a cytoplasmic localization distinct from Bcl-2 or Bcl-x(L). J.Cell Biol. 149 (3):623-634, 2000.

M. M. Hill, C. Adrain, P. J. Duriez, E. M. Creagh, and S. J. Martin. Analysis of the composition, assembly kinetics and activity of native Apaf-1 apoptosomes. EMBO J. 23 (10):2134-2145, 2004.

L. H. Ho, R. Taylor, L. Dorstyn, D. Cakouros, P. Bouillet, and S. Kumar. A tumor suppressor function for caspase-2. Proc.Natl.Acad.Sci.U.S.A 106 (13):5336-5341, 2009.

P. K. Ho, A. M. Jabbour, P. G. Ekert, and C. J. Hawkins. Caspase-2 is resistant to inhibition by inhibitor of apoptosis proteins (IAPs) and can activate caspase-7. FEBS J. 272 (6):1401-1414, 2005.

S. Hoffarth, A. Zitzer, R. Wiewrodt, P. S. Hahnel, V. Beyer, A. Kreft, S. Biesterfeld, and M. Schuler. pp32/PHAPI determines the apoptosis response of non-small-cell lung cancer. Cell Death.Differ. 15 (1):161-170, 2008.

H. S. Hofmann, A. Simm, A. Hammer, R. E. Silber, and B. Bartling. Expression of inhibitors of apoptosis (IAP) proteins in non-small cell human lung cancer. J.Cancer Res.Clin.Oncol. 128 (10):554-560, 2002.

M. Holcik and R. G. Korneluk. Functional characterization of the X-linked inhibitor of apoptosis (XIAP) internal ribosome entry site element: role of La autoantigen in XIAP translation. Mol.Cell Biol. 20 (13):4648-4657, 2000.

M. Holcik, B. W. Gordon, and R. G. Korneluk. The internal ribosome entry site-mediated translation of antiapoptotic protein XIAP is modulated by the heterogeneous nuclear ribonucleoproteins C1 and C2. Mol.Cell Biol. 23 (1):280-288, 2003.

S. W. Hong, C. J. Kim, W. S. Park, J. S. Shin, S. D. Lee, S. G. Ko, S. I. Jung, I. C. Park, S. K. An, W. K. Lee, W. J. Lee, D. H. Jin, and M. S. Lee. p34SEI-1 inhibits apoptosis through the stabilization of the X-linked inhibitor of apoptosis protein: p34SEI-1 as a novel target for anti-breast cancer strategies. Cancer Res 69 (3):741-746, 2009.

http://data.euro.who.int/dmdb

http://www.svod.cz

Y. Hu, M. A. Benedict, L. Ding, and G. N++-ez. Role of cytochrome c and dATP/ATP hydrolysis in Apaf-1-mediated caspase-9 activation and apoptosis. The EMBO journal 18 (13):3586-3595, 1999.

Y. Hu, G. Cherton-Horvat, V. Dragowska, S. Baird, R. G. Korneluk, J. P. Durkin, L. D. Mayer, and E. C. LaCasse. Antisense oligonucleotides targeting XIAP induce apoptosis and enhance chemotherapeutic activity against human lung cancer cells in vitro and in vivo. Clin.Cancer Res 9 (7):2826-2836, 2003.

C. L. Huang, D. Liu, J. Nakano, H. Yokomise, M. Ueno, K. Kadota, and H. Wada. E2F1 overexpression correlates with thymidylate synthase and survivin gene expressions and tumor proliferation in non small-cell lung cancer. Clin.Cancer Res. 13 (23):6938-6946, 2007.

M. Izawa, T. Mori, T. Satoh, K. Teramachi, and T. Sairenji. Identification of an alternative

form of caspase-9 in human gastric cancer cell lines: a role of a caspase-9 variant in apoptosis resistance. Apoptosis. 4 (5):321-325, 1999.

A. K. Jarvinen, R. Autio, S. Kilpinen, M. Saarela, I. Leivo, R. Grenman, A. A. Makitie, and O. Monni. High-resolution copy number and gene expression microarray analyses of head and neck squamous cell carcinoma cell lines of tongue and larynx. Genes Chromosomes.Cancer 47 (6):500-509, 2008.

A. Jemal, F. Bray, M. M. Center, J. Ferlay, E. Ward, and D. Forman. Global cancer statistics. CA.Cancer J.Clin. 61 (2):69-90, 2011.

M. R. Jenkins and G. M. Griffiths. The synapse and cytolytic machinery of cytotoxic T cells. Current opinion in immunology 22 (3):308-313, 2010.

X. Jiang and X. Wang. Cytochrome c promotes caspase-9 activation by inducing nucleotide binding to Apaf-1. J.Biol.Chem. 275 (40):31199-31203, 2000.

X. Jiang, H. E. Kim, H. Shu, Y. Zhao, H. Zhang, J. Kofron, J. Donnelly, D. Burns, S. C. Ng, S. Rosenberg, and X. Wang. Distinctive roles of PHAP proteins and prothymosin-alpha in a death regulatory pathway. Science 299 (5604):223-226, 2003.

X. Jiang and X. Wang. Cytochrome C-mediated apoptosis. Annual review of biochemistry 73 (1):87-106, 2004.

Q. Jin, L. Feng, C. Behrens, B. N. Bekele, I. I. Wistuba, W. K. Hong, and H. Y. Lee. Implication of AMP-activated protein kinase and Akt-regulated survivin in lung cancer chemopreventive activities of deguelin. Cancer Res. 67 (24):11630-11639, 2007.

C. E. Johnson, Y. Y. Huang, A. B. Parrish, M. I. Smith, A. E. Vaughn, Q. Zhang, K. M. Wright, T. Van Dyke, R. J. Wechsler-Reya, S. Kornbluth, and M. Deshmukh. Differential Apaf-1 levels allow cytochrome c to induce apoptosis in brain tumors but not in normal neural tissues. Proc.Natl.Acad.Sci.U.S.A 104 (52):20820-20825, 2007.

K. Kagedal, A. C. Johansson, U. Johansson, G. Heimlich, K. Roberg, N. S. Wang, J. M. Jurgensmeier, and K. Ollinger. Lysosomal membrane permeabilization during apoptosis–involvement of Bax? Int.J.Exp.Pathol. 86 (5):309-321, 2005.

N. Keller, J. Mare+, O. Zerbe, and M. G. Gr+-tter. Structural and biochemical studies on procaspase-8: new insights on initiator caspase activation. Structure 17 (3):438-448, 2009.

J. F. Kerr, A. H. Wyllie, and A. R. Currie. Apoptosis: a basic biological phenomenon with wide-ranging implications in tissue kinetics. Br.J.Cancer 26 (4):239-257, 1972.

Z. Khan, R. P. Tiwari, N. Khan, G. B. Prasad, and P. S. Bisen. Induction of apoptosis and sensitization of head and neck squamous carcinoma cells to cisplatin by targeting survivin gene expression. Curr.Gene Ther. 12 (6):444-453, 2012.

H. E. Kim, F. Du, M. Fang, and X. Wang. Formation of apoptosome is initiated by cytochrome c-induced dATP hydrolysis and subsequent nucleotide exchange on Apaf-1. Proc. Natl. Acad. Sci. U.S.A 102 (49):17545-17550, 2005.

H. E. Kim, X. Jiang, F. Du, and X. Wang. PHAPI, CAS, and Hsp70 promote apoptosome formation by preventing Apaf-1 aggregation and enhancing nucleotide exchange on Apaf-1. Mol.Cell 30 (2):239-247, 2008.

H. R. Kim, E. J. Kim, S. H. Yang, E. T. Jeong, C. Park, J. H. Lee, M. J. Youn, H. S. So, and R. Park. Trichostatin A induces apoptosis in lung cancer cells via simultaneous activation of the death receptor-mediated and mitochondrial pathway? Exp.Mol.Med. 38 (6):616-624, 2006.

J. Kim, A. B. Parrish, M. Kurokawa, K. Matsuura, C. D. Freel, J. L. Andersen, C. E. Johnson, and S. Kornbluth. Rsk-mediated phosphorylation and 14-3-3varepsilon binding of Apaf-1 suppresses cytochrome c-induced apoptosis. EMBO J. 31 (5):1279-1292, 2012.

D. C. Ko, E. R. Gamazon, K. P. Shukla, R. A. Pfuetzner, D. Whittington, T. D. Holden, M. J. Brittnacher, C. Fong, M. Radey, C. Ogohara, A. L. Stark, J. M. Akey, M. E. Dolan, M. M. Wurfel, and S. I. Miller. Functional genetic screen of human diversity reveals that a methionine salvage enzyme regulates inflammatory cell death. Proc.Natl.Acad.Sci.U.S.A 109 (35):E2343-E2352, 2012.

B. W. Konicek, J. R. Stephens, A. M. McNulty, N. Robichaud, R. B. Peery, C. A. Dumstorf, M. S. Dowless, P. W. Iversen, S. Parsons, K. E. Ellis, D. J. McCann, J. Pelletier, L. Furic, J. M. Yingling, L. F. Stancato, N. Sonenberg, and J. R. Graff. Therapeutic inhibition of MAP kinase interacting kinase blocks eukaryotic initiation factor 4E phosphorylation and suppresses outgrowth of experimental lung metastases. Cancer Res. 71 (5):1849-1857, 2011.

E. Krepela, J. Prochazka, X. Liul, P. Fiala, and Z. Kinkor. Increased expression of Apaf-1 and procaspase-3 and the functionality of intrinsic apoptosis apparatus in non-small cell lung carcinoma. Biol.Chem. 385 (2):153-168, 2004.

E. Krepela, J. Prochazka, P. Fiala, P. Zatloukal, and P. Selinger. Expression of apoptosome pathway-related transcripts in non-small cell lung cancer. J.Cancer Res Clin.Oncol. 132 (1):57-68, 2006.

E. Krepela, P. Dankova, E. Moravcikova, A. Krepelova, J. Prochazka, J. Cermak, J. Schutzner, P. Zatloukal, and K. Benkova. Increased expression of inhibitor of apoptosis proteins, survivin and XIAP, in non-small cell lung carcinoma. Int.J.Oncol. 35 (6):1449-1462, 2009.

M. Kurokawa, C. Zhao, T. Reya, and S. Kornbluth. Inhibition of apoptosome formation by suppression of Hsp90beta phosphorylation in tyrosine kinase-induced leukemias. Mol.Cell Biol. 28 (17):5494-5506, 2008.

M. Kurokawa and S. Kornbluth. Caspases and kinases in a death grip. Cell 138 (5):838-854, 2009.

E. C. LaCasse, D. J. Mahoney, H. H. Cheung, S. Plenchette, S. Baird, and R. G. Korneluk. IAP-targeted therapies for cancer. Oncogene 27 (48):6252-6275, 2008.

S. L. Lai, R. P. Perng, and J. Hwang. p53 gene status modulates the chemosensitivity of non-small cell lung cancer cells. Journal of biomedical science 7 (1):64-70, 2000.

K. Lauber, H. A. Appel, S. F. Schlosser, M. Gregor, K. Schulze-Osthoff, and S. Wesselborg. The adapter protein apoptotic protease-activating factor-1 (Apaf-1) is proteolytically processed during apoptosis. J.Biol.Chem. 276 (32):29772-29781, 2001.

C. Leo, C. Richter, L. C. Horn, A. Schutz, H. Pilch, and M. Hockel. Expression of Apaf-1 in cervical cancer correlates with lymph node metastasis but not with intratumoral hypoxia. Gynecol.Oncol. 97 (2):602-606, 2005.

C. Leo, L. C. Horn, C. Rauscher, B. Hentschel, C. E. Richter, A. Schutz, C. P. Leo, and M. Hockel. Lack of apoptotic protease activating factor-1 expression and resistance to hypoxia-induced apoptosis in cervical cancer. Clin.Cancer Res. 13 (4):1149-1153, 2007.

P. Li, D. Nijhawan, I. Budihardjo, S. M. Srinivasula, M. Ahmad, E. S. Alnemri, and X. Wang. Cytochrome c and dATP-dependent formation of Apaf-1/caspase-9 complex initiates an apoptotic protease cascade. Cell 91 (4):479-489, 1997.

L. Liu, T. Sakai, N. H. Tran, R. Mukai-Sakai, R. Kaji, and K. Fukui. Nucling interacts with nuclear factor-kappaB, regulating its cellular distribution. FEBS J. 276 (5):1459-1470, 2009.

L. Liu, D. Xing, W. R. Chen, T. Chen, Y. Pei, and X. Gao. Calpain-mediated pathway dominates cisplatin-induced apoptosis in human lung adenocarcinoma cells as determined by real-time single cell analysis. Int.J.Cancer 122 (10):2210-2222, 2008 a.

Y. Liu, H. Xing, X. Han, X. Shi, F. Liang, G. Cheng, Y. Lu, and D. Ma. Apoptosis of HeLa cells induced by cisplatin and its mechanism. J.Huazhong.Univ Sci.Technolog.Med.Sci. 28 (2):197-199, 2008 b.

W. H. Liu, H. W. Hsiao, W. I. Tsou, and M. Z. Lai. Notch inhibits apoptosis by direct interference with XIAP ubiquitination and degradation. EMBO J. 26 (6):1660-1669, 2007.

L. Liu, T. Sakai, N. Sano, and K. Fukui. Nucling mediates apoptosis by inhibiting expression of galectin-3 through interference with nuclear factor kappaB signalling. Biochem.J. 380 (Pt 1):31-41, 2004.

J. R. Liu, A. W. Opipari, L. Tan, Y. Jiang, Y. Zhang, H. Tang, and G. Nunez. Dysfunctional apoptosome activation in ovarian cancer: implications for chemoresistance. Cancer Res. 62 (3):924-931, 2002.

J. Lu, L. Bai, H. Sun, Z. Nikolovska-Coleska, D. McEachern, S. Qiu, R. S. Miller, H. Yi, S. Shangary, Y. Sun, J. L. Meagher, J. A. Stuckey, and S. Wang. SM-164: a novel, bivalent Smac mimetic that induces apoptosis and tumor regression by concurrent removal of the blockade of cIAP-1/2 and XIAP. Cancer Res 68 (22):9384-9393, 2008.

B. Lu, Y. Mu, C. Cao, F. Zeng, S. Schneider, J. Tan, J. Price, J. Chen, M. Freeman, and D. E. Hallahan. Survivin as a therapeutic target for radiation sensitization in lung cancer. Cancer Res 64 (8):2840-2845, 2004.

A. U. Luthi and S. J. Martin. The CASBAH: a searchable database of caspase substrates. Cell Death.Differ. 14 (4):641-650, 2007.

P. D. Mace and S. J. Riedl. Molecular cell death platforms and assemblies. Curr.Opin.Cell Biol. 22 (6):828-836, 2010.

P. D. Mace, S. Shirley, and C. L. Day. Assembling the building blocks: structure and function of inhibitor of apoptosis proteins. Cell Death.Differ. 17 (1):46-53, 2010.

G. Makin and C. Dive. Modulating sensitivity to drug-induced apoptosis: the future for chemotherapy? Breast Cancer Research 3 (3):150-153, 2001.

S. Malladi, M. Challa-Malladi, H. O. Fearnhead, and S. B. Bratton. The Apaf-1*procaspase-9 apoptosome complex functions as a proteolytic-based molecular timer. EMBO J. 28 (13):1916-1925, 2009.

C. Manzl, G. Krumschnabel, F. Bock, B. Sohm, V. Labi, F. Baumgartner, E. Logette, J. Tschopp, and A. Villunger. Caspase-2 activation in the absence of PIDDosome formation. J.Cell Biol. 185 (2):291-303, 2009.

C. Manzl, L. Peintner, G. Krumschnabel, F. Bock, V. Labi, M. Drach, A. Newbold, R. Johnstone, and A. Villunger. PIDDosome-independent tumor suppression by Caspase-2. Cell Death.Differ. 19 (10):1722-1732, 2012.

W. E. Marissen and R. E. Lloyd. Eukaryotic translation initiation factor 4G is targeted for proteolytic cleavage by caspase 3 during inhibition of translation in apoptotic cells. Mol.Cell Biol. 18 (12):7565-7574, 1998.

W. E. Marissen, A. Gradi, N. Sonenberg, and R. E. Lloyd. Cleavage of eukaryotic translation initiation factor 4GII correlates with translation inhibition during apoptosis. Cell Death.Differ. 7 (12):1234-1243, 2000.

A. G. Martin and H. O. Fearnhead. Apocytochrome c blocks caspase-9 activation and Bax-induced apoptosis. J.Biol.Chem. 277 (52):50834-50841, 2002.

M. C. Martin, L. A. Allan, E. J. Mancini, and P. R. Clarke. The docking interaction of caspase-9 with ERK2 provides a mechanism for the selective inhibitory phosphorylation of caspase-9 at threonine 125. J.Biol.Chem. 283 (7):3854-3865, 2008.

G. Martinez-Ruiz, V. Maldonado, G. Ceballos-Cancino, J. P. Grajeda, and J. Melendez-Zajgla. Role of Smac/DIABLO in cancer progression. J.Exp.Clin.Cancer Res 27:48, 2008.

H. Marusawa, S. Matsuzawa, K. Welsh, H. Zou, R. Armstrong, I. Tamm, and J. C. Reed. HBXIP functions as a cofactor of survivin in apoptosis suppression. EMBO J. 22 (11):2729-2740, 2003.

C. Mary, P. Duek, L. Salleron, P. Tienz, D. Bumann, A. Bairoch, and L. Lane. Functional Identification of APIP as Human mtnB, a Key Enzyme in the Methionine Salvage Pathway. PLoS.One. 7 (12):e52877, 2012.

A. Massiello and C. E. Chalfant. SRp30a (ASF/SF2) regulates the alternative splicing of caspase-9 pre-mRNA and is required for ceramide-responsiveness. J.Lipid Res. 47 (5):892-897, 2006.

P. P. Massion, P. M. Taflan, Y. Shyr, S. M. Rahman, P. Yildiz, B. Shakthour, M. E. Edgerton, M. Ninan, J. J. Andersen, and A. L. Gonzalez. Early involvement of the phosphatidylinositol 3-kinase/Akt pathway in lung cancer progression. Am.J.Respir.Crit Care Med. 170 (10):1088-1094, 2004.

R. Mazroui, S. Di Marco, E. Clair, C. von Roretz, S. A. Tenenbaum, J. D. Keene, M. Saleh, and I. E. Gallouzi. Caspase-mediated cleavage of HuR in the cytoplasm contributes to pp32/PHAP-I regulation of apoptosis. J.Cell Biol. 180 (1):113-127, 2008.

S. A. Mitchell, E. C. Brown, M. J. Coldwell, R. J. Jackson, and A. E. Willis. Protein factor requirements of the Apaf-1 internal ribosome entry segment: roles of polypyrimidine tract binding protein and upstream of N-ras. Mol.Cell Biol. 21 (10):3364-3374, 2001.

S. A. Mitchell, K. A. Spriggs, M. J. Coldwell, R. J. Jackson, and A. E. Willis. The Apaf-1 internal ribosome entry segment attains the correct structural conformation for function via interactions with PTB and unr. Mol.Cell 11 (3):757-771, 2003.

J. Moldvay. [Personalized therapy in non-small cell lung cancer: from diagnosis to therapy]. Orv.Hetil. 153 (23):909-916, 2012.

J. R. Molina, P. Yang, S. D. Cassivi, S. E. Schild, and A. A. Adjei. Non-small cell lung cancer: epidemiology, risk factors, treatment, and survivorship. Mayo Clin.Proc. 83 (5):584-594, 2008.

E. Moravcikova, E. Krepela, J. Prochazka, I. Rousalova, J. Cermak, and K. Benkova. Down-regulated expression of apoptosis-associated genes APIP and UACA in non-small cell lung carcinoma. Int.J.Oncol. 40 (6):2111-2121, 2012.

Y. Morizane, R. Honda, K. Fukami, and H. Yasuda. X-linked inhibitor of apoptosis functions as ubiquitin ligase toward mature caspase-9 and cytosolic Smac/DIABLO. J.Biochem. 137 (2):125-132, 2005.

Z. Nahle, J. Polakoff, R. V. Davuluri, M. E. McCurrach, M. D. Jacobson, M. Narita, M. Q. Zhang, Y. Lazebnik, D. Bar-Sagi, and S. W. Lowe. Direct coupling of the cell cycle and cell death machinery by E2F. Nat.Cell Biol. 4 (11):859-864, 2002.

K. Nakanishi, T. Kawai, F. Kumaki, S. Hiroi, M. Mukai, and E. Ikeda. Survivin expression in atypical adenomatous hyperplasia of the lung. Am.J.Clin.Pathol. 120 (5):712-719, 2003.

J. Nakano, C. L. Huang, D. Liu, M. Ueno, S. Sumitomo, and H. Yokomise. Survivin gene expression is negatively regulated by the p53 tumor suppressor gene in non-small cell lung cancer. Int.J.Oncol. 27 (5):1215-1221, 2005.

A. Oberst, C. Pop, A. G. Tremblay, V. Blais, J. B. Denault, G. S. Salvesen, and D. R. Green. Inducible dimerization and inducible cleavage reveal a requirement for both processes in caspase-8 activation. J.Biol.Chem. 285 (22):16632-16642, 2010.

T. Ogawa, K. Shiga, S. Hashimoto, T. Kobayashi, A. Horii, and T. Furukawa. APAF-1-ALT, a novel alternative splicing form of APAF-1, potentially causes impeded ability of undergoing DNA damage-induced apoptosis in the LNCaP human prostate cancer cell line. Biochem.Biophys.Res.Commun. 306 (2):537-543, 2003.

M. Olsson, H. Vakifahmetoglu, P. M. Abruzzo, K. Hogstrand, A. Grandien, and B. Zhivotovsky. DISC-mediated activation of caspase-2 in DNA damage-induced apoptosis. Oncogene 28 (18):1949-1959, 2009.

R. Panniers. Translational control during heat shock. Biochimie 76 (8):737-747, 1994.

S. L. Petersen, L. Wang, A. Yalcin-Chin, L. Li, M. Peyton, J. Minna, P. Harran, and X. Wang. Autocrine TNFalpha signaling renders human cancer cells susceptible to Smac-mimetic-induced apoptosis. Cancer cell 12 (5):445-456, 2007.

C. Pop, J. Timmer, S. Sperandio, and G. S. Salvesen. The apoptosome activates caspase-9 by dimerization. Mol.Cell 22 (2):269-275, 2006.

C. Pop, P. Fitzgerald, D. R. Green, and G. S. Salvesen. Role of proteolysis in caspase-8 activation and stabilization. Biochemistry 46 (14):4398-4407, 2007.

D. Prevot, J. L. Darlix, and T. Ohlmann. Conducting the initiation of protein synthesis: the role of eIF4G. Biol.Cell 95 (3-4):141-156, 2003.

C. Purring-Koch and G. McLendon. Cytochrome c binding to Apaf-1: the effects of dATP and ionic strength. Proc.Natl.Acad.Sci.U.S.A 97 (22):11928-11931, 2000.

X. Qi, L. Wang, and F. Du. Novel small molecules relieve prothymosin alpha-mediated inhibition of apoptosome formation by blocking its interaction with Apaf-1. Biochemistry 49 (9):1923-1930, 2010.

D. Raina, P. Pandey, R. Ahmad, A. Bharti, J. Ren, S. Kharbanda, R. Weichselbaum, and D. Kufe. c-Abl tyrosine kinase regulates caspase-9 autocleavage in the apoptotic response to DNA damage. J.Biol.Chem. 280 (12):11147-11151, 2005.

J. C. Reed. Apoptosis-targeted therapies for cancer. Cancer cell 3 (1):17, 2003.

M. Renatus, H. R. Stennicke, F. L. Scott, R. C. Liddington, and G. S. Salvesen. Dimer formation drives the activation of the cell death protease caspase 9. Proc.Natl.Acad.Sci.U.S.A 98 (25):14250-14255, 2001.

T. F. Reubold, S. Wohlgemuth, and S. Eschenburg. Crystal structure of full-length Apaf-1: how the death signal is relayed in the mitochondrial pathway of apoptosis. Structure. 19 (8):1074-1083, 2011.

T. F. Reubold and S. Eschenburg. A molecular view on signal transduction by the apoptosome. Cell Signal. 24 (7):1420-1425, 2012.

S. J. Riedl, W. Li, Y. Chao, R. Schwarzenbacher, and Y. Shi. Structure of the apoptotic protease-activating factor 1 bound to ADP. Nature 434 (7035):926-933, 2005.

J. D. Robertson, M. Enoksson, M. Suomela, B. Zhivotovsky, and S. Orrenius. Caspase-2 acts upstream of mitochondria to promote cytochrome c release during etoposide-induced apoptosis. J.Biol.Chem. 277 (33):29803-29809, 2002.

J. Rodriguez and Y. Lazebnik. Caspase-9 and APAF-1 form an active holoenzyme. Genes Dev. 13 (24):3179-3184, 1999.

A. Rosato, C. Menin, D. Boldrin, S. D. Santa, L. Bonaldi, M. C. Scaini, P. Del Bianco, D. Zardo, M. Fassan, R. Cappellesso, and A. Fassina. Survivin expression impacts prognostically on NSCLC but not SCLC. Lung Cancer 79 (2):180-186, 2013.

I. Rousalova and E. Krepela. Granzyme B-induced apoptosis in cancer cells and its regulation (review). Int.J.Oncol. 37 (6):1361-1378, 2010.

I. Rousalova, E. Krepela, J. Prochazka, J. Cermak, and K. Benkova. Expression of proteinase inhibitor-9/serpinB9 in non-small cell lung carcinoma cells and tissues. Int.J.Oncol. 36 (1):275-283, 2010.

T. Sakai, L. Liu, Y. Shishido, and K. Fukui. Identification of a novel, embryonal carcinoma cell-associated molecule, nucling, that is up-regulated during cardiac muscle differentiation. J.Biochem. 133 (4):429-436, 2003.

T. Sakai, L. Liu, X. Teng, R. Mukai-Sakai, H. Shimada, R. Kaji, T. Mitani, M. Matsumoto, K. Toida, K. Ishimura, Y. Shishido, T. W. Mak, and K. Fukui. Nucling recruits Apaf-1/pro-caspase-9 complex for the induction of stress-induced apoptosis. J.Biol.Chem. 279 (39):41131-41140, 2004.

A. K. Samraj, E. Keil, N. Ueffing, K. Schulze-Osthoff, and I. Schmitz. Loss of caspase-9 provides genetic evidence for the type I/II concept of CD95-mediated apoptosis. J.Biol.Chem. 281 (40):29652-29659, 2006.

Z. T. Schafer, A. B. Parrish, K. M. Wright, S. S. Margolis, J. R. Marks, M. Deshmukh, and S. Kornbluth. Enhanced sensitivity to cytochrome c-induced apoptosis mediated by PHAPI in breast cancer cells. Cancer Res. 66 (4):2210-2218, 2006.

Z. T. Schafer and S. Kornbluth. The apoptosome: physiological, developmental, and pathological modes of regulation. Dev.Cell 10 (5):549-561, 2006.

H. Schagger and G. von Jagow. Tricine-sodium dodecyl sulfate-polyacrylamide gel electrophoresis for the separation of proteins in the range from 1 to 100 kDa. Anal.Biochem. 166 (2):368-379, 1987.

K. Schleich, U. Warnken, N. Fricker, S. Ozturk, P. Richter, K. Kammerer, M. Schnolzer, P. H. Krammer, and I. N. Lavrik. Stoichiometry of the CD95 death-inducing signaling complex: experimental and modeling evidence for a death effector domain chain model. Mol.Cell 47 (2):306-319, 2012.

K. Schleich, P. H. Krammer, and I. N. Lavrik. The chains of death: A new view on caspase-8 activation at the DISC. Cell Cycle 12 (2):193-194, 2013.

Z. T. Schug, F. Gonzalvez, R. H. Houtkooper, F. M. Vaz, and E. Gottlieb. BID is cleaved by caspase-8 within a native complex on the mitochondrial membrane. Cell Death.Differ. 18 (3):538-548, 2011.

F. L. Scott, J. B. Denault, S. J. Riedl, H. Shin, M. Renatus, and G. S. Salvesen. XIAP inhibits caspase-3 and -7 using two binding sites: evolutionarily conserved mechanism of IAPs. EMBO J. 24 (3):645-655, 2005.

J. M. Seeger, K. Brinkmann, B. Yazdanpanah, D. Haubert, C. Pongratz, O. Coutelle, M. Kronke, and H. Kashkar. Elevated XIAP expression alone does not confer chemoresistance. Br.J.Cancer 102 (12):1717-1723, 2010.

A. Seifert and P. R. Clarke. p38alpha- and DYRK1A-dependent phosphorylation of caspase-9 at an inhibitory site in response to hyperosmotic stress. Cell Signal. 21 (11):1626-1633, 2009.

D. W. Seol and T. R. Billiar. A caspase-9 variant missing the catalytic site is an endogenous inhibitor of apoptosis. J.Biol.Chem. 274 (4):2072-2076, 1999.

K. W. Sherrill, M. P. Byrd, M. E. Van Eden, and R. E. Lloyd. BCL-2 translation is mediated via internal ribosome entry during cell stress. J.Biol.Chem. 279 (28):29066-29074, 2004.

E. N. Shiozaki, J. Chai, and Y. Shi. Oligomerization and activation of caspase-9, induced by Apaf-1 CARD. Proc.Natl.Acad.Sci.U.S.A 99 (7):4197-4202, 2002.

E. N. Shiozaki, J. Chai, D. J. Rigotti, S. J. Riedl, P. Li, S. M. Srinivasula, E. S. Alnemri, R. Fairman, and Y. Shi. Mechanism of XIAP-mediated inhibition of caspase-9. Mol.Cell 11 (2):519-527, 2003.

J. C. Shultz, R. W. Goehe, D. S. Wijesinghe, C. Murudkar, A. J. Hawkins, J. W. Shay, J. D. Minna, and C. E. Chalfant. Alternative splicing of caspase 9 is modulated by the phosphoinositide 3-kinase/Akt pathway via phosphorylation of SRp30a. Cancer Res. 70 (22):9185-9196, 2010.

J. C. Shultz, R. W. Goehe, C. S. Murudkar, D. S. Wijesinghe, E. K. Mayton, A. Massiello, A. J. Hawkins, P. Mukerjee, R. L. Pinkerman, M. A. Park, and C. E. Chalfant. SRSF1 regulates the alternative splicing of caspase 9 via a novel intronic splicing enhancer affecting the chemotherapeutic sensitivity of non-small cell lung cancer cells. Mol.Cancer Res. 9 (7):889-900, 2011.

P. K. Smith, R. I. Krohn, G. T. Hermanson, A. K. Mallia, F. H. Gartner, M. D. Provenzano, E. K. Fujimoto, N. M. Goeke, B. J. Olson, and D. C. Klenk. Measurement of protein using bicinchoninic acid. Anal.Biochem. 150 (1):76-85, 1985.

M. S. Soengas, P. Capodieci, D. Polsky, J. Mora, M. Esteller, X. Opitz-Araya, R. McCombie, J. G. Herman, W. L. Gerald, Y. A. Lazebnik, C. Cordon-Cardo, and S. W. Lowe. Inactivation of the apoptosis effector Apaf-1 in malignant melanoma. Nature 409 (6817):207-211, 2001.

S. M. Srinivasula, T. Fernandes-Alnemri, J. Zangrilli, N. Robertson, R. C. Armstrong, L. Wang, J. A. Trapani, K. J. Tomaselli, G. Litwack, and E. S. Alnemri. The Ced-3/interleukin 1+- converting enzyme-like homolog Mch6 and the lamin-cleaving enzyme Mch2+- are substrates for the apoptotic mediator CPP32. Journal of Biological Chemistry 271 (43):27099-27106, 1996.

S. M. Srinivasula, M. Ahmad, T. Fernandes-Alnemri, and E. S. Alnemri. Autoactivation of procaspase-9 by Apaf-1-mediated oligomerization. Molecular cell 1 (7):949-957, 1998.

S. M. Srinivasula, M. Ahmad, Y. Guo, Y. Zhan, Y. Lazebnik, T. Fernandes-Alnemri, and E. S. Alnemri. Identification of an endogenous dominant-negative short isoform of caspase-9 that can regulate apoptosis. Cancer Res. 59 (5):999-1002, 1999.

S. M. Srinivasula, R. Hegde, A. Saleh, P. Datta, E. Shiozaki, J. Chai, R. A. Lee, P. D. Robbins, T. Fernandes-Alnemri, Y. Shi, and E. S. Alnemri. A conserved XIAP-interaction motif in caspase-9 and Smac/DIABLO regulates caspase activity and apoptosis. Nature 410 (6824):112-116, 2001.

S. M. Srinivasula and J. D. Ashwell. IAPs: what's in a name? Mol.Cell 30 (2):123-135, 2008.

H. R. Stennicke, J. M. J+-rgensmeier, H. Shin, Q. Deveraux, B. B. Wolf, X. Yang, Q. Zhou, H. M. Ellerby, L. M. Ellerby, and D. Bredesen. Pro-caspase-3 is a major physiologic target of caspase-8. Journal of Biological Chemistry 273 (42):27084-27090, 1998.

T. E. Stinchcombe and M. A. Socinski. Current treatments for advanced stage non-small cell lung cancer. Proc.Am.Thorac.Soc. 6 (2):233-241, 2009a.

T. E. Stinchcombe and M. A. Socinski.Treatment paradigms for advanced stage non-small cell lung cancer in the era of multiple lines of therapy.J.Thorac.Oncol.4 (2):243-250, 2009b.

M. Stoneley, T. Subkhankulova, J. P. Le Quesne, M. J. Coldwell, C. L. Jopling, G. J. Belsham, and A. E. Willis. Analysis of the c-myc IRES; a potential role for cell-type specific trans-acting factors and the nuclear compartment. Nucleic Acids Res. 28 (3):687-694, 2000.

H. Sun, Z. Nikolovska-Coleska, C. Y. Yang, D. Qian, J. Lu, S. Qiu, L. Bai, Y. Peng, Q. Cai, and S. Wang. Design of small-molecule peptidic and nonpeptidic Smac mimetics. Acc.Chem.Res 41 (10):1264-1277, 2008.

Y. Sun, S. Orrenius, S. Pervaiz, and B. Fadeel. Plasma membrane sequestration of apoptotic protease-activating factor-1 in human B-lymphoma cells: a novel mechanism of chemoresistance. Blood 105 (10):4070-4077, 2005.

Y. Suzuki, Y. Nakabayashi, and R. Takahashi. Ubiquitin-protein ligase activity of X-linked inhibitor of apoptosis protein promotes proteasomal degradation of caspase-3 and enhances its anti-apoptotic effect in Fas-induced cell death. Proc.Natl.Acad.Sci.U.S.A 98 (15):8662-8667, 2001.

X. L. Tan, A. M. Moyer, B. L. Fridley, D. J. Schaid, N. Niu, A. J. Batzler, G. D. Jenkins, R. P. Abo, L. Li, J. M. Cunningham, Z. Sun, P. Yang, and L. Wang. Genetic variation predicting cisplatin cytotoxicity associated with overall survival in lung cancer patients receiving platinum-based chemotherapy. Clin.Cancer Res. 17 (17):5801-5811, 2011.

X. Teng, T. Sakai, L. Liu, R. Sakai, R. Kaji, and K. Fukui. Attenuation of MPTP-induced neurotoxicity and locomotor dysfunction in Nucling-deficient mice via suppression of the apoptosome pathway. J.Neurochem. 97 (4):1126-1135, 2006.

A. Terman, T. Kurz, B. Gustafsson, and U. T. Brunk. Lysosomal labilization. IUBMB life 58 (9):531-539, 2006.

J. Thiery, D. Keefe, S. Saffarian, D. Martinvalet, M. Walch, E. Boucrot, T. Kirchhausen, and J. Lieberman. Perforin activates clathrin-and dynamin-dependent endocytosis, which is required for plasma membrane repair and delivery of granzyme B for granzyme-mediated apoptosis. Blood 115 (8):1582-1593, 2010.

J. C. Timmer and G. S. Salvesen. Caspase substrates. Cell Death.Differ. 14 (1):66-72, 2007.

A. Tinel and J. Tschopp. The PIDDosome, a protein complex implicated in activation of caspase-2 in response to genotoxic stress. Science Signalling 304 (5672):843, 2004.

A. Tinel, S. Janssens, S. Lippens, S. Cuenin, E. Logette, B. Jaccard, M. Quadroni, and J.

Tschopp. Autoproteolysis of PIDD marks the bifurcation between pro-death caspase-2 and pro-survival NF-kappaB pathway. EMBO J. 26 (1):197-208, 2007.

N. J. Topham and E. W. Hewitt. Natural killer cell cytotoxicity: how do they pull the trigger? Immunology 128 (1):7-15, 2009.

W. D. Travis. Pathology and genetics of tumours of the lung, pleura, thymus and heart, Iarc, 2004.

W. D. Travis. Pathology of lung cancer. Clin.Chest Med. 32 (4):669-692, 2011.

D. Twiddy, D. G. Brown, C. Adrain, R. Jukes, S. J. Martin, G. M. Cohen, M. Macfarlane, and K. Cain. Pro-apoptotic proteins released from the mitochondria regulate the protein composition and caspase-processing activity of the native Apaf-1/caspase-9 apoptosome complex. J.Biol.Chem. 279 (19):19665-19682, 2004.

D. Twiddy, G. M. Cohen, M. Macfarlane, and K. Cain. Caspase-7 is directly activated by the approximately 700-kDa apoptosome complex and is released as a stable XIAP-caspase-7 approximately 200-kDa complex. J.Biol.Chem. 281 (7):3876-3888, 2006.

N. H. Ungureanu, M. Cloutier, S. M. Lewis, N. de Silva, J. D. Blais, J. C. Bell, and M. Holcik. Internal ribosome entry site-mediated translation of Apaf-1, but not XIAP, is regulated during UV-induced cell death. J.Biol.Chem. 281 (22):15155-15163, 2006.

UniProt Consortium. Reorganizing the protein space at the Universal Protein Resource (UniProt). Nucleic Acids Res 40:D71-D75, 2012.

J. Vadakara and H. Borghaei. Personalized medicine and treatment approaches in non-small-cell lung carcinoma. Pharmgenomics.Pers.Med. 5:113-123, 2012.

H. Vakifahmetoglu, M. Olsson, C. Tamm, N. Heidari, S. Orrenius, and B. Zhivotovsky. DNA damage induces two distinct modes of cell death in ovarian carcinomas. Cell Death.Differ. 15 (3):555-566, 2008.

P. Van Damme, S. Maurer-Stroh, K. Plasman, J. Van Durme, N. Colaert, E. Timmerman, P. J. De Bock, M. Goethals, F. Rousseau, and J. Schymkowitz. Analysis of protein processing by N-terminal proteomics reveals novel species-specific substrate determinants of granzyme B orthologs. Molecular & Cellular Proteomics 8 (2):258-272, 2009.

Walle L. Vande, E. Wirawan, M. Lamkanfi, N. Festjens, J. Verspurten, X. Saelens, T. Vanden Berghe, and P. Vandenabeele. The mitochondrial serine protease HtrA2/Omi cleaves RIP1 during apoptosis of Ba/F3 cells induced by growth factor withdrawal. Cell Res 20 (4):421-433, 2010.

A. Vazquez, E. E. Bond, A. J. Levine, and G. L. Bond. The genetics of the p53 pathway, apoptosis and cancer therapy. Nat.Rev.Drug Discov. 7 (12):979-987, 2008.

K. Viktorsson and R. Lewensohn. Apoptotic signaling pathways in lung cancer. J.Thorac.Oncol. 2 (3):175-179, 2007.

B. Vischioni, der van, V, S. W. Span, F. A. Kruyt, J. A. Rodriguez, and G. Giaccone. Expression and localization of inhibitor of apoptosis proteins in normal human tissues. Hum.Pathol. 37 (1):78-86, 2006.

M. Vogler, H. Walczak, D. Stadel, T. L. Haas, F. Genze, M. Jovanovic, U. Bhanot, C. Hasel, P. Moller, J. E. Gschwend, T. Simmet, K. M. Debatin, and S. Fulda. Small molecule XIAP inhibitors enhance TRAIL-induced apoptosis and antitumor activity in preclinical models of pancreatic carcinoma. Cancer Res 69 (6):2425-2434, 2009.

K. Wachmann, C. Pop, B. J. van Raam, M. Drag, P. D. Mace, S. J. Snipas, C. Zmasek, R. Schwarzenbacher, G. S. Salvesen, and S. J. Riedl. Activation and specificity of human caspase-10. Biochemistry 49 (38):8307-8315, 2010.

P. Wang, T. Shi, and D. Ma. Cloning of a novel human caspase-9 splice variant containing only the CARD domain. Life Sci. 79 (10):934-940, 2006.

B. B. Wolf, M. Schuler, W. Li, B. Eggers-Sedlet, W. Lee, P. Tailor, P. Fitzgerald, G. B. Mills, and D. R. Green. Defective cytochrome c-dependent caspase activation in ovarian cancer cell lines due to diminished or absent apoptotic protease activating factor-1 activity. J.Biol.Chem. 276 (36):34244-34251, 2001.

K. Yamada, S. Senju, T. Nakatsura, Y. Murata, M. Ishihara, S. Nakamura, S. Ohno, A. Negi, and Y. Nishimura. Identification of a novel autoantigen UACA in patients with panuveitis. Biochem.Biophys.Res Commun. 280 (4):1169-1176, 2001.

Q. Yin, H. H. Park, J. Y. Chung, S. C. Lin, Y. C. Lo, L. S. da Graca, X. Jiang, and H. Wu. Caspase-9 holoenzyme is a specific and optimal procaspase-3 processing machine. Mol.Cell 22 (2):259-268, 2006.

N. J. Yoo, S. H. Lee, E. G. Jeong, and S. H. Lee. Expression of phosphorylated caspase-9 in gastric carcinomas. APMIS 115 (4):354-359, 2007.

X. Yu, D. Acehan, J. F. Menetret, C. R. Booth, S. J. Ludtke, S. J. Riedl, Y. Shi, X. Wang, and C. W. Akey. A structure of the human apoptosome at 12.8 A resolution provides insights into this cell death platform. Structure. 13 (11):1725-1735, 2005.

S. Yuan, X. Yu, M. Topf, S. J. Ludtke, X. Wang, and C. W. Akey. Structure of an apoptosome-procaspase-9 CARD complex. Structure. 18 (5):571-583, 2010.

S. Yuan, X. Yu, J. M. Asara, J. E. Heuser, S. J. Ludtke, and C. W. Akey. The holo-apoptosome: activation of procaspase-9 and interactions with caspase-3. Structure. 19 (8):1084-1096, 2011.

Y. Zermati, S. Mouhamad, L. Stergiou, B. Besse, L. Galluzzi, S. Boehrer, A. L. Pauleau, F. Rosselli, M. D'Amelio, R. Amendola, M. Castedo, M. Hengartner, J. C. Soria, F. Cecconi, and G. Kroemer. Nonapoptotic role for Apaf-1 in the DNA damage checkpoint. Mol.Cell 28 (4):624-637, 2007.

H. Zhang, R. Gogada, N. Yadav, R. K. Lella, M. Badeaux, M. Ayres, V. Gandhi, D. G. Tang, and D. Chandra. Defective molecular timer in the absence of nucleotides leads to inefficient caspase activation. PLoS.One. 6 (1):e16379, 2011.

X. Zhang, J. Zhang, H. Wei, and Z. Tian. STAT3-decoy oligodeoxynucleotide inhibits the growth of human lung cancer via down-regulating its target genes. Oncol.Rep. 17 (6):1377-1382, 2007.

H. Zou, R. Yang, J. Hao, J. Wang, C. Sun, S. W. Fesik, J. C. Wu, K. J. Tomaselli, and R. C. Armstrong. Regulation of the Apaf-1/caspase-9 apoptosome by caspase-3 and XIAP. J.Biol.Chem. 278 (10):8091-8098, 2003.

Selected publications